

Chain-End Functionalization and Modification of Polymers using Modular Chemical Reactions

Dissertation

von

Zoya Zarafshani

Eingereicht an der mathematisch-naturwissenschaftlichen Fakultät der Universität
Potsdam zur Erlangung des akademischen Grades Dr. rer. nat. in der
Wissenschaftsdisziplin Polymerchemie

Abgabe: 18.01.2012

Betreuer: Prof. Dr. André Laschewsky

Published online at the
Institutional Repository of the University of Potsdam:
URL <http://opus.kobv.de/ubp/volltexte/2012/5972/>
URN [urn:nbn:de:kobv:517-opus-59723](http://nbn-resolving.org/urn:nbn:de:kobv:517-opus-59723)
<http://nbn-resolving.org/urn:nbn:de:kobv:517-opus-59723>

Table of Contents

Chapter 1.....	5
General introduction and scientific objectives of the thesis	5
1.1. General Introduction.....	6
1.2. Goals of the thesis.....	10
Chapter 2.....	15
Theoretical part.....	15
2.1. Controlled polymerisation techniques	16
2.2. Controlled Radical Polymerizations (CRP).....	16
2.2.1. Nitroxide mediated radical polymerisation (NMP)	18
2.2.2. Reversible addition-fragmentation chain transfer (RAFT)	20
2.2.3. Atom Transfer Radical Polymerization (ATRP).....	22
2.2.3.1. ATRP monomers.....	24
2.2.3.2. ATRP catalysts	25
2.2.3.3 ATRP initiators.....	27
2.3. ATRP as a convenient way to induce functionality	27
2.3.1. Various initiators to induce some typical α -functionalities	28
2.3.2. Activated ester containing initiators.....	32
2.4. Different approaches to induce ω -functionalities in polymers synthesized by ATRP	33
2.5. Click Chemistry.....	35
2.5.1. Mechanism of copper-catalyzed alkyne-azide cycloaddition	38
2.5.2. “Metal-free” click strategies	39
2.5.3. Metal-free nitrile oxide-alkyne Huisgen cycloaddition.....	41
2.6. Some biological applications of thermoresponsive polymers	43
2.6.1. PEGylated chromatography: Thermoresponsive stationary phases for bioseparation.....	45
2.6.2. Activated ester end-functionalized thermoresponsive polymers for bioconjugation: Smart PEGylation of trypsin.....	46
Chapter 3.....	54
Functionalization of polymer chain ends via CuAAC	54
3.1. <i>In situ</i> functionalization of thermoresponsive polymeric micelles using CuAAC.....	55
3.2. <i>In situ</i> click cycloaddition of the pre-formed micelles in water with a “low molecular weight” model molecule	57

3.2.1. Preparation of azide end functional polymers	61
3.2.2. Self-organization of the macrosurfactants in water	61
3.2.3. <i>In situ</i> “click” functionalization of co/polymers with a model low molecular weight alkyne in aqueous solution.....	64
3.3. <i>In situ</i> aqueous click cycloaddition of the corona of micellar aggregates with large polymeric molecules	68
3.3.1. Synthesis of ω -azido-functional diblock copolymer PS- <i>b</i> -POEGA 1.....	70
3.3.2. Synthesis of α -alkyne functional homopolymer POEGA 2.....	75
3.3.3. CuAAC of diblock copolymer PS- <i>b</i> -POEGA 1 and homopolymer POEGA 2.....	78
3.3.4. Optimization of the click reaction conditions	79
3.3.5. Investigation of the main-chain hydrolysis of the formed triblock copolymer 3	81
3.4. Synthetic Procedures	84
3.4.1. <i>In situ</i> CuAAC of the pre-formed micelles in water with propargyl alcohol	84
3.4.1.1. Synthesis of the ATRP initiator cholesteryl-2-bromoisobutyrate	84
3.4.1.2. General procedure for the bulk atom transfer radical copolymerization of EEO ₂ A and OEGA	84
3.4.1.3. General procedure for the atom transfer radical copolymerization of MEO ₂ MA and OEGMA	85
3.4.1.4. Preparation of azide end functionalized polymers.....	85
3.4.1.5. General procedure for the aqueous “click” functionalization of the amphiphilic copolymers	86
3.4.2. <i>In situ</i> aqueous click cycloaddition of the corona of micellar aggregates with POEGA 2.....	86
3.4.2.1. Synthesis of polystyrene macroinitiator via atom transfer radical polymerization	86
3.4.2.2. Synthesis of the ω -azido functional block copolymer PS- <i>b</i> -POEGA 1.....	87
3.4.2.3. Procedure for the synthesis of the α -alkyne functional homopolymer POEGA 2	87
3.4.2.4. Procedure for the aqueous click ligation of PS- <i>b</i> -POEGA 1 and POEGA 2	88
Chapter 4.....	89
Functionalization of polymer chain ends through methods other than CuAAC.....	89
4.1. Introduction	90
4.2. Chain-end modification of biocompatible polymers via a “metal-free” cycloaddition of nitrile oxides and alkynes	91
4.2.1. Nitrile oxide-alkyne cycloaddition (NOAC) reactions on α -alkyne-functionalized polymers....	93
4.3. Orthogonal modification of polymers chain-ends via sequential nitrile oxide-alkyne and azide-alkyne Huisgen cycloadditions.....	97

4.3.1. Synthesis of well-defined α -alkyne, ω -azido heterotelechelic polystyrene	98
4.3.2. Nitrile oxide-alkyne cycloaddition (NOAC) step.....	105
4.3.3. Copper-catalyzed azide-alkyne cycloaddition (CuAAC) step	106
4.4. Inducing some other α -functionalities in co/polymers synthesized by ATRP	107
4.4.1. Synthesis of protected α -amino functionalized co/polymer P(OEGMA-co-MEO ₂ MA).....	107
4.4.2. Synthesis of the α -aldehyde functionalized copolymer P(OEGMA-co-MEO ₂ MA)	109
4.5. Synthetic procedures.....	111
4.5.1. Chain-end modification of biocompatible polymers via a “metal-free” cycloaddition of nitrile oxides and alkynes.....	111
4.5.1.1. TMS-protected copolymer P(OEGMA-co-MEO ₂ MA) P1 by ATRP	111
4.5.1.2. Synthesis of the homopolymer P2 by ATRP	112
4.5.1.3. Nitrile oxide click reactions on polymer alkynes P1 and P2.....	112
4.5.1.4. 2-nitrobenzo nitrile oxide click reactions on polymer alkyne P1.....	113
4.5.2. Orthogonal modification of polymer chain ends via sequential nitrile oxide-alkyne and azide-alkyne Huisgen cycloadditions	114
4.5.2.1. Nitrile oxide-alkyne cycloaddition (NOAC) step.....	114
4.5.2.2. Copper-catalyzed azide-alkyne cycloaddition (CuAAC) step	114
4.5.3. Inducing some other α -functionalities in co/polymers synthesized by ATRP	115
4.5.3.1. Synthesis of ATRP initiator, 2-hydroxyethyl bromoisobutyrate (HEBB)	115
4.5.3.2. α -aldehyde copolymer of P(OEGMA-co-MEO ₂ MA)	115
4.5.3.3. t-Boc protected α -amino functionalized co/polymer P(OEGMA-co-MEO ₂ MA).....	116
Chapter 5.....	117
Activated ester-functionalized polymers	117
5.1. Activated ester derivatives as ATRP initiators	118
5.2. PEGylated chromatography: Thermoresponsive stationary phases for bioseparation.....	119
5.2.1. Functionalization of the Silica monoliths.....	120
5.2.2. Chromatographic performance of the P(OEGMA-co-MEO ₂ MA)-grafted stationary phases ..	121
5.3. Smart PEGylation of trypsin	123
5.3.1. Characterizaion of P(MEO ₂ MA-co-OEGMA ₄₇₅) copolymers	124
5.3.2. Polymer Conjugation of Trypsin.....	127
5.4. Characterization of the conjugates of MEO ₂ MA-OEGMA ₄₇₅ copolymers with trypsin	128
5.4.1. SDS-PAGE	129
5.4.2. Turbidimetry	132

5.4.3. Enzyme activity tests.....	133
5.5. Synthetic procedures	137
5.5.1. NHS-containing or activated ester initiators for ATRP.....	137
5.5.1.1. Synthesis of ATRP initiator N-succinimidyl-2-bromopropionate.....	137
5.5.1.2. Synthesis of the ATRP initiator <i>N</i> -Succinimidyl 2-bromo-bromoisobutyrate	137
5.5.2. Functionalization of Silica monoliths	138
Chapter 6.....	139
Summary and Outlook	139
Chapter 7.....	144
Analytical methods	144
7.1. Nuclear Magnetic Resonance (NMR)	145
7.2. Size exclusion chromatography (SEC)	145
7.3. Cloud point measurements (Turbidimetry)	145
7.4. FT-IR spectroscopy	145
7.5. Enzyme activity tests.....	146
References	147

Chapter 1

General introduction and scientific objectives of the thesis

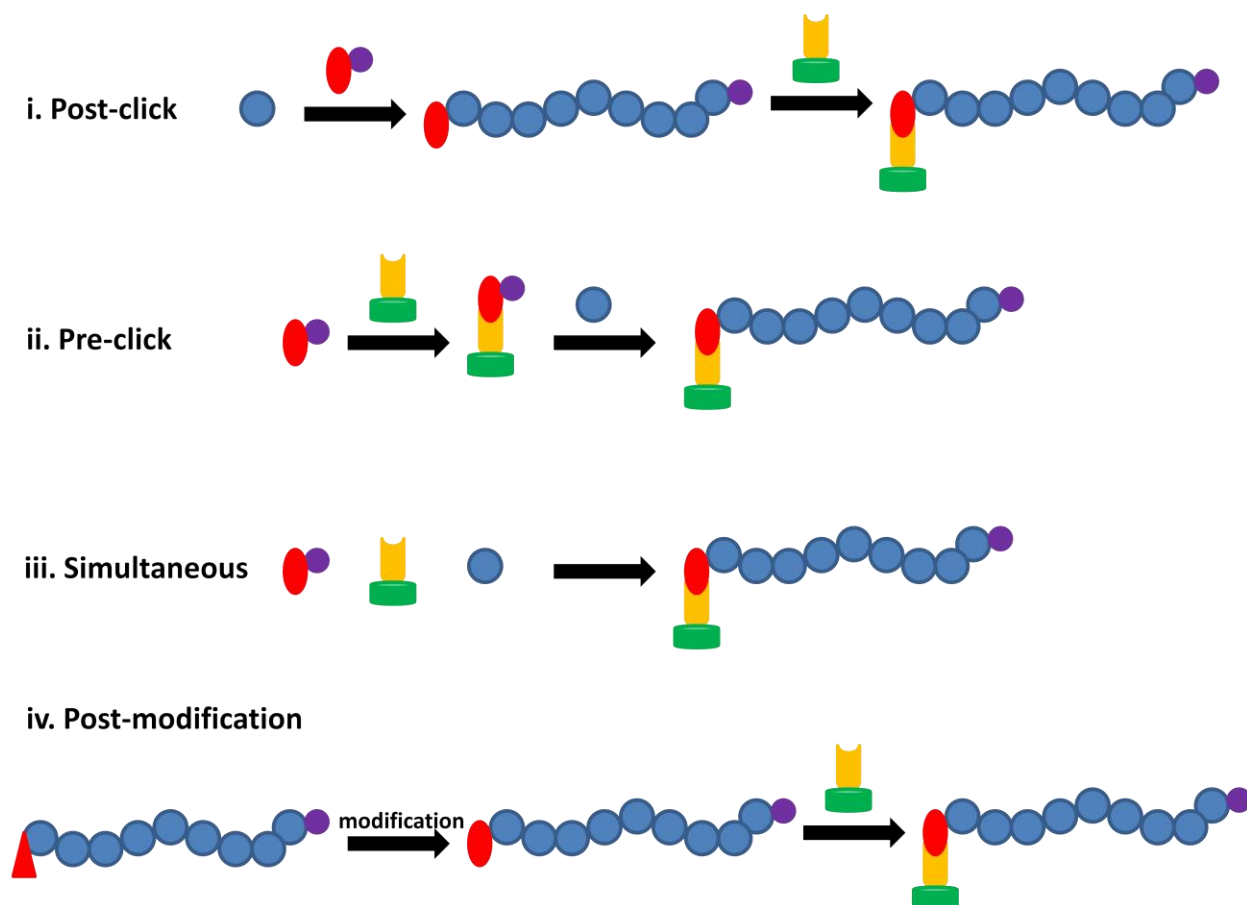
1.1. General Introduction

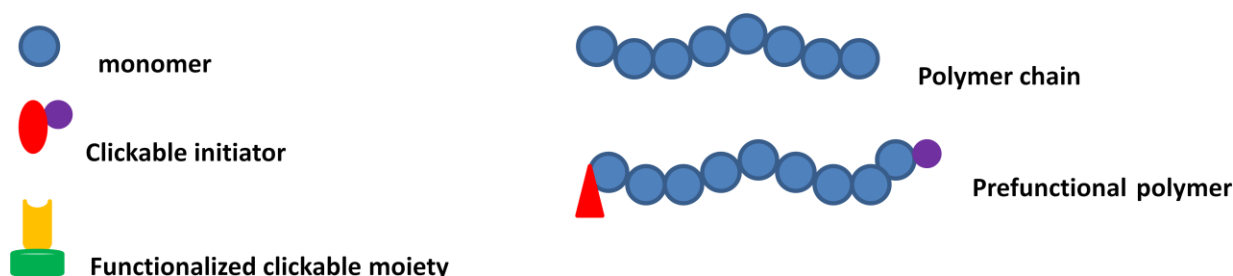
Functionalization of macromolecules at α - or ω - chain ends or side chains is an important challenge of polymer chemistry^{1,2}. Functionalization of polymers has found many applications for example in making telechelic polymers, surface modification, grafting onto approaches and bioconjugation. In many applications these functionalization should be selective and only at specific sites of the polymer molecule.

Functionality could be induced through pre-functionalized monomers and initiators or through end capping methods. However, in many cases functionality of monomer or initiator interferes with polymerization process and kinetics or causes side reactions to happen. Consequently, control over final polymer properties such as polydispersity, composition and structure becomes more difficult. In order to overcome this problem, functional groups may be protected. Nevertheless, combination of controlled radical polymerization (CRP) techniques such as Atom Transfer Radical Polymerization (ATRP), Reversible Addition-Fragmentation chain Transfer (RAFT) and Nitroxide Mediated Polymerization (NMP) with click- type efficient reactions in recent years has opened new opportunities for functionalization of well-defined polymeric structures^{3,4}. Furthermore, simple ordinary reactions of organic chemistry such as amidification or esterification in combination with CRP methods have been used to attach functional moieties on polymers at different sites.

“Click-type” reactions are particularly efficient for binding functionalities on polymers since these high-yielding reactions do not need harsh experimental conditions and often can be performed even in aqueous solution at room temperature. For performing a click reaction at the chain ends of a polymer, the α - and ω - ends of the polymers should have suitable functionalities. Click chemistry is indeed one of the approaches to couple two molecules containing complementary functionalities, each of them located on one of the species. In materials science, there are different methods to covalently joint or bind two species, in almost all of them useful functionalities should be induced on both molecules and efficient and easy chemical tools should be applied to couple these species. Functionalities could be on planar surfaces, particles, biomolecules, synthetic polymers, self-assembled aggregates in selective solvents and other species.

Different types of click reactions combined with CRP techniques have been used so far. The main strategies to combine CRP and click include pre-click, post-click, one pot/simultaneous approach and post-modification methods (scheme 1.1). Depending on the type of click reaction aimed for functionalization, different clickable moieties should be induced at α - and ω - chain ends or as pendant groups along the chains. Some of the most widely used click reactions include the copper-catalyzed azide-alkyne 1,3 dipolar cycloaddition (CuAAC)⁴, nitrile oxide-alkyne cycloaddition (NOAC)⁵, thiol-ene radical addition^{6,7,8}, thiol-yne radical addition^{9,10} Diels-Alder reactions (DA)^{11,12,13} and hetero Diels-Alder reactions (HDA)^{12,14}.

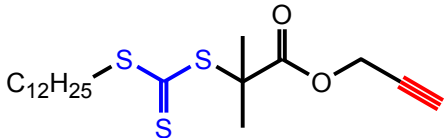
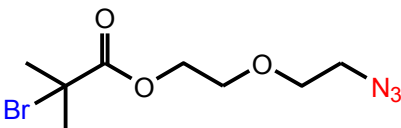
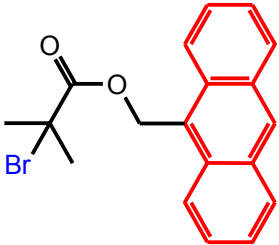
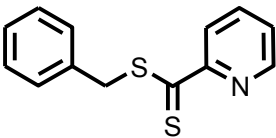




Scheme 1.1. Different strategies to combine CRP and click techniques to get well-defined functionalized polymeric structures. Here, only the α - chain end modification of the polymers are schematically displayed. (i) post-click: in this approach polymers are synthesized using functional initiators or monomers having clickable moieties. Clicking is performed after polymerization on the polymer molecules. (ii) Pre-click strategy: in this strategy functional clickable initiators or monomers are clicked before polymerization. (iii) Simultaneous strategy: CRP and click reaction occur at the same time during polymerization. (iv) Post-modification: in this method prefunctional polymers are synthesized by CRP and then modified with some clickable moieties to get clickable polymers.

In order to incorporate clickable moieties in a polymer chain, suitable clickable monomers, initiators or chain transfer agents should be used, depending on the type of the CRP method applied. In general, the initiator or chain transfer agent suitable for a controlled polymerization and consequent functionalization should consist of two fragments: i) a fragment designed so that a CRP reaction could happen, such as the halogenated part of the ATRP initiator or typical chain transfer agent (CTA) structure for RAFT, as in xanthates or trithiocarbonates and ii) a clickable fragment which is responsible for the click reaction, such as alkyne or azide groups for CuAAC or maleimide functionalities for Diels-Alder reactions. In Table 1.1 structures of some of these initiators/CTAs which have been applied in CRP/click approaches are shown.

Table 1.1. Structure of CTAs for RAFT and halogenated ATRP initiators used in a CRP/click approach. Segments shown in blue represent CRP-related part and segments in red show the clickable moieties. In the case of (RAFT polymerization-HDA click) CRP-related and clickable moiety are both located in the dithioester function.

Initiator/chain transfer agent	Polymerization method	Click strategy	References
	RAFT	CuAAC	15,16,17,18,19,20,21
	ATRP	CuAAC	22
	ATRP	DA	23,24,25,26,27
	RAFT	HDA	12

One of the challenges of functionalization of polymers is to develop easy and robust methods to perform it. In some cases, functionalization should be done *in situ* which might be inside the human body or on biological species which are sensitive to harsh temperatures and reaction conditions and additionally have many other functional groups which might interfere with the chemistry of functionalization reaction. At the same time, these reactions should be efficient enough and proceed at high yields in a short time scale²⁸.

1.2. Goals of the thesis

The above-mentioned reasoning shows the importance of research on click chemistry and click-type reactions to functionalize macromolecules for different goals. The motivation to do different projects of the present thesis was to try different types of straightforward reactions (click-type, amidification) in combination with CRP methods and discover the scope and applicability of these reactions in functionalizing well-controlled polymeric structures. The CRP technique applied in this work was ATRP. Co/polymers synthesized and utilized for further functionalization or modification steps were designed to be thermoresponsive to make the whole system “smart”. These graft co/polymers with oligo (ethylene glycol) side chains exhibit adjustable lower critical solution temperature (LCST) values in water^{29,30}. A typical structure of this category of co/polymers is shown in scheme 1.2.

In the third chapter of this thesis, copper-catalyzed azide-alkyne cycloadditions (CuAAC) were studied for the functionalization of thermoresponsive co/polymers. In order to study this concept, first a model low molecular weight functional molecule (propargyl alcohol) was chosen for *in situ* functionalization of micellar aggregates through CuAAC in water (scheme 1.2 (II).a). In this stage, click reaction conditions (catalyst system used, reaction time and temperature) were optimized. Two catalytic systems were chosen which were extracted from previous studies, namely CuSO₄/sodium ascorbate and CuBr/Bipyridyl (Bipy). For each catalytic system yield and efficiency of the click reaction was studied. After optimization of click conditions, synthesized co/polymers were functionalized with a high molecular weight molecule (polymer) to investigate the efficiency of the click method for clicking high molecular weight species, scheme 1.2 (II).b). It should be mentioned that the efficiency of a click reaction between two polymers is not expected to be necessarily as high as the efficiency of the same click reaction with the same conditions between a polymer and a low molecular weight molecule.

Another theme which was studied in the present thesis was to examine the catalyst (copper) free click reactions for functionalization of well-defined thermoresponsive polymers with some low molecular weight functional molecules (scheme 1.2 (II).c). This project was done in

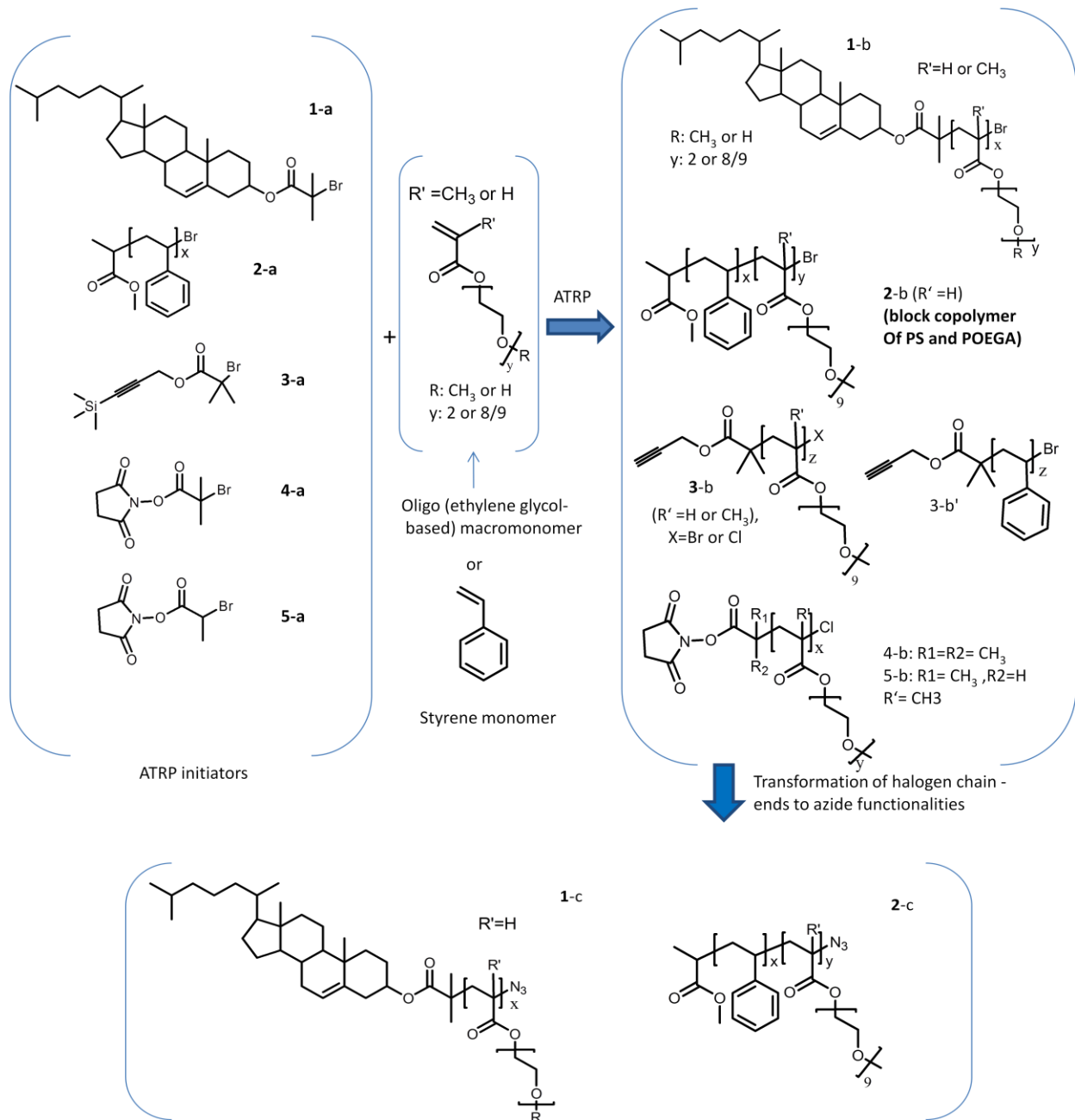
collaboration with research group of F. Heaney in Ireland. Because of the toxicity of many metal ions (e.g. copper), it is important to develop metal-free click methods, especially for biological or *in situ* applications. In order to remove metal catalyst, researchers have proposed different approaches. In this work, we chose metal-free 1,3-dipolar cycloaddition of nitrile oxide and alkynes (NOAC). First, co/polymers of oligo (ethylene glycol) methacrylates with an alkyne functionality at α position were synthesized. Then these polymers were clicked with some substituted model nitrile oxides. After investigating the efficiency of NOAC in functionalization of polymers with some model molecules, in a second collaboration project, the applicability of sequential nitrile oxide-alkyne (NOAC) and copper-catalyzed azide-alkyne (CuAAC) Huisgen cycloadditions for orthogonal modification of polymer chain-ends was tested (scheme 1.2 (II).d). First, α -alkyne, ω -azido telechelic polystyrene was synthesized, then α and ω chain ends of the polystyrene were modified by NOAC and CuAAC respectively in two consequent steps.

Another approach to modify polymeric structures is the insertion of activated ester functionalities along the chain or at the chain ends. These activated esters can then react with amino groups on other functionalized molecules. This strategy was used in two different projects in the present thesis. Oligo (ethylene glycol)-based thermoresponsive polymers with reactive ester chain ends were synthesized and characterized. In order to induce reactive ester functionality at α position of the polymers, N-hydroxysuccinimide (NHS) activated ester initiators (N-succinimidyl-2-bromopropionate and N-succinimidyl 2-bromo-bromoisobutyrate (scheme 1.2 (I) initiators 5.a and 4.a, respectively)) were used for polymerization.

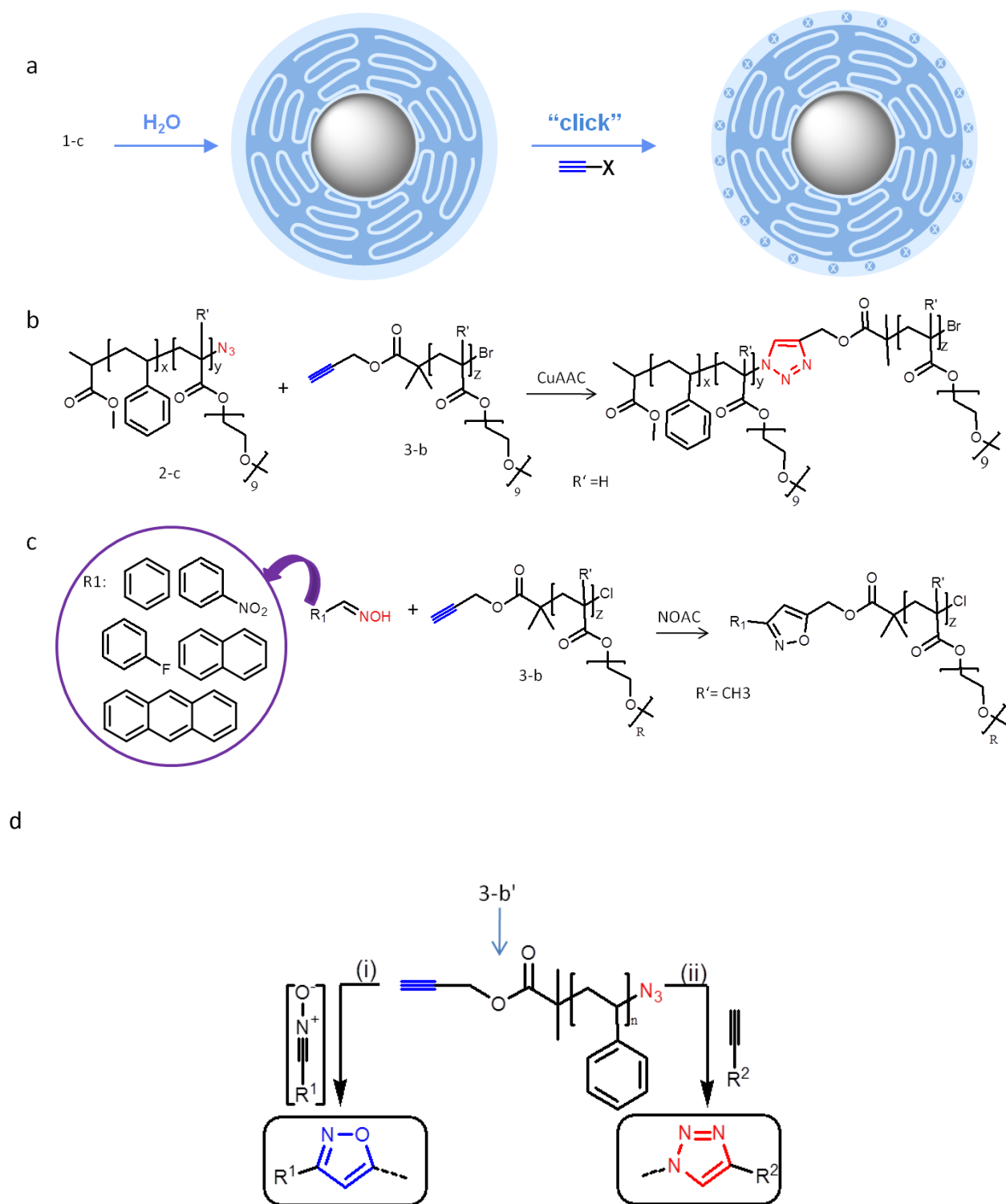
In the first project in collaboration with Max Planck Institute of Colloids and Interfaces, these polymers were grafted onto amino-functionalized silica monoliths to generate thermoresponsive stationary phases for chromatography (scheme 1.2 (III).e).

In the second work, these polymers were coupled to trypsin, which is a protein (scheme 1.2 (III).f). In this approach active ester chain ends of polymers were reacted with the amino groups of lysine residues of trypsin enzyme. The second project is an example of bioconjugation or coupling of synthetic polymers to biomolecules such as proteins. The polymers used for bioconjugation have adjustable LCSTs in the useful range of room to body temperature. Therefore, trypsin could be purified or recovered through precipitation at low temperatures

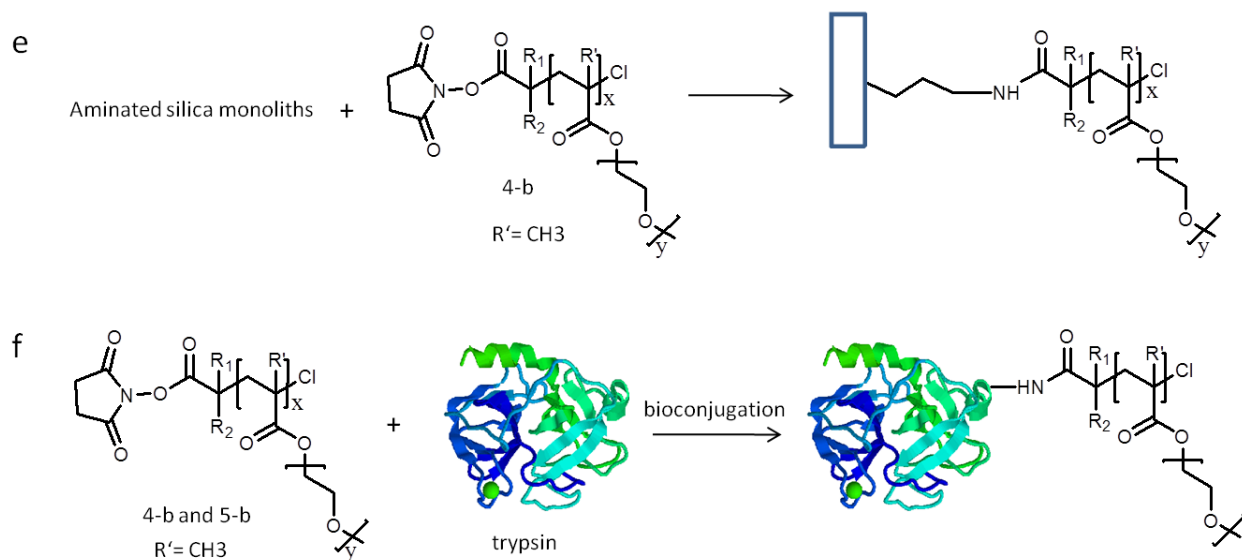
which is necessary for this enzyme to avoid its self-digestion. Moreover, the influence of bioconjugation on enzyme bioactivity was investigated.



Scheme 1.2 (I). Scheme of the different initiators and polymers used in this thesis. These polymers were functionalized further and applied in coupling and bioconjugation strategies. Copolymer **2-c** is the block copolymer of polystyrene and POEGA (PS-*b*-POEGA).



Scheme 1.2 (II). Scheme of the different approaches explored in this thesis, to investigate different chemical tools for functionalization of polymers, and further application of these polymers in coupling and bioconjugation strategies: copper-catalyzed azide-alkyne Huisgen cycloaddition (CuAAC) and nitrile oxide-alkyne cycloaddition (NOAC).



Scheme 1.2 (III). Scheme of the different approaches explored in this thesis, to investigate different chemical tools for functionalization of polymers, and further application of these polymers in coupling and bioconjugation strategies: N-hydroxysuccinimide (NHS) activated ester functionalized polymers applied for (e) making thermoresponsive stationary phases for chromatography and (f) polymer-trypsin bioconjugation.

Chapter 2

Theoretical part

2.1. Controlled polymerisation techniques

It is of much interest in polymer and materials science to get well-defined polymeric structures with controlled chain length, end-functionality and low polydispersity. To achieve this goal, different “living” polymerisation techniques have been developed. In a living polymerization process initiation should be fast and termination must be negligible so that almost all chains could grow simultaneously. For many years, most of the focus on living polymerisation methods was on anionic (discovered by Szwarc in 1956)^{31,32}, cationic and coordination polymerisations. These ionic methods, however, need strict reaction conditions and are sensitive to many functional groups and impurities and the number of monomers capable to be polymerised by these methods is also limited. Because of all these limitations, during last decades researchers have been trying to develop radical processes which behave close to ‘living’, these methods have the advantage of robustness of radical processes and at the same time can be well controlled.

2.2. Controlled Radical Polymerizations (CRP)

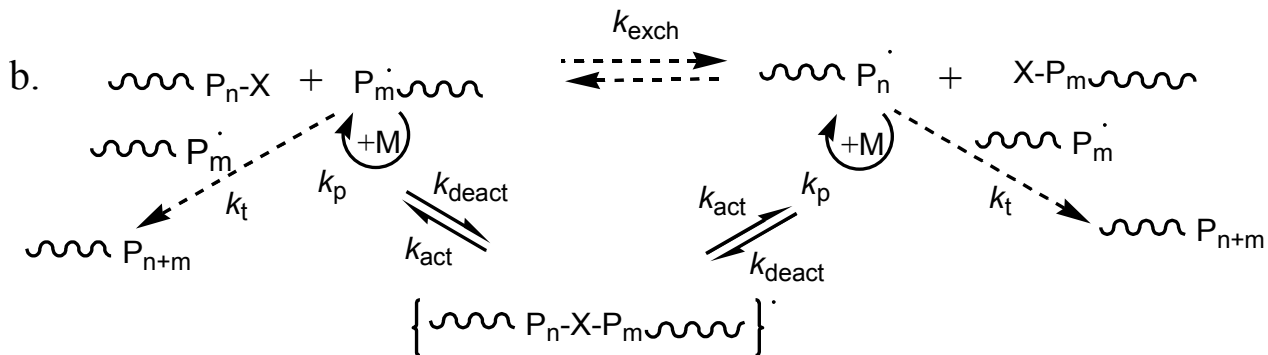
In free radical polymerisation (FRP) the highly active chain ends are radicals which can react easily with monomer, solvent, initiator or other chain ends via combination or disproportionation, so the control over molecular weight and molecular weight distribution is an issue here. To achieve control over FRP, new techniques of controlled radical polymerisations (CRP) have been developed in which the chain ends are reversibly deactivated. All of the CRP methods are based on establishing a rapid dynamic equilibrium between a minute amount of growing free radicals and a large majority of dormant species. The dormant chains may be alkyl halides, as in atom transfer radical polymerisation (ATRP) or degenerative transfer (DT), thioesters, as in reversible addition fragmentation chain transfer processes (RAFT), or alkoxyamines, as in nitroxide mediated polymerisation (NMP). Radicals may either be reversibly trapped in a deactivation/activation process (This mechanism relies on the Persistent

Radical Effect (PRE)³³), or may go through a “reversible transfer”, degenerative exchange process³⁴(Scheme 2.1.a and 2.1.b respectively).

A controlled radical polymerization process has some general features:

1. Polymerization rate (R_p) with respect to the monomer concentration ($[M]$) increases linearly with time (first order kinetics behaviour). First order kinetics is also observed in free radical polymerization (FRP) due to the “steady state”. In this state, the concentration of the active species ($[P^*]$) remains constant.
2. Degree of polymerization and molecular weight can be pre-determined, since the initiation is fast and termination and transfer can be almost ignored.
3. The molecular weight distribution is narrow, because the initiation rate is comparable to propagation rate, termination can be neglected and the exchange between species with different reactivity is faster than propagation.
4. The majority of chains remain active for long time, until almost all monomer is consumed. If monomer is added, polymerization can restart again (suitable for block copolymer synthesis).

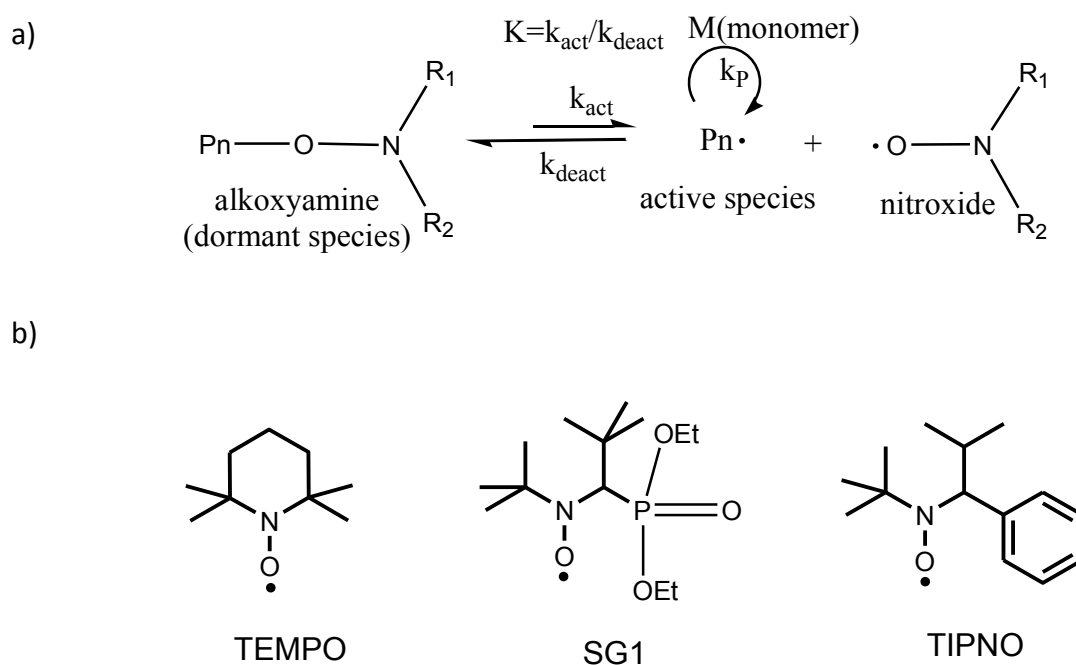
All the CRP methods include activation and deactivation steps (with rate constants k_{act} and k_{deact}). A general scheme of CRP methods is shown in Scheme 1.

reference³⁴.

2.2.1. Nitroxide mediated radical polymerisation (NMP)

propagating radicals and generates the dormant species ^{35,36}. Like other CRP methods, when the equilibrium between dormant and active species is shifted towards the dormant form, the

irreversible chain termination becomes negligible (scheme 2.3.a). This method is metal free and effective in the controlled polymerisation of a broad range of monomers. One of the first systems developed for NMP was the use of a bimolecular initiator which requires the combination of a free radical initiator as BPO or AIBN with a nitroxide (2,2,6,6-tetramethylpiperidinyloxy(TEMPO)). Georges *et al.* reported the controlled polymerization of styrene using BPO and TEMPO³⁷. NMP mediated by TEMPO was limited mainly to styrene and derivatives. Then, substituted TEMPO derivatives had been used for polymerization of acrylates. Later on, other types of nitroxides than TEMPO were developed to overcome limitations of the TEMPO mediated systems³⁸. Some examples of these nitroxides are shown in scheme 2.3.b. NMP has been carried out successfully in aqueous dispersed systems, especially in miniemulsion using N-(2-methylpropyl)-N-(1-diethylphosphono-2,2-dimethylpropyl)-N-oxyl (SG1) and 2,2,5-tri-methyl-4-phenyl-3-azahexane-3-nitroxide (TIPNO) or their derivatives as nitroxides^{39,40,41}.



Scheme 2.3.a) General mechanism of Nitroxide Mediated Radical Polymerization (NMP). b) different nitroxide structures useful for NMP.

2.2.2. Reversible addition-fragmentation chain transfer (RAFT)

RAFT polymerisation discovered by researchers at CSIRO in Australia, was reported in the late 1990s^{42, 43}. Around the same time researchers in France described a process operating through an identical addition-fragmentation chain transfer mechanism they named MADIX for Macromolecular Design by Interchange of Xanthate⁴⁴. These two techniques exploit an identical mechanism, but MADIX refers specifically to those polymerisations mediated by xanthates. RAFT includes systems using all other thiocarbonylthio mediating agents.

RAFT operates on the principle of degenerative chain transfer. The appropriate choice of a so-called RAFT chain transfer agent (CTA) plays a key role for a successful RAFT of a given monomer. These are mostly thiocarbonylthio compounds belonging to one of these general families: dithioesters (**A**), trithiocarbonates (**B**), xanthate (**C**), and dithiocarbamates (**D**) as shown in Fig. 2.1. The key structural properties of RAFT agents are the so-called Z and R groups. The Z group for dithioesters (**A**) can be alkyl or aryl functional group, such as CH₃ or phenyl. In trithiocarbonates (**B**) the Z group is an –SR functionality, in xanthates (**C**), an O-Y functionality, and in dithiocarbamates (**D**) an –NYY' species. The Z group determines the general reactivity of the C=S bond towards radical addition and affects the lifetime of the intermediate radical resulting from the addition of a radical species across the C=S bond. As a general rule, dithioesters are the most susceptible to radical addition. The structure of the R group allows for the fine tuning of the overall reactivity and effects polymerisation kinetics and the overall degree of control. The R group must be first of all a good free radical (homolytic) leaving group, and secondly, the radical generated from the homolytic dissociation must be able to initiate polymerisation.

One of the advantageous features of RAFT is the wide range of functional and non-functional monomers and reaction conditions applicable in this method⁴⁵. However, if not fully controlled, RAFT process can result in ill-defined polymeric structures. For example, in the case of block copolymer synthesis via RAFT by sequential addition of comonomers, the first polymeric thiocarbonyl thiol compound which is used to prepare the macro-CTA for the second

comonomer polymerization, must have a high transfer constant to the monomer in the subsequent polymerization. In other words the leaving ability of the first block should be comparable to that of the propagating radical of the second block, otherwise second block could not be produced or is not fully generated in a reasonable time⁴⁶. There are also other limitations and considerations regarding RAFT such as polymerization of monomers bearing primary or secondary amine groups or homogeneous aqueous RAFT limitations⁴⁵. In many cases, alternative methods such as coupling of two blocks by click chemistry or amidification are much more straightforward to produce block copolymers.

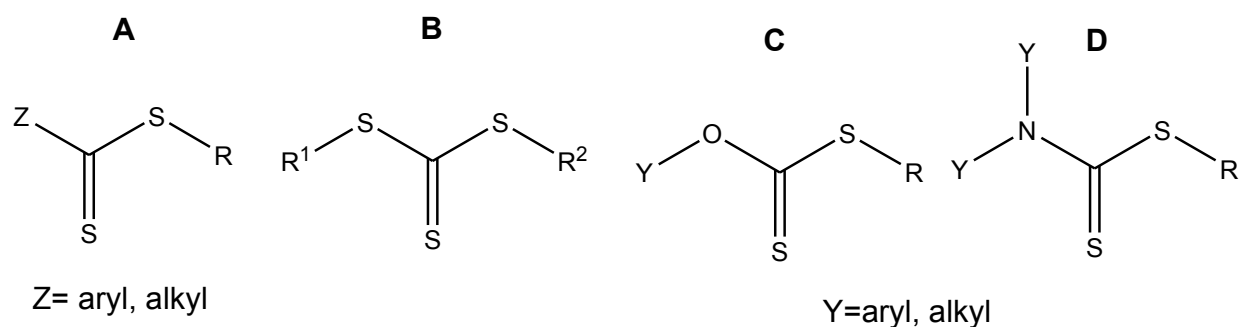
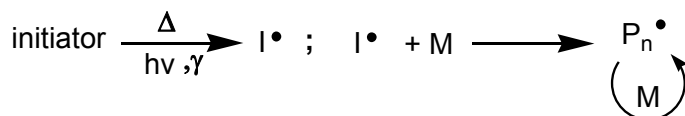


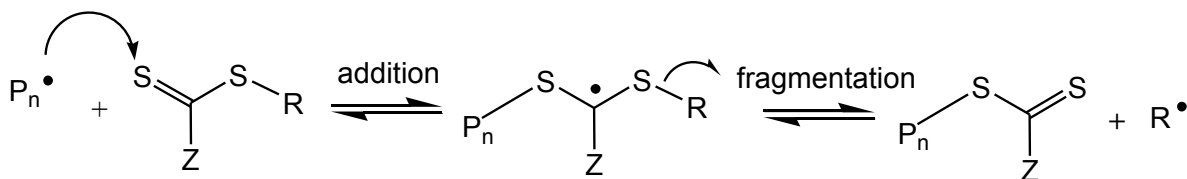
Figure 2.1. General structures of common thiocarbonylthio RAFT agents.

The general scheme of RAFT mechanism is shown in scheme 2.2. Like any other free radical polymerization method, the first step of RAFT is the radical generation step. For this step, traditional initiators such as AIBN are applied. Radicals can be generated by irradiation or heat (thermal initiation).

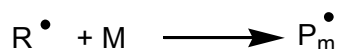
Radical generation



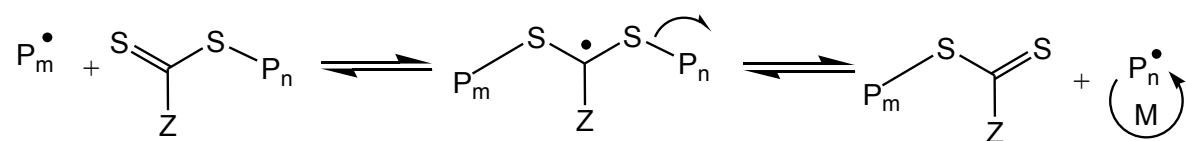
CTA activation/Addition/Fragmentation



Reinitiation



RAFT equilibrium



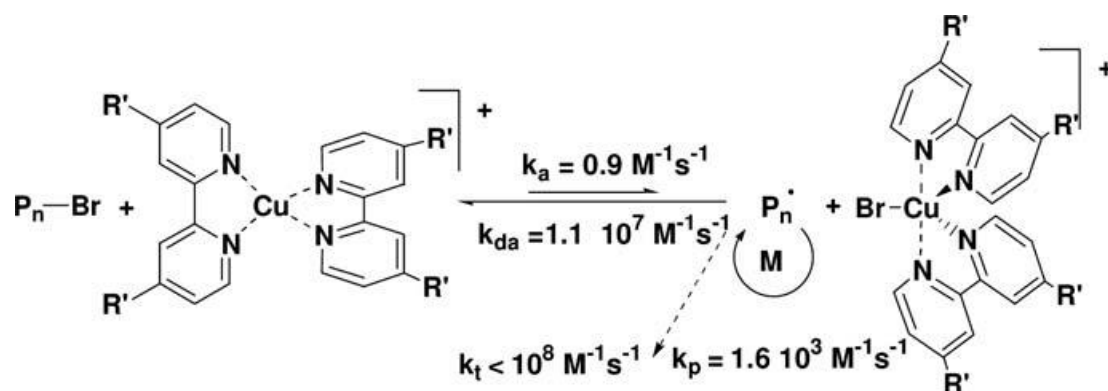
Scheme 2.2. General mechanism of reversible addition-fragmentation chain transfer (RAFT)

2.2.3. Atom Transfer Radical Polymerization (ATRP)

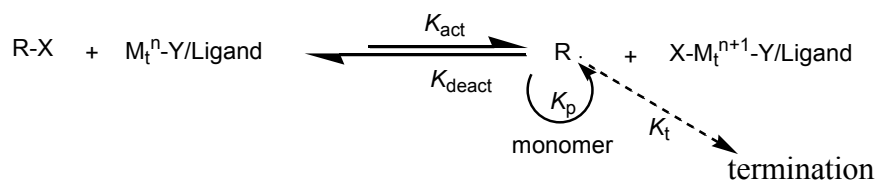
ATRP is based on the homolytic cleavage of an alkyl halide bond R-X (or macromolecular $\text{P}_n\text{-X}$), considered as the initiator, by a transition metal complex Mt_n/L (such as CuBr/bpy_2), considered as the catalyst (a representative example of this process is illustrated in Scheme 2.4). This reaction generates reversibly (with the activation rate constant, k_a) the corresponding higher oxidation state metal halide complex $\text{X-Mt}_{n+1}/\text{L}$ (such as $\text{CuBr}_2/\text{bpy}_2$) and an alkyl radical R^\bullet . The so-called active species or R^\bullet radicals propagate with monomer (k_p), terminate by coupling and/or disproportionation (k_t), or are reversibly deactivated by $\text{X-Mt}_{n+1}/\text{L}$ (k_{da}) (scheme 2.5). In a typical ATRP, termination reactions are insignificant due to the persistent radical effect. In the nonstationary stage and the beginning of the polymerization process, termination reactions occur and this increases the concentration of oxidized metal complexes (X-Mt_t^{n+1}), which act as

persistent radicals and decrease the stationary concentration of growing radicals R^\bullet , and consequently termination reactions. For a well-controlled ATRP, all polymer chains should grow simultaneously. In other words termination should be almost negligible, reversible deactivation should be rapid and initiation should be fast enough to produce an almost constant concentration of active species during the whole polymerization process. However when very high molecular weight polymers are targeted, termination and other side reactions become more pronounced.

In some alternative ways such as reverse ATRP or AGET (activators generated by electron transfer), deactivator in higher oxidation state (for example Cu^{II}) is used in the beginning of polymerization and lower oxidation state transition metal activator (for example Cu^I) is generated *in situ*. These ATRP techniques were developed to avoid the problem of catalyst oxidation, especially in large scale synthesis. In another type of ATRP called ARGET (activators regenerated by electron transfer) ATRP, the relative concentration of transition metal catalyst to initiator is much lower than in normal ATRP. Here, a reducing agent is used in excess to constantly regenerate the lower oxidation state of the transition metal (Cu^I) activating species.



Scheme 2.4. A representative example of ATRP process of styrene polymerization at 110°C , the illustration is taken from reference ⁴⁷.



Scheme 2.5. General Mechanism of Atom Transfer Radical Polymerization (ATRP)

In the absence of any side reactions other than radical termination by coupling or disproportionation, the magnitude of the equilibrium constant ($K_{eq}=k_a/k_{da}$) determines the polymerisation rate. If K_{eq} is too small, ATRP will not happen or will occur very slowly. If K_{eq} is too large, the resulting high radical concentration will lead to a large amount of termination and lack of control. Equation 2.1 shows that polymerization rate (R_p) is proportional to the ratio of concentrations of activator and deactivator ($[Mt_n/L]/[X-Mt_{n+1}/L]$), and also increases with the initiator concentration. It also shows that polymerisation rate is first order with respect to the monomer and initiator. Polydispersity decreases with monomer conversion (p) and concentration of deactivator as shown in equation 2.2^{48, 49}.

$$R_p = -d[M]/dt = k_p[M][P^*] = k_p[M](k_a[P-X][Mt^n/L]/(k_{da}[X-Mt^{n+1}/L])) \quad (2.1)$$

$$M_w/M_n = 1 + 1/DP_n + [(k_p[RX]_0)/(k_{da}[X-Mt^{n+1}/L])](2/p - 1) \quad (2.2)$$

2.2.3.1. ATRP monomers

Various monomers have been successfully polymerised via ATRP. Styrenes, (meth)acrylates), (meth)acrylamides, and acrylonitrile are typical monomers polymerised by ATRP. Each monomer has its characteristic atom transfer equilibrium constant. In the case of styrenic

monomers, polymerisation of monomers with electron withdrawing groups is faster because of the increased monomer activity and large propagation rate, and the decreased stability of dormant species, which both result in larger atom transfer constants. As a matter of fact, an electron-withdrawing substituent destabilizes the partial positive charge on the benzylic carbon and consequently the bond dissociation energy is decreased⁵⁰.

The order of the ATRP equilibrium constants of some typical monomers (acrylonitrile > methacrylates > styrene ~ acrylates > acrylamides > vinyl chloride > vinyl acetate) must be followed in order to prepare block copolymers efficiently³⁴. For example, in the case of methacrylate-based monomers the ATRP equilibrium constant is high and activation of the dormant species is easy. Due to the difference in the monomer nature and reactivity, the initiation efficiency in the ATRP of methacrylate monomer from less reactive macroinitiators such as acrylate or styrene-based macroinitiators is not high enough to give a monomodal distribution of molecular weight. However, to overcome this problem some methods like 'halogen exchange' approaches are applied. In this technique a macroinitiator in the form of alkyl bromide could be extended with a less reactive monomer by using a CuCl catalyst⁵¹.

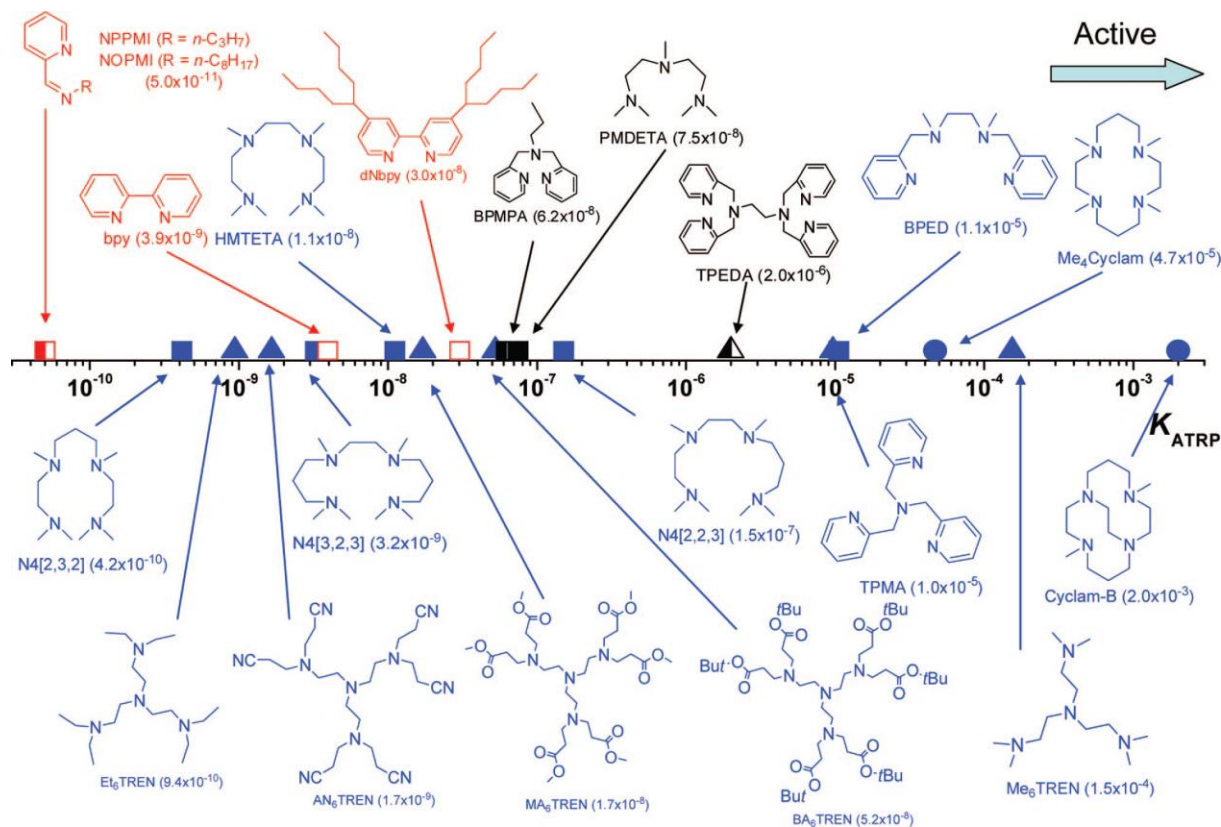
Three major categories of monomers are difficult to be polymerised using ATRP. The first class includes acidic monomers, because they can protonate ligands and prohibit the polymerisation to proceed. However there are some approaches like using less basic ligands, which can to some extent prevent loss of ligands. The second type of monomers, which cause problems when polymerised through ATRP, are monomers with very low intrinsic reactivity in radical polymerisations and often have very low ATRP equilibrium constants. This category includes halogenated alkenes, alkyl-substituted olefins, and vinyl esters. The third group of monomers which could cause problems in ATRP, are nitrogen containing monomers. In this case, monomer or polymer complexation to the catalyst makes them less reactive.

2.2.3.2. ATRP catalysts

Transition metal copper (Cu) complexes with polydentate N-containing ligands are one of the most efficient ATRP catalytic systems. The ligand adjusts the atom transfer equilibrium and

improves catalyst solubility. The catalyst becomes more active when the Cu^{II} state of the catalyst is better stabilized by the ligand⁵².

Some general rules describe the ligand structure-catalyst activity correlations: 1) the order of activities of complexes with various ligands is as the following: alkyl amine ~ pyridine > alkyl imine >> aryl imine > aryl amine; 2) the higher the number of carbon atoms between N atoms in ligand is, the less the activity of the catalyst is expected to be (C4 << C3 < C2); 3) topology of the ligand is another determining factor for activity (cyclic ~linear < branched). Halidophilicity, i.e., the affinity of the halide anion to the transition metal complex in its higher oxidation state is another factor, which influences ATRP equilibrium constant and catalyst activity. The activities of some typical N-based ligands for ATRP are compared in scheme 2.6⁵².



Scheme 2.6. ATRP equilibrium constants K_{ATRP} for various N-based ligands with the initiator ethyl 2-bromoisobutyrate (EtBrIB) in the presence of CuBr in MeCN at 22°C. Color key: (red) N2; (black) N3 and N6; (blue) N4. Symbol key: (solid) amine/imine; (open) pyridine; (left-half-solid) mixed; (O) linear; (4) branched; (O) cyclic. (scheme 2.6 is taken from the reference⁵²).

2.2.3.3 ATRP initiators

Different categories of initiators can be applied for ATRP. A good ATRP initiator should have a reactivity, which is at least comparable to that of the growing chains. In other words, the R-X bond should be more labile than the P_n -X bond. Normally, alkyl halides having inductive or resonance stabilizing groups are effective initiators to start ATRP. Clearly, all initiators are not suitable for polymerization of all monomers. Usually, initiators with structural similarity to the monomer to be polymerized have the good chance to be suitable for polymerization. For example, for polymerization of styrene, the most commonly used initiator is 1-phenylethyl halide⁵³. Generally, initiators having very low reactivity will result in uncontrolled ATRP and polymers with high polydispersities. Also very reactive initiators which produce many radicals in a short time increase the termination rate in early stages of polymerization and reduce the efficiency of initiation. They also generate too much of deactivating species and slow down the polymerization. Different categories of initiators used in ATRP include halogenated alkanes, benzylic halides, α -haloesters, α -haloketones, α -halonitriles and sulfonyl halides. When using alkyl halides as ATRP initiators, tertiary alkyl halides are better initiators than secondary ones, which are better than primary alkyl halides. The reason is that tertiary radicals are better stabilized than secondary and primary radicals. Halogen end groups resulting from ATRP can be converted to other functional groups by different synthetic ways. They can be replaced either directly by other functionalities (e.g. substitution of halogen with azide group), or can react with other molecules having complementary functionalities in their structure.

2.3. ATRP as a convenient way to induce functionality

ATRP is a robust and efficient CRP method, through which well-defined polymers with controlled topology (linear, star, comb/brush, network/crosslinked or dendritic/hyperbranched macromolecules), composition (homopolymers, random or alternative copolymers, block copolymers, graft copolymers and gradient copolymers) and functionality (side chain or chain-

end functionalities, telechelic polymers or multifunctional macromolecules) can be pre-designed and prepared¹.

By using ATRP as the polymerisation method, not only functional monomers can be polymerised and as a result polymers with pendant functional groups are prepared, but also end-groups of the polymers can be well controlled. Because of the “living” characteristics of ATRP, this method can be used to obtain block copolymers: since the proportion of terminated chains can be often neglected (in a well-controlled ATRP, less than 5% of the chains are terminated), most of the chains still contain halide end-functionality at ω -position to be used as potential macroinitiators for another ATRP or any other CRP method (grafting from approach). Suitable end-functionalities can be introduced also at α -position of the polymer chains through functionalities of the ‘R’ side of the ATRP initiator. Eventually by direct reaction of these functional groups or by converting them into other end groups, one can take the advantage of many organic reactions to couple synthetic polymers or biomolecules to the synthesized polymer to prepare block copolymers or bioconjugates (grafting to approach). As an example, by using initiators containing activated ester groups like N-hydroxysuccinimide (NHS), it is possible to prepare polymers having an activated ester end group, which is well-suited to react with the amine functionality to form an amide bond under mild reaction conditions. The amine group can be on a biomolecule, as in peptides, and therefore this method opens new approaches for covalent attachment of synthetic polymers with biological polymers⁵⁴. Different NHS containing ATRP initiators have been synthesized, as N-hydroxysuccinimide-2-bromo-2-methylpropionate which was used as a successful ATRP initiator for the polymerisation of styrene⁵⁵, or N-hydroxysuccinimide-2-bromopropionate was used as initiator for the living copolymerization of poly (ethylene glycol) methyl ether methacrylate (PEGMA₄₇₅) and hostasol methacrylate (HMA)⁵⁶.

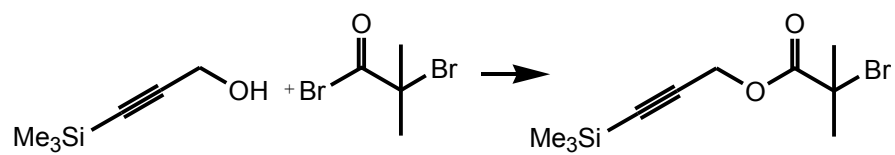
2.3.1. Various initiators to induce some typical α -functionalities

For typical ATRP monomers (styrene, (meth) acrylates), different initiators with appropriate efficiencies are used. A wide range of ester group- containing initiators can be derived from the

esterification of substituted moieties bearing targeted functionalities with 2-bromoisobutyryl bromide or 2-chloroisobutyryl chloride (scheme 2.7) ⁵³.

In table 2.1 some examples of functionalized ATRP initiators are illustrated. For example, initiator 2 bears a t-Boc protected amino group, which can react with maleic anhydride groups of other molecules after polymerization and deprotection. In another example (initiator 3), the pyridyl disulfide functionality bound to the initiator makes it reactive to thiol groups on other molecules after polymerization. Some of these initiators (4,5,6,7) contain end groups which could go through click-type reactions with other species after polymerization. Initiators incorporating an α -aldehyde end functionality or activated ester derivatives in α position have been also synthesized ^{57,56,58,59}. These end functionalities are reactive towards amine groups of other molecules. A typical example of initiator with active ester end group is initiator 8. Depending on application, many other types of functionalized initiators for ATRP could be designed and synthesized. These initiators should be also efficient for the polymerization of the monomers used. For instance, polymerisation of MMA initiated by cholesteryl 2-bromoisobutyrate (to induce cholesteryl functionality) or polymerisation of styrene or MMA with a range of functionalized phenolic esters derived from esterification of substituted phenols with 2-bromoisobutyryl bromide or 2-chloroisobutyryl chloride can be mentioned ⁶⁰. In order to get acidic α -functionality, protected α -halocarboxylic acid and carboxylic acid initiators with remote halogens can be used, since unprotected carboxylic groups can go through intramolecular cyclization reactions with monomers like styrene. In order to obtain epoxy and hydroxyl end-functionalities, one can use allyl bromide or allyl chloride initiators and the transform them to epoxy or hydroxyl groups.

Multifunctional initiators can be synthesized from molecules with multiple reactive sites which can be further converted to ATRP initiating sites. Examples of multifunctional initiators are bifunctional ATRP initiators obtained from ethylene glycol reacted with 2-bromopropionyl bromide ⁶¹, four-armed star initiators derived from pentaerythritol and six-armed star initiators such as hexakis (bromomethyl) benzene, which is used to synthesize six-armed star polystyrene⁶².



Scheme 2.7. Synthesis of a trimethylsilyl (TMS) protected alkyne functionalized ATRP initiator by esterification. Reagents and conditions: a) Et_3N , THF, 0°C ; b) room temperature, 1h, 93%⁶³.

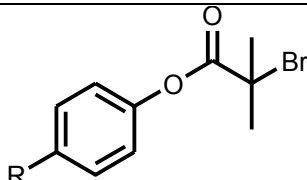
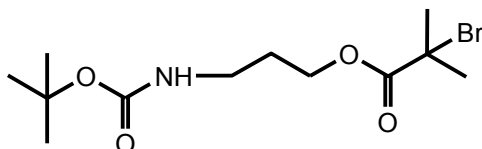
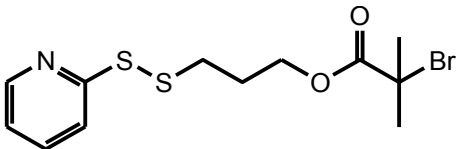
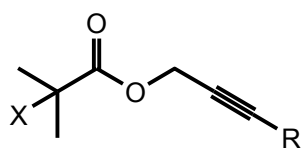
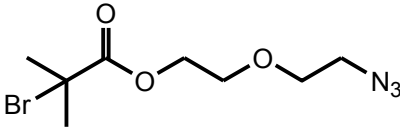
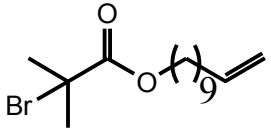
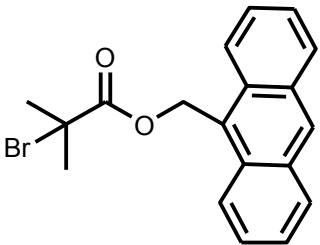
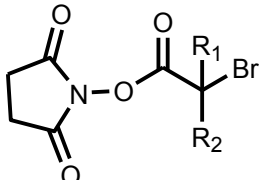
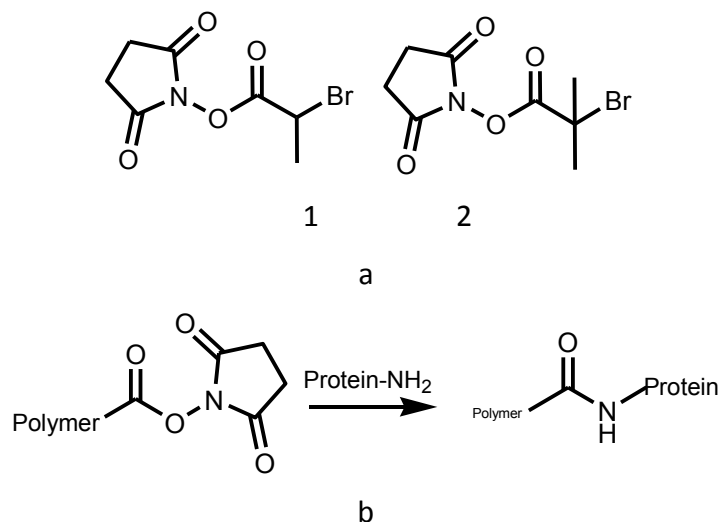
	ATRP initiator	comments	reference
1		R=H, NH ₂ , NO ₂ , CHO, OCH ₃ ,...	60
2		t-Boc protected amine	64
3		pyridyl disulfide for bioconjugation	65
4		X=Br, Cl R= TMS, TIPS, H for 3+2 dipolar cycloaddition	63, 66,67, 68,69, 70,71, 72
5		Used for CuAAC	22
6		for Thiol-ene reaction	73
7		for Diels-Alder reaction	27
8		R ₁ =R ₂ =CH ₃ or R ₁ =CH ₃ and R ₂ =H for coupling to amines	56,58,59

Table 2.1. Some examples of functionalized ATRP initiators

2.3.2. Activated ester containing initiators

One of the important categories of functional ATRP initiators is activated ester derivatives. These initiators make the α position of the polymers reactive towards amine functionalities existing e.g. on proteins and biomolecules or on synthetic polymers or low molecular weight species for post-functionalization. Activated ester derived initiators are very useful for covalent linking of amine and carboxylic acid groups and forming amide bonds ⁵⁹.

Ringsdorf and coworkers and Ferruti et al. did pioneering research in the field of polymers based on activated esters in 1972 ^{74,75}. Later, in other research groups e.g. of D.Haddleton, N-succinimidyl ester functionalized initiators were synthesized and used further for ATRP of various monomers such as poly (ethylene glycol) methyl ether methacrylates ^{56,58}. Then, the polymers obtained were reacted with amine groups on the protein molecules (bioconjugation). The structures of some N-hydroxy succinimide (NHS) based initiators (1 and 2) and their reaction with amine groups on proteins is shown in scheme 2.8.



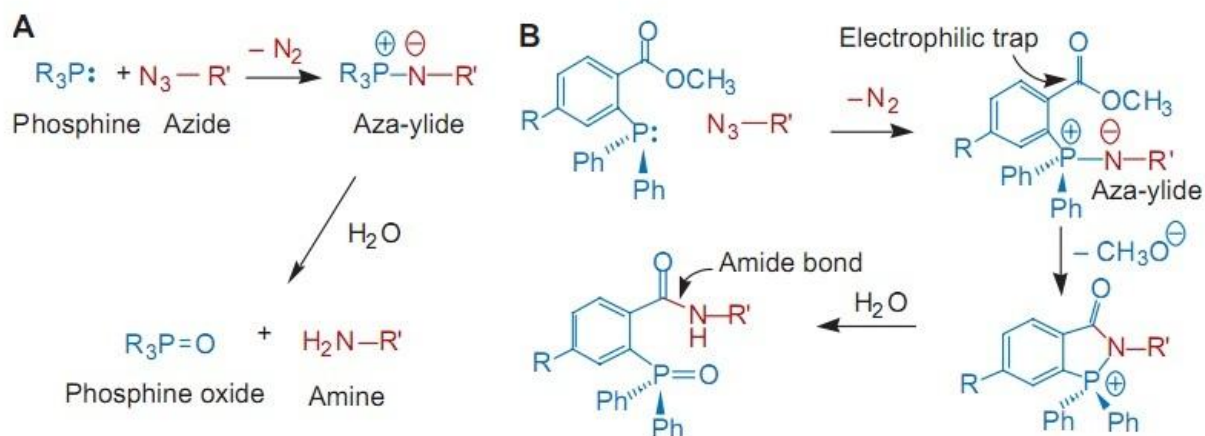
Scheme 2.8. a) Structures of N-hydroxy succinimide activated initiators (1 and 2), b) schematic reaction of NHS-activated polymers with amine groups of proteins

2.4. Different approaches to induce ω -functionalities in polymers synthesized by ATRP

After synthesis of well-defined polymers by ATRP, one can transform the halide end group into other functionalities by several procedures. For further functionalization of the polymers through ω chain ends (to prepare telechelic or block copolymers for example), It is important to have enough halogenated chain ends still existing on the polymer chains after ATRP, so normally in order to do further chemistry on the ω chain ends, it is common to stop the polymerisation at lower conversion (below 90% conversion)⁷⁶. It was shown that at this low conversion, other side reactions such as elimination reaction is negligible⁷⁶.

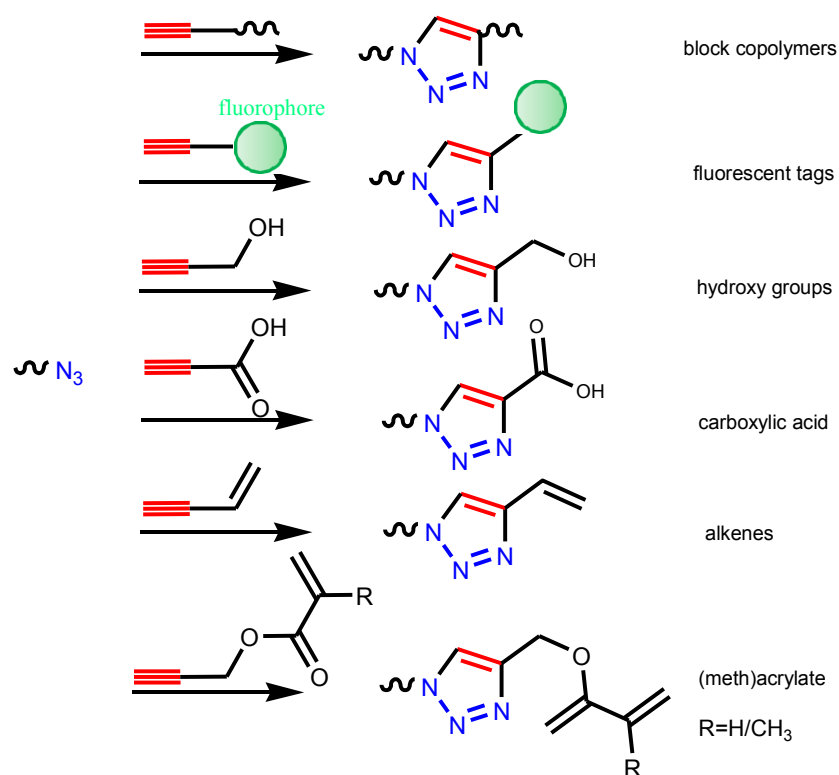
One example for chain end transformation is the nucleophilic substitution on the halogenated chain ends. Amidst the examples of nucleophilic substitution, one can mention the substitution of bromine end groups with primary amines to insert additional functionalities, like reacting poly (St-Br) with excess of ethanolamine at room temperature to get hydroxyl end functionality. Another example is the replacement of bromine end group by acetate in DMSO, adding a 25-fold excess of sodium acetate.

A typical nucleophile often used is sodium azide that converts the halogen end group to azide end functionality. Azide end groups are interesting, because they can be further converted into different other functionalities like amino groups. Alternatively, azide group could selectively act as a reactive functional group towards a limited number of reactants. Moreover, azide functionality is almost absent in most of the biological molecules and this results in bioorthogonality. As an example, the Staudinger ligation reaction of azide and phosphine to produce aza-ylide can be cited^{77,78,79}. Nevertheless, the aza-ylide adduct is not stable in water, and therefore, this method is not applicable in many biological media. Saxon and Bertozzi solved this problem by designing a new type of phosphin which enables rearrangement of the unstable aza-ylide (scheme 2.9). In the structure of this phosphin derivative an electrophilic trap such as a methyl ester group is designed so that the phosphin goes through an intramolecular cyclization with the nucleophilic aza-ylide and a stable amide bond is generated as the result⁷⁷.



Scheme 2.9. (A) The classical Staudinger reaction of phosphines and azides. Hydrolysis of the produced aza-ylide generates amine and phosphine oxide. (B) Modified Staudinger reaction which produces an amide-bond containing adduct, which is stable in water (scheme 2.9 is taken from the reference ⁷⁷).

The Huisgen 1,3 dipolar cycloaddition of azides and alkynes is another efficient reaction of azide-functionalized species. The efficiency and applicability of this ‘click’ type reaction, has made the nucleophilic substitution of halogen end groups of polymers with azide functionality even more popular. The concept of click chemistry was introduced by Sharpless and coworkers in 2001 ^{3, 80}. Shortly after the introduction of this general concept, polymer scientists took this idea and tried to use it as a tool in materials science. Even though other classes of chemical reactions can be categorized as ‘click’ reactions, the above-mentioned example has been used more often in materials science. Employing this type of click chemistry makes it possible to obtain a lot of end-functionalities in a more convenient way. For this approach halogen end functionality on the polymer is first converted to azide and the polymer is then reacted via 1,3 dipolar cycloaddition with another moiety having one alkyne end group and a functionality at the opposite end, which is going to be the final end group of the polymer (scheme 2.10). This type of click chemistry will be applied and discussed in detail in the next chapters.



Scheme 2.10. End functionalization of polymers using azide-alkyne cycloaddition with polymers (to make blocks), fluorophores, hydroxyl, carboxyl, vinyl, and (meth)acrylate groups

2.5. Click Chemistry

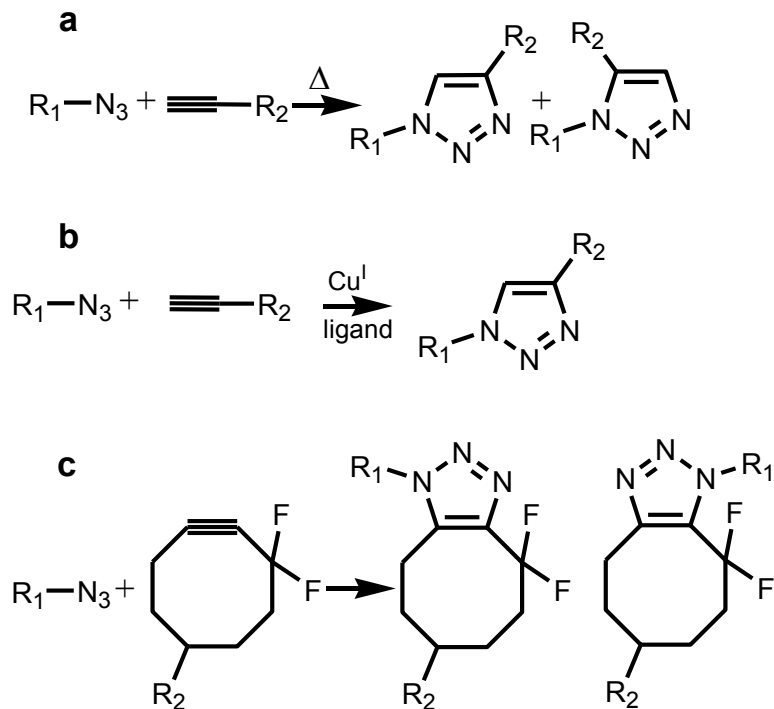
The concept of click chemistry was first proposed by ‘Sharpless’ in 2001³. A set of stringent criteria that a process must meet to be considered as a ‘click’ type reaction has been defined by Sharpless *et al.*, as reactions that: *“The reaction must be modular, wide in scope, give very high yields, generate only inoffensive byproducts that can be removed by nonchromatographic methods, and be stereospecific (but not necessarily enantioselective). The required process characteristics include simple reaction conditions (ideally, the process should be insensitive to oxygen and water), readily available starting materials and reagents, the use of no solvent or a solvent that is benign (such as water) or easily removed, and simple product isolation. Purification-if required- must be by nonchromatographic methods, such as crystallization or distillation, and the product must be stable under physiological conditions.”*³.

Typical examples of click reactions include Diels-Alder cycloaddition, thiol-ene additions, and copper catalysed Huisgen azide-alkyne cycloadditions (CuAAC). All of the click-type reactions

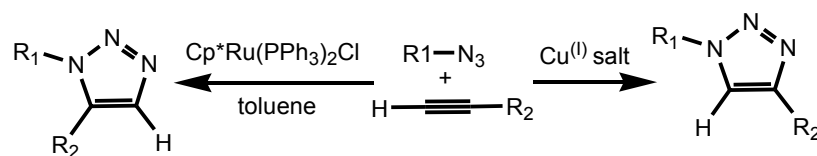
have the following characteristics in common: simplicity (mild and benign reaction conditions, simple workup and purification procedures) and efficiency (often giving quantitative yields). Although “click” toolbox includes different types of “simple” and “efficient” reactions ⁸⁰, the term click has been mostly restricted to the CuAAC in the literature. CuAAC is the copper catalyzed reaction of azides and terminal alkynes, which results in the formation of 1,2,3-triazoles. The Huisgen type of cycloaddition of azides and alkynes in the initial form that he proposed was without the use of catalytic transition metal and therefore was not regioselective (producing mixtures of the 1,4- and 1,5-regioisomers), and additionally this reaction was so slow that required high temperatures to get an acceptable yield (scheme 2.11.a). In 2002, Meldal and coworkers reported the use of catalytic amounts of copper(I), which resulted in fast, highly efficient and regioselective cycloaddition (1,4-regioisomer) at room temperature in organic media. (scheme 2.11.b) ⁸¹. Later, Sharpless and Fokin reported the CuAAC in polar media, such as *tert*-butyl alcohol, ethanol and pure water ⁸². For regioselective synthesis of 1,5-disubstituted 1,2,3 triazoles from azides and internal or terminal alkynes, a ruthenium(II)-based complex was used as catalyst ^{83,84} (scheme 2.12).

There has been a growing number of publications and research work of applying click chemistry in different areas, such as materials science, biomaterial synthesis (hydrogel, microgel), dendrimer synthesis, inorganic and organic chemistry, polymer chemistry, drug discovery, bioconjugation and many other branches of biochemistry ^{85,86,87,88,89,70}. For example, CuAAC has been used to couple end-functionalized polymers to modularly synthesize block copolymers. Opsteen and Hest coupled blocks of PEG and ATRP-derived polystyrene and poly(methyl methacrylate) to give A-B diblock or A-B-A triblock copolymers ⁶³. Azides and alkynes can be introduced easily into the molecules and are stable and inert to most organic and biological conditions. Click cycloaddition has shown to be relevant for biological applications, mostly because this reaction can be performed in pure water and at room or body temperature and doesn't need harsh conditions to proceed. Simultaneously, even in these mild conditions, very high yields are obtained. Moreover, since this reaction is very chemoselective and considering that in biological systems different functionalities exist, but rarely azide and alkyne ones, these two reactive groups are inert to other functionalities and in the presence of copper catalyst

react only with each other. Therefore, many protection/deprotection steps in biological reactions are unnecessary. Additionally, the triazole ring formed is thermally and hydrolytically stable in aqueous media. All of these features make CuAAC a very suitable synthetic tool for functionalization or ligation of biological species. Nevertheless, in many cases, *in vivo* and *in vitro*, the presence of transition metal catalysts in biological world might be an issue. For example, if CuAAC should be applied *in vivo*, copper in more than trace quantities would be toxic for living organisms. Because of this limitation of transition-metal catalyzed click cycloaddition, researchers have been trying to develop other “metal-free” or specifically “copper-free” cycloaddition methods which will be discussed in the following paragraphs.



Scheme 2.11. a. Thermal Huisgen cycloaddition of azides and alkynes. b. Copper-catalyzed Huisgen cycloaddition of azide and alkyne performed at room temperature. c. Copper-free cycloaddition of strained cyclooctynes and azides at room temperature.

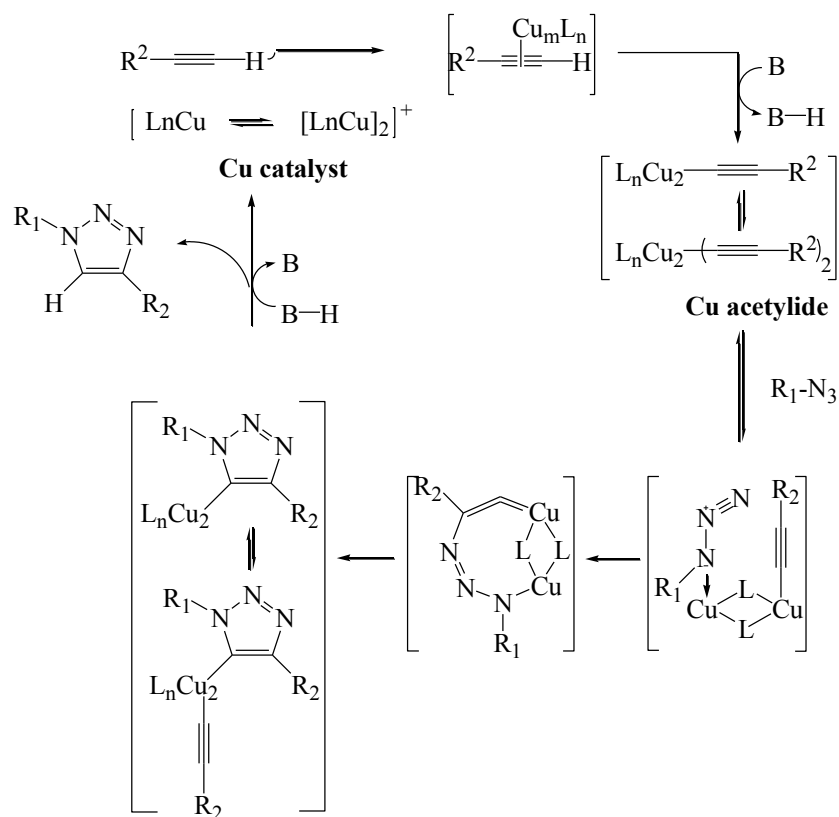


Scheme 2.12. Control of regioselectivity in 1,3 dipolar cycloaddition of azides and alkynes through catalyst selection: Cu(I) catalyzed cycloaddition produces 1,4-regioisomer, while Ru-cyclopentadiene complex catalyst generates 1,5-disubstituted triazole, Ph:phenyl, Cp*:cyclopentadienyl. Scheme 2.12 is taken from the reference⁸⁴.

2.5.1. Mechanism of copper-catalyzed alkyne-azide cycloaddition

The mechanism of Cu (I) catalysed alkyne-azide cycloaddition is not yet fully understood, however, a stepwise mechanism beginning with the formation of Cu(I) acetylide species through the π complex is proposed⁹⁰. The mechanism of the catalysed cycloaddition is shown in scheme 2.13. Electron-withdrawing substituents on the alkynes accelerate the cycloaddition. Since some kinetic studies show that the rate of the catalytic process is of second order for copper while one copper generates Cu(I) acetylide, it is suggested that the second copper atom activates the azide functionality in a dimer (scheme 2.13).

To produce a source of Cu(I) to catalyse the cycloaddition reaction, different ways are suggested: Cu(I) can be directly obtained from Cu(I) salts, or by reduction of a Cu(II) salt such as Cu(II) sulfate pentahydrate by e.g. sodium ascorbate. Another method to produce Cu(I) catalyst is by oxidation of Cu metal.



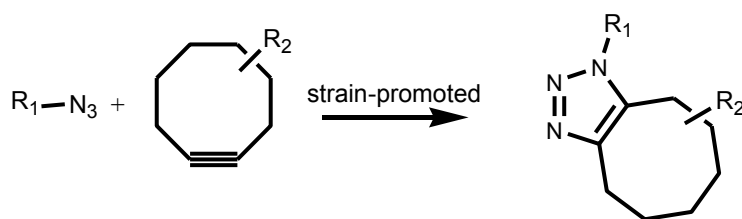
Scheme 2.13. Proposed mechanism of copper-catalyzed alkyne-azide cycloaddition⁹⁰

2.5.2. “Metal-free” click strategies

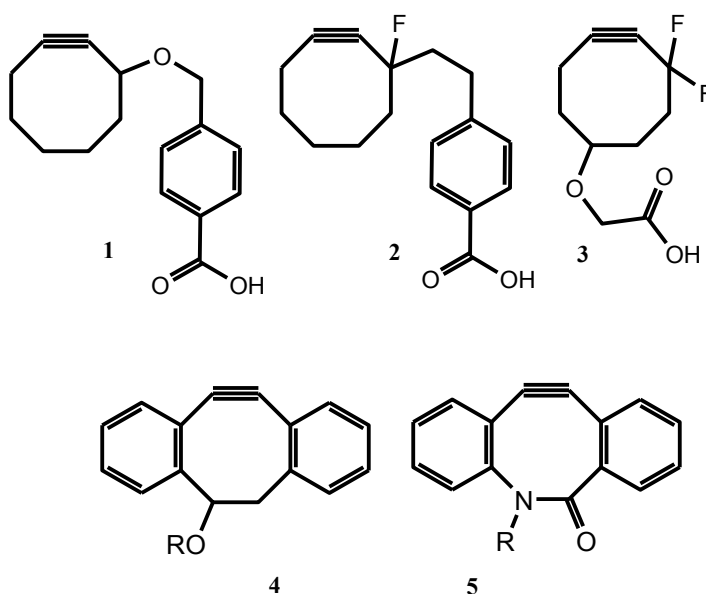
In recent years different metal free click strategies have been developed^{30,91}. In most of the approaches, the combination of ring strain and electron deficiency of alkyne moieties and use of electron rich azides and/or elevated temperatures are applied to compensate for the lack of metal-catalyst. For example, Cornelissen and coworkers investigated the metal-free cycloaddition of azides and oxanobornadienes instead of substituted alkynes; however this method results in the formation of furan which is a toxic byproduct⁹². In another example, Ju et al. increased the click reaction temperature up to 80°C⁹³. In another synthetic protocol, they used alkynes with at least one electron-withdrawing neighboring group to achieve reaction with azide at room temperature in water⁹⁴.

Another interesting copper-free azide-alkyne cycloaddition strategy was proposed by Bertozzi and coworkers^{95,96,97,98}. Following the early studies of Wittig and Krebs⁹⁹ they used strained cyclooctynes (scheme 2.11.c) in which the alkyne bond goes through a geometrical deformation due to the high ring strain. Bertozzi research group introduced different generations of substituted cyclooctynes (scheme 2.14.b). The first compound **1** undergoes copper-free click cycloaddition successfully with both azide-functionalized low molecular weight model molecules and biomolecules and living cells, nevertheless, the click cycloaddition in this case is slow. In order to improve the kinetics of copper-free click cycloadditions, next generations of substituted cyclooctynes were introduced by Bertozzi. In these cyclooctynes, electron-withdrawing substituents such as fluoro substituents were introduced in the α -position of the alkyne group (scheme 2.14.b, **2,3**). The cycloaddition of difluorinated cyclooctynes (DIFO, scheme 2.14.b, **3**) was very fast and efficient and applicable for functionalization of mammalian cells with fluorescent dyes within minutes. While the fluorine substituents increase the click rate through electronic effects of the alkyne, Boons and coworkers found another way to enhance the rate of click, i.e. via increasing strain energy¹⁰⁰. They used dibenzocyclooctynes (DIBO, scheme 2.14.b, **4**) which are stable, but undergo successful rapid copper-free click cycloaddition. Recently, Bertozzi research group developed a new class of substituted cyclooctynes, biarylazacyclooctynone (BARAC, scheme 2.14.b, **5**), which are more easily synthesized when compared to the previous cyclooctynes studied in their group¹⁰¹. In general, copper-free cycloaddition strategies open new doors in bioorthogonal chemical reactions e.g. for tagging and visualizing biomolecules¹⁰².

a)



b)



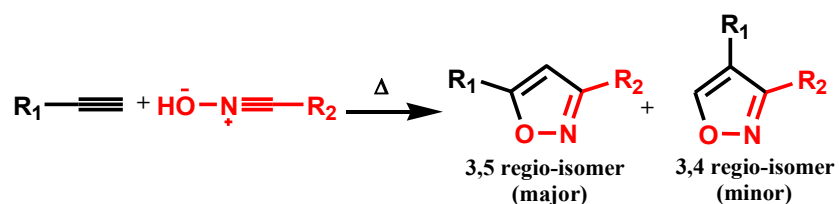
Scheme 2.14. a) strain-promoted [3+2] cycloaddition of azides and strained cyclooctyne derivatives b) Molecular structures of different substituted cyclooctynes used for copper-free cycloaddition with azides^{95,96,97,98}.

2.5.3. Metal-free nitrile oxide-alkyne Huisgen cycloaddition

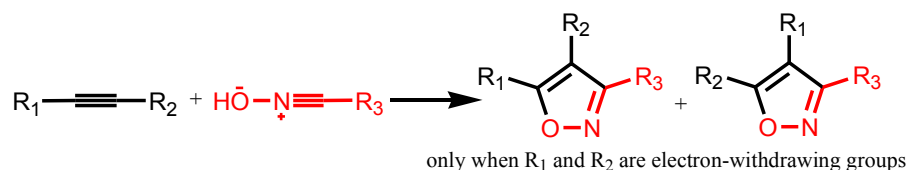
Another type of dipolar cycloaddition reaction which could be interesting especially in biological sciences is the Huisgen cycloaddition of nitrile oxides (as the dipole) and alkynes, which results in the synthesis of a five-membered nitrogen heterocycle, i.e. an isoxazole ring. The isoxazole ring is indeed embedded in many pharmaceutical and bioactive compounds^{103,104}. Some advantages of nitrile oxides as 1,3-dipoles for click cycloaddition over their azide counterparts are listed in the literature¹⁰⁵. For example, a dipole is formed *in situ* easily by using suitable dipole generating agents. Furthermore, cycloaddition of nitrile oxides with alkynes is $\sim 6 \text{ kcal mol}^{-1}$ lower than that for similar azides, this lower energy barrier makes the cycloaddition

reaction happen faster at room temperature. Additionally, reaction of nitrile oxides with monosubstituted alkynes is regioselective and generates 3,5-disubstituted adducts. Thermal cycloaddition of nitrile oxides with terminal alkynes generates both 3,4 and 3,5-disubstituted isomers, with the favorite formation of 3,5 regio-isomer (scheme 2.15.a). Thermal regioselective cycloaddition of nitrile oxides with internal alkynes occurs only when alkyne is highly activated through electron-withdrawing substituents and is not sterically hindered (scheme 2.15.b). So, in the absence of a metal-catalyst nitrile oxide/alkyne cycloaddition reaction seems to be more advantageous over its azide/alkyne counterparts, because it is highly regioselective and can be done at mild temperatures. However, this cycloaddition reaction might be catalyzed by copper or ruthenium-based complexes. Fokin and coworkers showed that both copper (I)-catalyzed cycloaddition process as well as ruthenium (II)-catalyzed synthesis resulted in the regioselective and efficient preparation of all isomers of isoxazoles in very short reaction times^{106,107}. Nevertheless, it was reported recently that isoxazole modified oligonucleotides^{105,108} and steroidal glycoconjugates¹⁰⁹ were prepared by uncatalyzed nitrile oxide/alkyne cycloadditions. These reactions exhibited almost perfectly all the characteristics of a “click” type reaction.

a



b



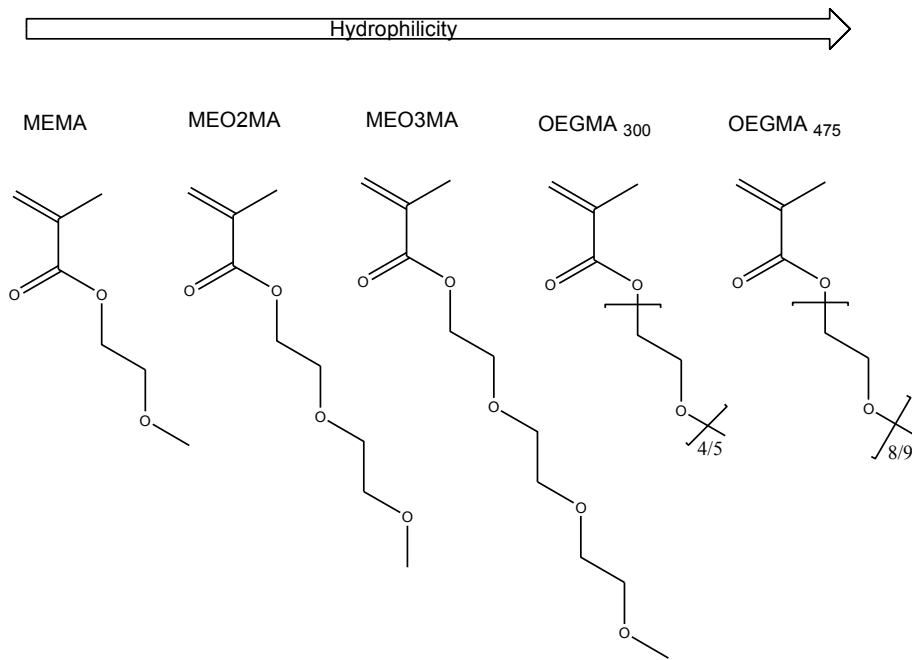
Scheme 2.15. a. Thermal metal-free cycloaddition of nitrile oxides with terminal alkynes is region-selective and produces preferentially 3,5-regioisomer. b. Catalyst-free thermal cycloaddition of nitrile oxides with substituted internal alkynes occurs only when the substituents are electron withdrawing groups.

2.6. Some biological applications of thermoresponsive polymers

Poly (ethylene glycol) PEG is well known for its biocompatibility and water solubility. However, many requirements of biosciences could not be accomplished by using just linear PEG. Indeed, other than biocompatibility of PEG a certain 'smart' characteristic is also needed. Therefore attempts have been done to develop new categories of biocompatible polymers which are simultaneously 'responsive' to external triggers, such as stimuli responsive polymers which change their conformation when exposed to external stimuli like pH, temperature, ionic strength and irradiation. Poly (N-isopropylacrylamide) (PNIPAM) is a typical example of these thermoresponsive polymers which is vastly applied. Still, there are some limitations in using PNIPAM. Firstly, it is not possible to play with the thermoresponsive characteristics of PNIPAM, the lower critical solution temperature (LCST) of PNIPAM is around 32°C and if any other temperature range is required, the LCST of this polymer could not be adjusted. Another issue with the thermoresponsive behaviour of PNIPAM is that its phase transitions show a hysteresis, which means above LCST, PNIPAM chains which are dehydrated globules start to make some intramolecular and intermolecular hydrogen bonding because of the amide groups present in the structure of PNIPAM. These extra interactions lead to some hindrance in the cooling process of PNIPAM and rehydration of the collapsed state.

The requirement to have both PEG biocompatibility and smartness of PNIPAM in one single polymer led to progress in synthesis of a new category of polymers. Such polymers are not linear PEG, but have PEG grafted as side chains to a carbon-carbon backbone. A common group of macromonomers which are also commercially available are oligo (ethylene glycol) (meth) acrylates which can be polymerized by CRP methods to produce brush co/polymeric structures through "grafting through" method. These monomers have a hydrophobic backbone and a hydrophilic PEG side chain and by adjusting the length of this PEG side chain the hydrophobic/hydrophilic balance of the macromonomer could be adjusted and a range of macromonomers starting from very hydrophobic to very hydrophilic ones are obtained. The molecular structures of some of these macromonomers are shown in scheme 2.16.

Furthermore, our group reported that the LCST of the copolymers synthesized from comonomers with different PEG lengths in the side chains can be adjusted precisely by adjusting the molar fraction of the comonomers in the copolymers¹¹⁰. As a result, for different applications, different required LCSTs can be reached by varying the comonomer ratios. Also, in these types of copolymers the hysteresis behaviour observed in PNIPAM is not detected and the phase transitions are reversible, because in the collapsed state above LCST, no strong H-bond donor exists in the molecular structure of these polymers. So, this class of macromonomers are very suitable candidates to be used in biomedical applications²⁹, since they combine both properties of linear PEG and thermoresponsive polymers like PNIPAM.



Scheme 2.16. Structures of different oligo (ethylene glycol) methacrylates

2.6.1. PEGylated chromatography: Thermoresponsive stationary phases for bioseparation

Thermoresponsive stationary phases have been used in the recent years for controlling the separation of bioanalytes^{111,112}. These stationary phases are prepared by grafting smart thermoresponsive polymers, polymers that show property alteration by applying an external stimulus such as temperature, onto preformed chromatographic supports such as silica or polymer-based beads or monoliths. Such chromatography system is based on the changes in hydrophilicity of the grafted co(polymers) upon temperature changes.

These smart chromatographic materials have some advantages for separation of mixtures of biomolecules. Firstly, they use a greener technology compared to conventional reversed-phased chromatography based on organic solvent gradients for separation, since the mobile phase here is pure water and separation occurs under isocratic conditions¹¹³. Secondly, in aqueous solution there is no risk of denaturation of biomolecules to be separated. So far,

special attention has been given to poly(N-isopropylacrylamide) (PNIPAM) for preparing smart stationary chromatographic phase¹¹⁴. This polymer shows a LCST of around 32°C in pure water which is very close to body temperature and therefore is a suitable candidate for biological and biomedical applications. Moreover, the LCST of PNIPAM is insensitive to slight changes in environmental conditions such as pH or concentration¹¹⁵. However, as already mentioned, PNIPAM has some drawbacks in bioapplications. Besides all of these general drawbacks, for specific case of bioapplications, another limitation exists: it can interact with proteins and natural polyamides through strong hydrogen bonding of its secondary amide functionality. This feature is problematic in many bioapplications, especially in bioseparation of protein and enzymes. For example, in PNIPAM hydrogels it is demonstrated that even after shrinkage of the gel some encapsulated protein stays in the PNIPAM hydrogel because of the strong interaction of the protein with PNIPAM¹¹⁶.

Therefore, oligo (ethylene glycol)-based thermoresponsive polymers have been proposed as an alternative to PNIPAM¹¹⁷. These polymers contain bioinert ethylene oxide units and since there

is no H-bond donor in their molecular structure, there is much less possibility for them to interact intermolecularly or with amide-containing biomolecules and proteins. Furthermore, as already discussed, these polymers can be synthesized from commercially available monomers such as OEGMA and MEO₂MA which are nonlinear PEG analogues and as it was demonstrated in our group LCST of the copolymer of these comonomers can be precisely adjusted by changing the comonomer composition¹¹⁸. Thus, thermoresponsive P(OEGMA-*co*-MEO₂MA) copolymers have been exploited for preparing a variety of smart biocompatible materials^{119,120,121,122,123,124,125}.

2.6.2. Activated ester end-functionalized thermoresponsive polymers for bioconjugation: Smart PEGylation of trypsin

One application of N-succinimidyl functionalized polymers is to use them for coupling or conjugating with proteins or biomolecules. Bioconjugation is the covalent bonding of a protein to a synthetic polymer or another natural polymer to obtain a new macromolecule with different properties. Polymer bioconjugation or the modification of proteins with synthetic polymer chains to prepare hybrid structures having both properties of synthetic water soluble polymers and functional native proteins and biomolecules is a very interesting topic in bioscience⁵⁴. If the synthetic polymer coupled to the protein is a poly(ethylene glycol) (PEG)-based polymer, which is a non-toxic polymer, the bioconjugation is termed “PEGylation”. PEGylation of proteins improves their pharmacokinetics, and results in reduced immunogenicity, prolonged plasma half-life, and increased solubility comparing to non-PEGylated proteins. Furthermore, in pharmaceutical chemistry, conjugation with polymers has developed new synthetic ways especially in the field of enzyme-polymer conjugation, for which in most cases enzyme activity is remained or even increased^{126,127,128}.

Since many proteins are suitable candidates to be used as drugs, there have been attempts to develop methods other than oral or injection to deliver these proteins in the desired bodily target, because through oral delivery or injection, proteins are degraded by *in vivo* proteolytic digestion. Furthermore, proteins have a short life time in the body and may cause immunological reactions. So, in order to improve protein delivery and also enhance its solubility

and stability, protein surface could be masked by water soluble PEG chains through covalent coupling mechanisms randomly or at specific sites¹²⁸. In this approach, functional PEG chains react with the accessible functionalities (e.g., thiols or primary amines) located on the protein surface. However, standard linear PEG is a passive molecule since its properties are not adjustable. In the recent years, “smarter” macromolecules, such as temperature or pH-responsive polymers have been grafted on proteins¹²⁹. Pioneering research in this area was performed by Hoffman and Stayton and co-workers^{130,131}. The thermoresponsive polymer they studied most extensively is PNIPAM, which has a LCST at 32°C in aqueous media and therefore its solubility in water could be easily shifted between room and body temperature¹¹⁴. For example, PNIPAM conjugation could be used in biocatalysis, as e.g. PNIPAM-enzyme conjugates can be easily recycled via thermoprecipitation¹³². It is also possible to control or switch the catalytic activity of enzymes through site-specific conjugation of stimuli-responsive polymers like PNIPAM near the active sites of enzymes¹³³. Different approaches have been investigated for grafting PNIPAM on enzyme or on globular proteins. Typically, the lysine amino groups or N-terminus are the reactive sites of the proteins for random conjugation of polymers and the chemistry used for coupling is the N-succinimide coupling. However, conjugation could happen through other functionalities than amino groups which are accessible on the proteins, e.g. –COOH, –OH or –SH groups. Reaction conditions, especially pH and the active groups existing on polymer determine which site is the most probable site on the protein for conjugation to happen. In order to induce the fitting functionality on the polymer, it is relevant to use functionalized initiators and CRP techniques such as ATRP and RAFT to synthesize defined heterotelechelic polymers that can react with proteins^{70, 134, 135, 136, 137}. Indeed, controlled radical polymerization techniques are relevant methods for synthesis of the functionalized PNIPAM for conjugation^{138,139}.

However, PNIPAM has its own drawbacks. For example, specifically in protein-related applications, it should be considered that amide functions of PNIPAM could interact nonspecifically with proteins^{116,140}. Therefore, some alternatives to PNIPAM have been proposed and developed in the recent years. To date, the most investigated alternatives are elastin-like polypeptides¹⁴¹, poly(alkyl oxazolines)^{142,143} and poly(meth)acrylates with short

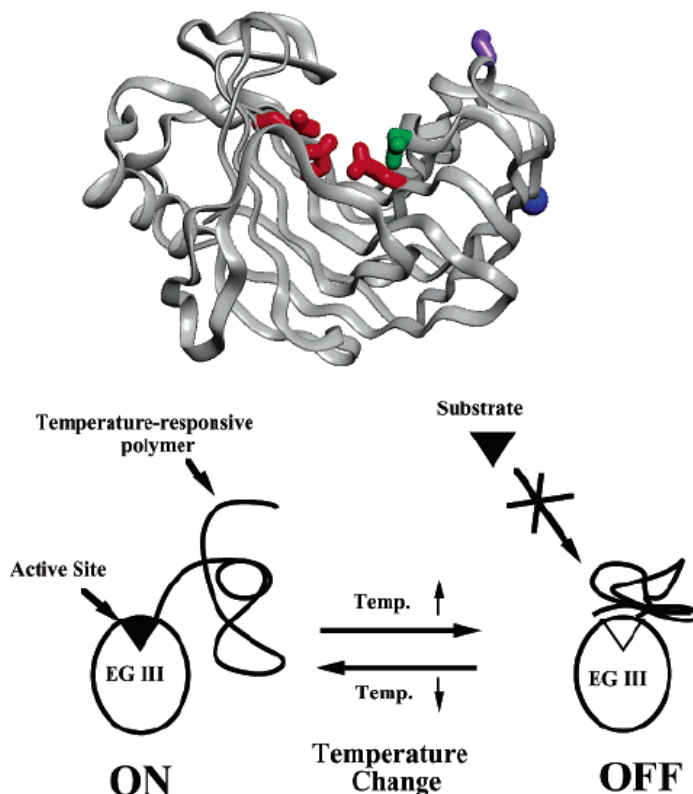
oligo(ethylene glycol) side chains^{117,144,145,146}. As mentioned above, the latter group of polymers is extensively investigated in our group. Particularly, it was demonstrated that the thermoresponsive behavior of these polymers can be precisely tuned via a controlled copolymerization process. For instance, atom transfer radical copolymerization of different ratios of 2-(2-methoxyethoxy)ethyl methacrylate (MEO₂MA) and oligo(ethylene glycol) methyl ether methacrylate (OEGMA) (e.g., OEGMA₄₇₅, M_n=475 g·mol⁻¹ or OEGMA₃₀₀, M_n=300 g·mol⁻¹) leads to the formation of bioinert and biocompatible^{147,148,149} thermoresponsive copolymers with sharp reversible phase transitions in aqueous solution^{118,150,151,152}. So these polymers have been used for a broad range of stimuli-responsive materials such as hydrogels^{153,154,155}, microgels^{156,157}, micellar assemblies^{158,159,160}, modified inorganic nano-objects^{120,123}, and switchable surfaces^{119,161,162,163}. Nevertheless, these copolymers have been rarely used for smart protein conjugation. Theato and co-workers described the synthesis of PMEO₂MA-protein conjugates without studying the thermoresponsiveness of the conjugates^{164,165}. Moreover, the modification of peptides and proteins with poly(meth)acrylates having long oligo(ethylene glycol) side chains has been reported^{57,166,167,168,169,170,171}. Still, these polymers are permanently hydrophilic with LCST which is generally above 85°C and therefore behave like linear PEG and lead to passive PEGylation^{117,172,173}. Therefore, bioconjugation of proteins with copolymers of OEGMA and MEO₂MA having adjustable LCST values, combines the advantages of both PEG (such as hydrophilicity, protection and biorepellency) and PNIPAM (thermoresponsivity).

As already mentioned, a common way for protein conjugation is the reaction of terminally-activated polymers with the amino groups of lysine residues and the N-terminal amino group present in polypeptides. Abuchowski *et al.* did the pioneering work in protein bioconjugation field^{174,175}. They attached methoxypolyethylene glycols of 1900 and 5000 Daltons covalently to bovine liver catalase. PEG-1900-catalase and PEG-5000-catalase showed enhanced circulating lives in the blood of mice. Also, proteolytic digestion of catalase and PEG-catalase by trypsin was compared. PEG-catalase lost its activity very slowly compared to unmodified catalase. After conjugation, immunogenicity of the enzyme is reduced, since PEG provides a shell around enzyme which prevents the recognition of the interior enzyme as a foreign substance against

which immune response could be provoked. Since most of the enzymes entered to human body as drugs are taken from other animal species, plants or microorganisms, patient's immune system produces antibodies specific for that enzyme and recognizes this protein as a foreign substance. Additionally, these immune reactions can reduce the clearance time of the drug in the body and eliminate its function¹⁷⁶. Simultaneously, this PEG shell is still permeable for small substrates, so no loss of enzymatic activity is observed. The improved enzymatic properties shown by this work of Abuchowski opened new doors for enzyme therapy methods. Since these results, many research groups have been interested in this area.

Later, other applications were found for PEGylation, such as enzyme recovery approaches. Due to the catalytic efficiency and chemoselectivity of enzymes, they can be employed in many organic synthesis processes. However, one of the challenges in this field is the separation of the products generated after enzymatic reaction and the recovery of the enzyme. A common strategy to solve this problem is to immobilize enzyme on an insoluble or conditionally soluble support¹⁷⁷. Different approaches have been suggested to immobilize enzyme including non-covalent adsorption or deposition, covalent attachment, entrapment in a polymeric gel, membrane or capsule or crosslinking of the enzyme. There are also examples of immobilization of enzyme on magnetic nanoparticles¹⁷⁸. All of these immobilization methods should be a compromise between maintaining the catalytic activity of the enzyme and gaining the advantages of immobilization. Hoffman and co-workers reported temperature-induced switching of enzyme activity with smart polymer-enzyme conjugates¹³³. For this purpose a site-specific conjugation of stimuli-responsive polymers near the active sites of proteins is utilized, so the enzyme can be switched 'on' and 'off' thermally. Since the smart polymer switches reversibly between expanded and collapsed states when increasing the temperature from below LCST (Lower Critical Solution Temperature) to above LCST, and this polymer is conjugated specifically near the enzyme active site, this active site is somehow available for the substrate below LCST (activity on) and inaccessible to the substrate above LCST (activity off); (scheme 2.17). In another work by Hoffman, these thermoresponsive polymer-enzyme conjugates (PNIPAM was used as thermoresponsive polymer) are exploited to recover enzyme and purify the product of the enzymatic reaction from the reaction solution¹⁷⁹. This way of bioseparation is much easier than dialysis, membrane ultrafiltration, or gel chromatographic

separation. Polymer-enzyme conjugate is soluble in the reaction solution below its LCST and above the LCST it is phase separated from the solution and can be recovered. The product remains in the solution and can be also recovered from the supernatant.



Scheme2.17. Switchable enzyme activity induced by conjugated thermoresponsive polymers (scheme 2.17 is taken from reference¹³³)

In chapter 5 of this thesis, thermoresponsive oligo (ethylene glycol)-based copolymers were investigated for trypsin conjugation. Trypsin is a digestive enzyme that cleaves protein chains¹⁸⁰. Trypsin was chosen as a model enzyme for this 'smart PEGylation', since its polymer conjugation has many advantages compared to the native trypsin. In addition to general advantages of PEGylation for proteins (increasing the water-solubility, thermal stability, overcoming the immunogenicity, extended blood circulating lives, etc.), it is observed so far that in the case of trypsin PEGylation, the conjugate product shows an increase in enzymatic activity (in many cases both esterase and amidase activities) compared to native trypsin¹⁸¹. This

phenomenon is due to changes in the local environment of the enzyme after conjugation¹⁸². However, sometimes both esterase and amidase activities do not increase concurrently as a result of bioconjugation¹⁷⁴. Different parameters influence the biological activity and other properties of the conjugated enzyme or protein. It has been tried to find some general trends to correlate structural properties of the conjugated polymer or protein (such as molecular weight and architecture of the polymer, number of polymer molecules coupled per protein, number of reactive sites on the polymer for coupling, linking site on the protein (distance from biologically-active site)) and applied linking chemistry to conjugate's final properties such as biological activity, thermal stability, autolysis, etc¹⁸³. Nevertheless, so far it does not seem straightforward to find general trends to predict systematically changes in protein/enzyme bioactivities and other properties of the bioconjugate after conjugation. However, for special case of trypsin coupled to specific polymers such as MPEG (α -methoxy-poly(ethylene glycol)) or PNIPAM under specified coupling conditions some trends were observed. Indeed, it was demonstrated that both PEG and PNIPAM conjugation enhance the *in vitro* behavior of trypsin^{174,184,181,185,179,186, 187}. For example, Ding *et al.* reported the conjugation of thermoresponsive PNIPAM to trypsin and observed a remarkable increase in both esterolytic and amidase activities of conjugated trypsin¹⁸⁵. These conjugates can catalyze enzymatic reactions in solution and might be separated from the solution through thermal precipitation and the enzyme could be recycled. Also, the conjugate shows more stability against autolysis compared to the native trypsin due to the steric hindrance of the attached polymer¹⁸⁷.

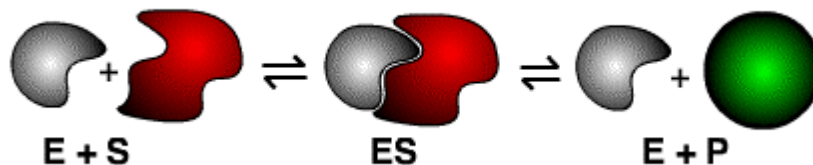
Enzymes are protein catalysts that bind temporarily to the substrate and lower the activation energy which is needed to convert the substrate to the product. The rate at which an enzyme works is influenced by several factors, for example: 1. The concentration of the substrate molecules: increasing the number of substrate molecules causes in faster collision and binding of the enzyme molecules to them. 2. Temperature: as the temperature increases, molecular motion and collision between enzyme and substrate becomes faster. But enzymes are proteins and there is an upper limit beyond which the enzyme becomes denatured and ineffective. 3. The presence of inhibitors: competitive inhibitors are molecules that bind to the active site of the enzyme and prevent the binding of the enzyme to the substrate. Noncompetitive inhibitors

are the inhibitors which reduce the enzyme activity. 4.pH: the conformation of a protein is influenced by pH and as enzyme activity is crucially dependent on its conformation, its activity is likewise affected¹⁸⁸.

The study of the rate at which an enzyme works is called enzyme kinetics. To study enzyme kinetics as a function of the substrate concentration, a series of tubes containing graded concentrations of substrate [S] are prepared. At time zero, a fixed amount of enzyme preparation is added and the concentration of the product which is formed is measured over the few minutes after reaction. If the product absorbs light, this concentration could be easily measured by a spectrophotometer. Early in the run, when the substrate amount is in substantial excess to the amount of enzyme, the observed rate is the initial velocity of V_i . In scheme 2.18(left) V_i is plotted as a function of [S]. At low values of [S], initial velocity, V_i increases almost linearly with [S]. As [S] increases, V_i levels off and a rectangular hyperbola is formed. The asymptote represents the maximum velocity of the reaction, V_{max} . The [S] value that produces a V_i equal to one-half of V_{max} is designated the Michaelis-Menten constant, K_m . K_m is roughly an inverse measure of the affinity between the enzyme and its substrate. The lower the K_m , the greater the affinity (so the lower the concentration of substrate needed to achieve a given rate)¹⁸⁸.

Plotting $1/V_i$ versus $1/[S]$ yields a „double-reciprocal“ or „Lineweaver-Burk“ plot (scheme 2.18, right). This plot provides a more precise way to determine V_{max} and K_m . V_{max} is calculated from the intercept of the $1/V_i$ axes and then K_m is calculated from the slope of the Lineweaver-Burk plot¹⁸⁸.

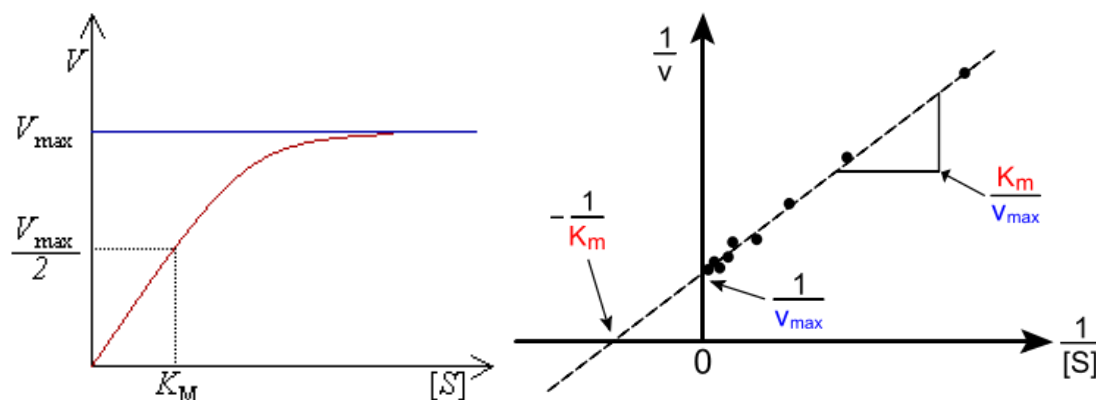
a)



b)

$$V_i = \frac{-d[S]}{dt} = \frac{d[Pr]}{dt} = \frac{V_{max} \cdot [S]}{K_m + [S]} \quad \text{or} \quad \frac{1}{V_i} = \frac{K_m}{V_{max}} \cdot \frac{1}{[S]} + \frac{1}{V_{max}}$$

Scheme 2.17. a) Schematic representation of an enzymatic reaction with substrate to produce Pr, product; b) The Michaelis-Menten equation which relates the initial reaction rate V_i to the initial substrate concentration $[S]$. $[S]$ = initial substrate concentration, K_m = Michaelis-Menten constant, $d[S]/dt$ = elimination rate of the substrate, $d[Pr]/dt$ = rate of product formation, V_{max} = the maximum velocity of the enzymatic reaction.



Scheme 2.18. Left: Saturation curve for an enzyme showing the relation between the initial concentration of substrate and initial reaction rate. Right: Lineweaver–Burk or double-reciprocal plot of kinetic data, showing the significance of the axis intercepts and gradient.

Chapter 3

Functionalization of polymer chain ends via CuAAC

3.1. *In situ* functionalization of thermoresponsive polymeric micelles using CuAAC

Individual molecules are integrated into larger functional and structural hierarchies very often in nature through self-assembly mechanisms (bottom-up strategy). Scientists have taken this strategy from nature to make functionalized materials from synthetic or bio molecules and their self-organization, which is through purely physical (noncovalent) interactions. For instance, self-assembly of macromolecular amphiphiles in water is one of the attractive areas in colloidal and materials science^{115,189, 190, 191}.

Amphiphilic block copolymers self-assemble in selective solvents into different nanoscale morphologies, like micelles, and analogous to low molecular weight surfactants they have CMC, however their CMC is much lower than low molecular weight surfactants and this makes them good candidates for nanocontainers for drug delivery. Self-organization of polymeric building blocks in selective solvent is derived by three main interactions of hydrophobicity, electrostatic forces and hydrogen bonding. For example, the mechanism of self-aggregation through hydrophobic effect is explained as follows: blocks which are not soluble in the main solvent tend to hide from the main phase (e.g. water) and blocks that are soluble in the main solvent try to make as much contact as possible with the solvent.

In this way, depending on the hydrophobic volume of the block copolymer aggregates with different morphologies are formed. Characteristic sizes and morphologies of these nanostructures can be predicted by knowing the volume fraction of the constituent blocks and the molecular weight of the polymers. For example, amphiphilic diblock copolymers composed of distinct hydrophilic and hydrophobic segments self-organize in water into spherical micelles, cylindrical micelles or vesicles, depending on their hydrophilic-hydrophobic balance^{192, 193,194,195}. More complex morphologies (multicompartment micelles, toroids, crew-cut micelles, nanotubes,...) may be obtained by using more elaborate molecular design (e.g. triblock copolymers or miktoarm stars) or by varying the experimental self-assembly conditions (using cosolvents, cosolutes as well as temperature or pH variations)^{194, 196,197,198, 199,200,201,202}.

In many applications such as targeted drug or gene delivery the “*in situ*” modification of pre-formed aggregates is of interest. Nevertheless, the chemical modification of preformed micellar aggregates is limited by the nature of the main solvent (in bioapplications mostly water) and solution conditions such as pH, aggregate concentration, temperature and all conditions in which the formed micelles are stable in solvent (water). Therefore, efficient chemical reactions which can be performed in dilute aqueous solutions and at relatively moderate temperatures (room or physiological temperature) should be chosen. The copper-catalyzed 1,3-dipolar cycloaddition of azides and terminal alkynes (CuAAC) is potentially a very suitable reaction for modifying *in situ* polymeric micelles. In fact, this reaction is highly chemo- and regioselective, and proceeds in very high yield in aqueous media. The starting materials do not need to be dissolved in the reaction solvent. As long as the solution is stirred adequately, reaction proceeds^{82,81}.

The *in situ* “functionalization” of micellar aggregates formed from copolymers prepared by ATRP of PEG-based macromonomers was performed. For this investigation, first a low molecular weight model molecule (propargyl alcohol) is clicked *in situ* on the corona of the pre-formed micelles in aqueous solution. After this successful click and optimization of click conditions, *in situ* functionalization of micellar aggregates by clicking larger polymeric molecules on their corona is investigated.

In the first example of “functionalization” of micellar aggregates with a low molecular weight molecule, a cholesterol-based moiety was chosen as the hydrophobic segment and homo- or co-polymers of oligo (ethylene glycol) acrylate formed the hydrophilic segments of the micelles. In the case of “functionalization” of micellar aggregates with polymeric species, the hydrophobic block of the micelles was composed of polystyrene (PS) and homo-polymers of oligo (ethylene glycol) acrylate were chosen as the hydrophilic segments of the micelles.

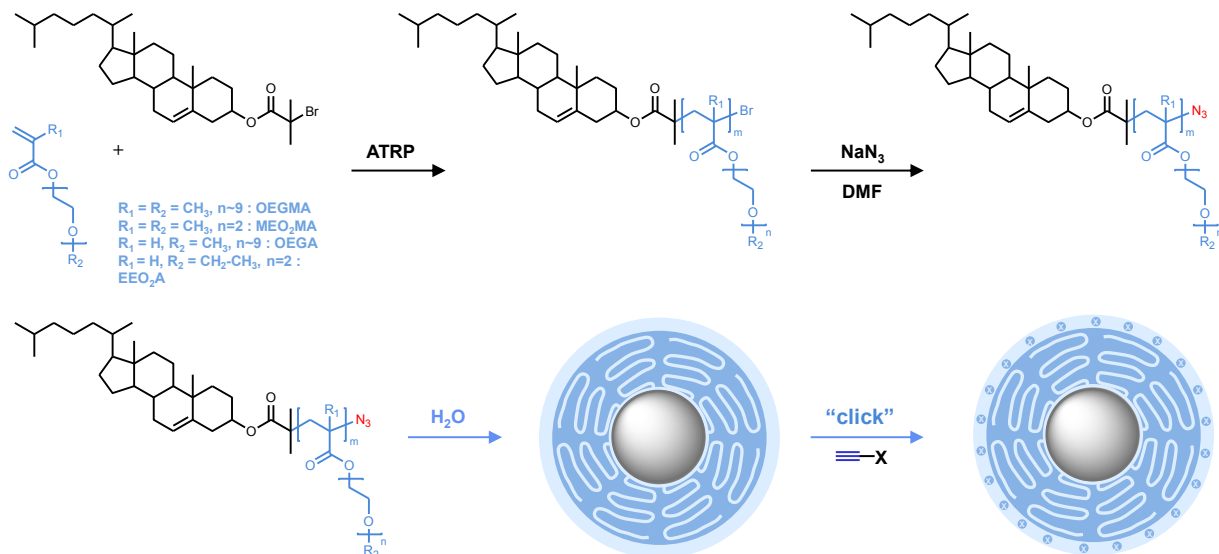
PEG-based macromonomers or oligo (ethylene glycol) (meth) acrylates were used as macromonomers to synthesize PEG-based copolymers in the present work. In order to obtain micelles, different lengths of hydrophilic and hydrophobic blocks and hydrophobic/hydrophilic ratios of the blocks were targeted. In some cases individually soluble polymers were obtained instead of micellar aggregates due to the high volume fraction of the hydrophilic block. In these

cases the hydrophobic volume fraction was increased in order to obtain micelles instead of soluble copolymers in subsequent syntheses.

The above-mentioned PEG-based polymers used as hydrophilic segments in both “functionalization” methods, and their advantages and properties are explained in detail in part 2.6 of the second chapter.

3.2. *In situ* click cycloaddition of the pre-formed micelles in water with a “low molecular weight” model molecule

In situ “functionalization” of micelles formed from the copolymers of PEG-based macromonomers is investigated. Here, polymeric micelles composed of a cholesterol-based hydrophobic core and a hydrophilic, thermoresponsive and biocompatible PEG-like corona are formed in aqueous solution (scheme 3.2.). The micellization behavior of these macrosurfactants was studied in aqueous solution by Dynamic Light Scattering (DLS), ^1H NMR and turbidometry. After micelle formation, the *in situ* CuAAC corona functionalization of the formed micelles was investigated in dilute aqueous conditions in the presence of a model functional alkyne (propargyl alcohol).



Scheme 3.2. Experimental pathways for the preparation of well-defined surfactants (top) and functionalized micelles (bottom).

Different oligo (ethylene glycol) (meth) acrylate homo/copolymers were synthesized by ATRP and using CBI (Cholesteryl-2-bromoisobutyrate) as initiator. Molecular characterization and polymerization conditions of these series of well-defined surfactants are listed in table 3.1. The formed homo and copolymers were characterized by size exclusion chromatography (SEC) in THF and ¹H NMR (see table 3.1.). In the case of acrylate-based monomers polymerizations were stopped at relatively low monomer conversions (Table 3.1., entries 5,6,7) to reach a high degree of halogen chain-ends, this precaution is essential for subsequent step of transformation of halogen end groups into azide functionalities^{76,169,203}.

Table 3.1. Molecular characterization and experimental conditions of the well-defined polymeric surfactants prepared by ATRP.^a

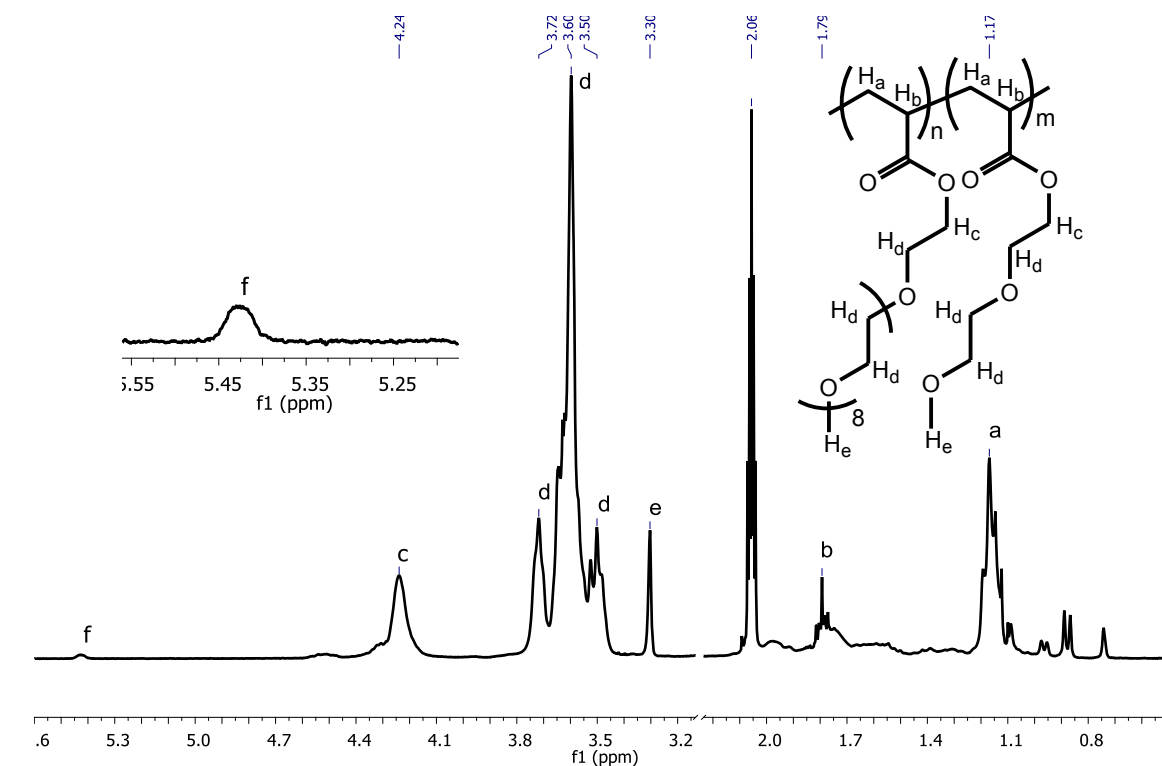
	M ₁	M ₂	M ₁ /M ₂ /CBI/Cu(I)/Bipy	T(°C)	t(h)	Conv. ^b	M _n ^c	M _w /M _n ^c
1	OEGMA	MEO ₂ MA	3/17/1/1/2	60	17	0.99	8500	1.20
2	OEGMA	MEO ₂ MA	6/34/1/1/2	60	14	0.98	10700	1.19
3	OEGMA	MEO ₂ MA	4/16/1/1/2	60	14	0.97	8500	1.19
4	OEGMA	MEO ₂ MA	8/32/1/1/2	60	14	0.99	12000	1.20
5	OEGA	-	40/-/1/1/2	90	3	0.29	4900	1.14
6	OEGA	-	40/-/1/1/2	90	1.5	0.21	3300	1.21
7	OEGA	EEO ₂ A	8/32/1/1/2	90	3	0.46	4000	1.49

^a Experimental conditions: copolymerization of methacrylates (entries 1-4) in ethanol solution (monomer/ethanol= 1:1.25 v/v) and in the presence of Cu(I)Cl; homopolymerization and copolymerization of acrylates (entries 5-7) in bulk and in the presence of Cu(I)Br. ^b Monomer conversion measured by ¹H NMR. ^c Measured by SEC in THF, calibration by linear PS standards (PSS, Germany).

¹H NMR spectrum of a homopolymer of cholesterol-*b*-OEGA and a copolymer of cholesterol-*b*-EEO₂A-co-OEGA and their characteristic peaks is shown in figure 3.1.

¹H NMR analysis confirmed that all formed polymers exhibit α- terminal cholesterol moieties. Two characteristic signals of the cholesterol moiety (f and g protons in figure 3.1) appear around 5.4 and 4.5 ppm, respectively. These two signals were observed in all ¹H NMR spectra (For example, zoom of the region 5-5.5 ppm in figure 3.1 shows clearly the f proton of cholesterol moiety.).

Other characteristic signals related to the polymers appear in different regions (figure 3.1). Five other regions could be recognized in the ¹H NMR spectra of co/polymers (a, b, c, d, e regions shown in Figure 3.1) which are characteristic of the main backbone and side chains protons of the co/polymers.



60

3.2.1. Preparation of azide end functional polymers

The halogen chain-ends of all acrylate-based macrosurfactants (table 3.1., entries 5-7) were transformed into azide functionalities by nucleophilic substitution in the presence of sodium azide. Azide end functional polymers were characterized by FTIR, which evidenced the formation of ω -azido chain-ends. After treatment with sodium azide and purification, an absorption peak at 2112 cm^{-1} , due to the asymmetric stretching vibration of the azide function, could be detected in the IR measurements of all polymers (Figure 3.2.B). As a proof, polymer samples before treatment with sodium azide are also measured by IR and compared to the samples after nucleophilic substitution.

3.2.2. Self-organization of the macrosurfactants in water

The aqueous self-organization of the azide-functionalized macrosurfactants was studied by dynamic light scattering (DLS) and turbidometry. Since the formation of micellar aggregates of copolymers in water is targeted, it is important to adjust their hydrophobic/hydrophilic balance so that a micellar solution could be obtained. Therefore, a series of macrosurfactants with different ratios of cholesterol and comonomers are designed and synthesized. The synthesis was started with a cholesterol-*b*-POEGA with the $M_{n(\text{SEC})}=4900$ (Table 3.1, entry 5) to get an estimation of the hydrophobic volume of the system. Since this cholesterol-*b*-POEGA (Table 3.1, entry 5) could not form micellar aggregates in water, investigation was continued with the synthesis of more hydrophobic co(polymers) to reach the suitable hydrophilic/hydrophobic balance for micelle formation (Table 3.1, entries 6,7).

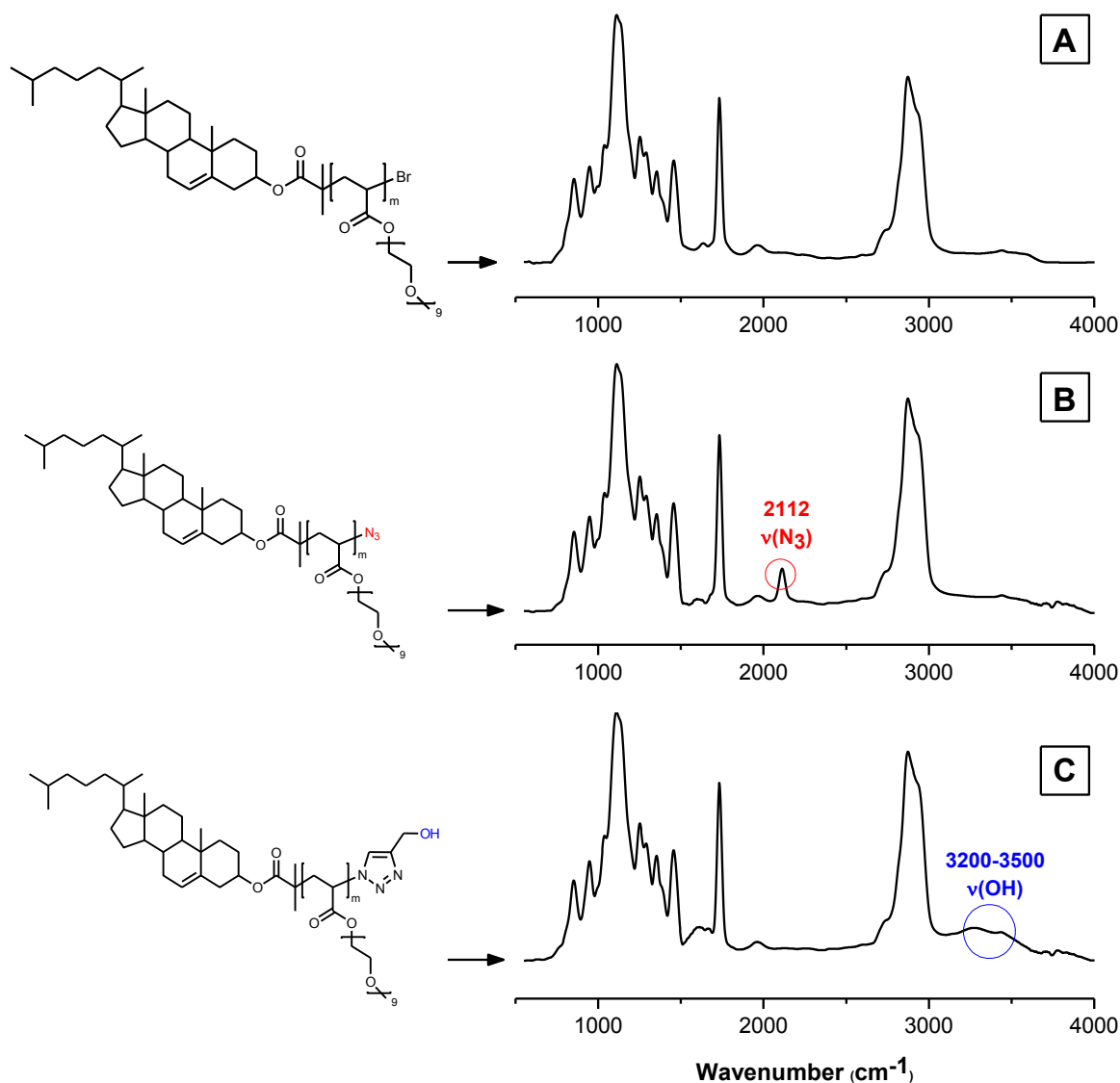


Figure 3.2. IR spectra recorded at room temperature for a cholesterol-*b*-POEGA surfactant (Table 3.1., entry 6) A) before reaction with sodium azide, B) after reaction with sodium azide and C) after click cycloaddition with propargyl alcohol in aqueous medium.

Typical size distributions measured by DLS for various acrylate-based macrosurfactants are shown in Figure 3.3.A. The aggregation behavior of these surfactants in pure deionized water depends on the volume fractions of their hydrophilic-hydrophobic segments. For example, cholesterol-*b*-POEGA macrosurfactants (Table 3.1., entries 5 and 6) did not form large

aggregates in pure water since hydrophilic volume fraction in these macrosurfactants is too high to form any aggregation and only small objects (5-6 nm in diameters) are observed by DLS (Table 3.2, entries 5a, 5b and 6). POEGA is indeed a very hydrophilic homopolymer, which is soluble in water at any temperature up to 100°C²⁰⁴. Therefore, even when cholesterol-based block is hydrophobic and the theoretical degree of polymerization of the hydrophilic POEGA block is as short as 11 or 8 units (Table 3.1. entries 5 and 6 respectively), DLS measurements show no aggregates and most probably only random coils are observed.

In order to get aggregation, a random copolymer of OEGA and EEO₂A (20 mol % of OEGA) is synthesized which is less hydrophilic than POEGA (Table 3.1., entry 7). Monomer EEO₂A is less hydrophilic than OEGA because it has shorter oligo (ethylene glycol) side chains (only 2 EO units). Random copolymers of cholesterol-*b*-P(EEO₂A-*co*-OEGA) self-organize in pure water into monodisperse aggregates with an average hydrodynamic diameter of 100 nm measured by DLS (Figure 3.3.A and Table 3.2, entries 7a and 7b).

Moreover, ¹H NMR of cholesterol-*b*-P(EEO₂A-*co*-OEGA) in D₂O confirmed the formation of aggregates, since protons of hydrophobic cholesterol moiety could not be detected in this case. In fact, these protons which are located in the core of the micellar aggregates are shielded from water by a hydrophilic outer corona.

As demonstrated before, well-defined copolymers of P(EEO₂A-*co*-OEGA) exhibit an LCST in water, which can be adjusted by varying the comonomer composition²⁰⁴. Aggregates of cholesterol-*b*-P(EEO₂A-*co*-OEGA) formed in aqueous solution were also characterized by turbidimetry and showed a broad phase transition around 45°C (Figure 3.3.B). The broadness of the observed phase transition is related to the short DP of the copolymers and chain- to chain deviations in comonomer composition¹⁵⁰.

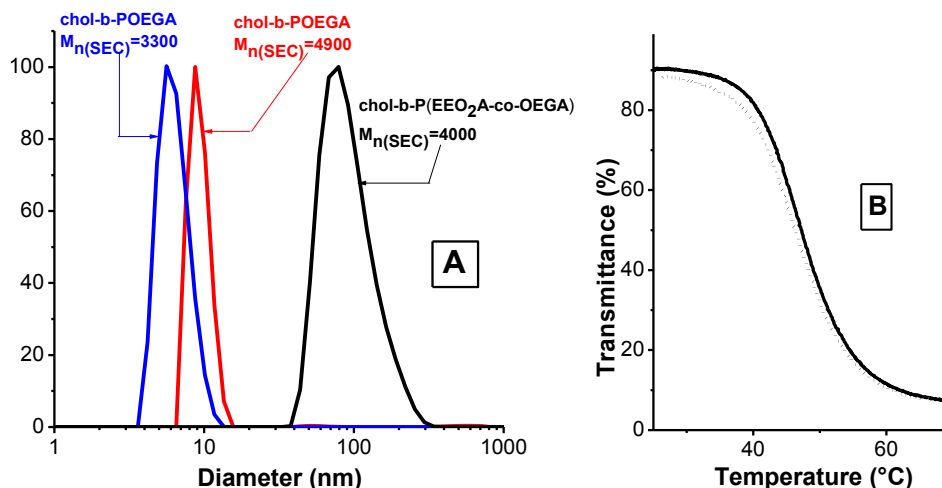


Figure 3.3. A) Size distribution measured by DLS at room temperature for solutions ($10 \text{ g}\cdot\text{L}^{-1}$) of cholesterol-*b*-POEGA samples (red line= Table 3.1, entry 5); blue line= Table 3.1, entry 6), or cholesterol-*b*-P(EEO₂A-co-OEGA) (black line=Table 3.1, entry 7) in pure deionized water. B) Plots of transmittance as a function of temperature measured for an aqueous solution ($1 \text{ g}\cdot\text{L}^{-1}$) of cholesterol-*b*-P(EEO₂A-co-OEGA) (Table 1, entry 7). Solid line: heating, dotted line: cooling.

3.2.3. *In situ* “click” functionalization of co/polymers with a model low molecular weight alkyne in aqueous solution

The click functionalization in pure water was first investigated with the water-soluble cholesterol-*b*-POEGA surfactants (Table 3.1., entries 5 and 6). Since these surfactants do not form aggregates in pure water, they could be used as models, in concentrated conditions ($50 \text{ g}\cdot\text{L}^{-1}$). After optimization of the click reaction with these model surfactants, the click could be performed on the micellar aggregates of cholesterol-*b*-P(EEO₂A-co-OEGA)(Table 3.1., entry 7). To optimize the click conditions, two different water soluble copper-based catalytic systems were chosen: (1) a combination of copper (II) sulfate and the reducing agent sodium L-ascorbate (Na-AsA), and (2) a combination of copper (I) bromide and the ligand Bipy. Propargyl alcohol was chosen as a model alkyne, because its click cycloaddition was already described in the literature^{89,169}. Click reactions were carried out at room temperature during 24 h.

Characterizations by FT-IR and ^1H NMR methods, confirmed that CuAAC successfully occurred in all cases.

FT-IR characterization of the samples showed that after click reaction with propargyl alcohol, the absorption peak of azide (2112 cm^{-1}) disappeared from the IR spectrum (Figure 3.2.C) and was replaced by a broad signal at $3200\text{-}3500\text{ cm}^{-1}$ corresponding to the stretching of H-bonded hydroxyl functions (terminal alcohol function in the ω -chain end after click with propargyl alcohol).

Additionally, new chain-end signals appeared in the NMR spectrum after click cycloadditions (Figure 3.4). A signal at $4.60\text{-}4.80\text{ ppm}$ is observed which could be assigned to the methylene protons neighbouring terminal alcohol function (H_h). Two other signals related to the cholesterol α -chain-end could be detected (ethylenic proton H_f at $5.40\text{-}5.50\text{ ppm}$ and a proton located in the α of the ester function H_g at $4.40\text{-}4.60\text{ ppm}$). H_g signal is shifted upfield as compared to that of the initiator CIB and therefore the protons H_g and H_h are not overlapping and therefore could be individually integrated. The yield of click reaction was calculated for both catalytic systems after 24 h of reaction at room temperature by comparing the integration of proton H_f of the α - chain-end (1H) to protons H_h (2H) of the ω - chain-end.

The results show that the catalyst $\text{CuSO}_4/\text{Na-AsA}$ gives much higher yields compared to CuBr/Bipy system (compare two spectra in Figure 3.4). So, the optimized catalyst for the CuAAC was selected to be $\text{CuSO}_4/\text{Na-AsA}$. This result agrees with previous studies which show that Bipy-based copper catalysts lead to slower cycloaddition reactions^{205,206}. Generally, aliphatic amine ligands lead to more rate enhancement of the cycloaddition reaction compared to pyridine-based ligands. One reason is that aliphatic amine ligands enhance Cu^{I} -alkyne π -complexation due to their electron-donating properties. Furthermore, aliphatic amine ligands have stronger basicity compared to pyridine ligands and this accelerates the CuAAC²⁰⁶.

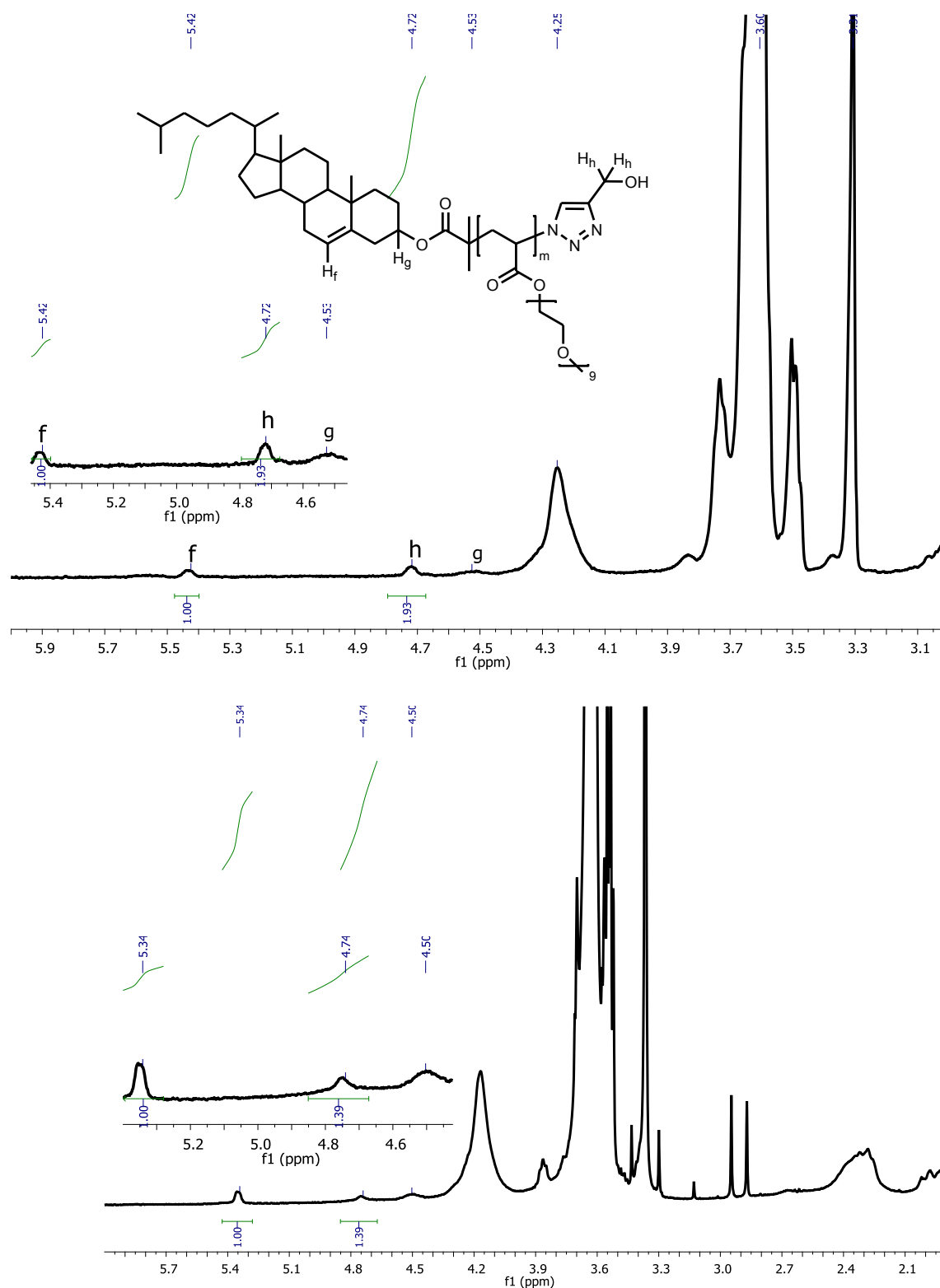


Figure 3.4. ^1H NMR spectra of the functionalized cholesterol-*b*-POEGA (Table 3.1., entry 5) micelles after cycloaddition in water, the spectrum was recorded at room temperature. Top: CuSO_4 and sodium ascorbate was chosen as catalyst. Bottom: CuBr and bipyridyl was used as catalytic system.

Based on the results obtained from CuAAC of the cholesterol-*b*-POEGA, the catalyst CuSO₄/Na-AsA was chosen for the CuAAC of cholesterol-*b*-P(OEGA-*co*-EEO₂A) micelles in dilute aqueous solution. For CuAAC with propargyl alcohol, two different concentrations of copolymers were chosen (1 and 10 g·L⁻¹).

At both concentrations of 1 and 10 g·L⁻¹ of cholesterol-*b*-P(EEO₂A-*co*-OEGA) surfactants in water, rather monodisperse aggregates with an average hydrodynamic diameter D_h of around 100 nm were formed (Table 3.2, entries 7a and 7b). After micelle formation and *in situ* CuAAC, the product was isolated and characterized. ¹H NMR measurements in acetone-*d*₆ confirmed the functionalization of the micellar aggregates and also proved in both dilutions very efficient click cycloaddition reactions in water and extremely high yields (Table 3.2, entries 7a and 7b). For example, in Figure 3.5 ¹H NMR spectrum of the click product of 10 g·L⁻¹ of cholesterol-*b*-P(EEO₂A-*co*-OEGA) surfactants in water (Table 3.2, entry 7a) with propargyl alcohol is demonstrated. As it is clear from this spectrum, the CuAAC yield in this case is very high and around 97%.

Table 3.2. CuAAC of azide-functionalized surfactants with propargyl alcohol in aqueous solution.^a

	surfactant	[surfactant] (g·L ⁻¹)	Diameter (nm) ^b	catalyst	CuAAC Yield (%) ^c
5a	Cholesterol- <i>b</i> -POEGA 5	50	5.5	CuSO ₄ /Na-AsA	95
5b	Cholesterol- <i>b</i> -POEGA 5	50	5.5	CuBr/Bipy	70
6	Cholesterol- <i>b</i> -POEGA 6	50	6	CuSO ₄ /Na-AsA	95
7a	Cholesterol- <i>b</i> -P(EEO ₂ A- <i>co</i> -OEGA) 7	10	100	CuSO ₄ /Na-AsA	97
7b	Cholesterol- <i>b</i> -P(EEO ₂ A- <i>co</i> -OEGA) 7	1	99	CuSO ₄ /Na-AsA	98

^a Experimental conditions: all experiments were performed in deionized water; room temperature, 24 h. ^b Average diameter of the aggregates measured by DLS. ^c calculated from ¹H NMR spectra in acetone-*d*₆.

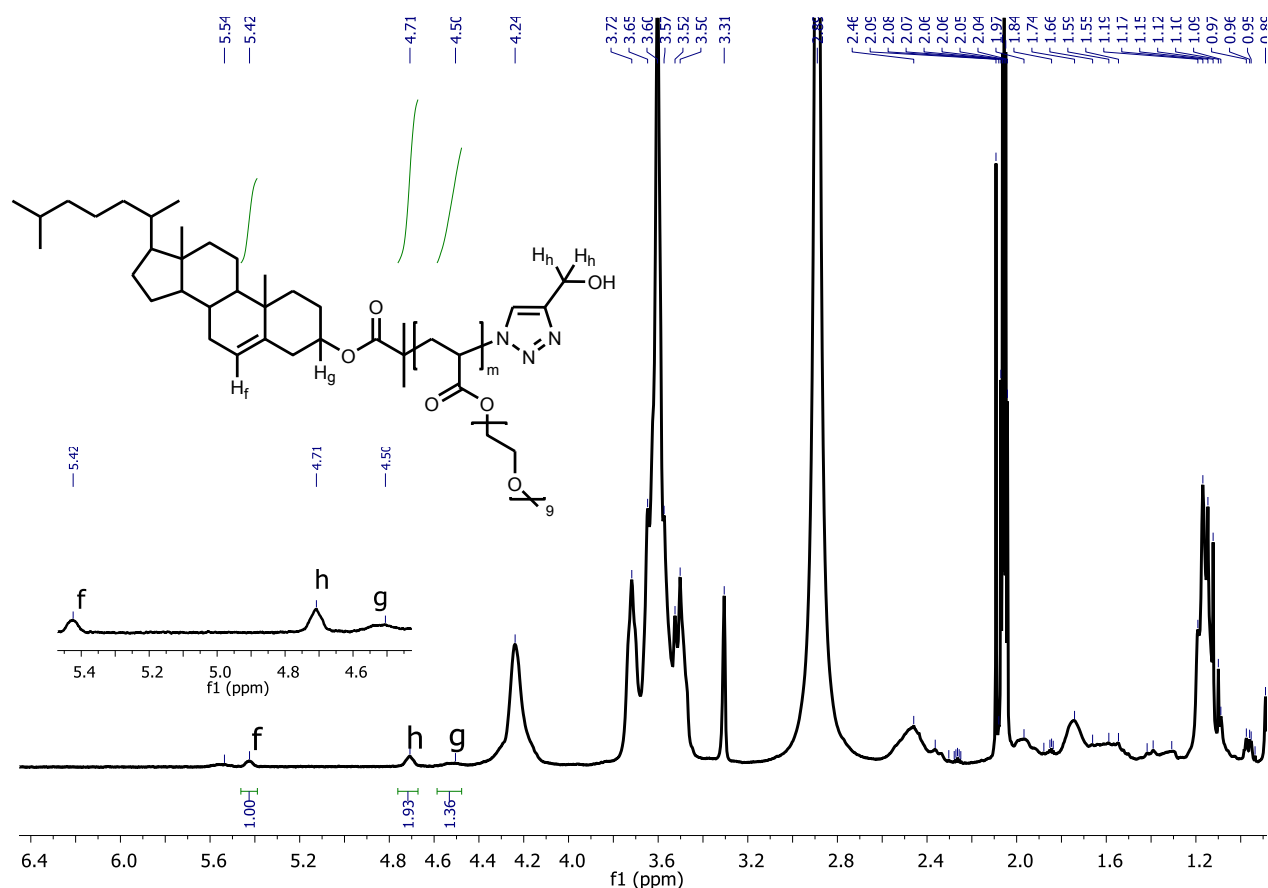


Figure 3.5. ^1H NMR spectrum of the click product of 10 mg/mL of cholesterol-*b*-P(EEO₂A-co-OEGA) surfactants in water (Table 3.2, entry 7a) with propargyl alcohol.

3.3. *In situ* aqueous click cycloaddition of the corona of micellar aggregates with large polymeric molecules

After successful *in situ* CuAAC of the model ‘low molecular weight’ alkyne with the azide functionality on the corona of the micellar aggregates, this technique was applied to couple *in situ* ‘high molecular weight’ species with pre-formed micelles in water.

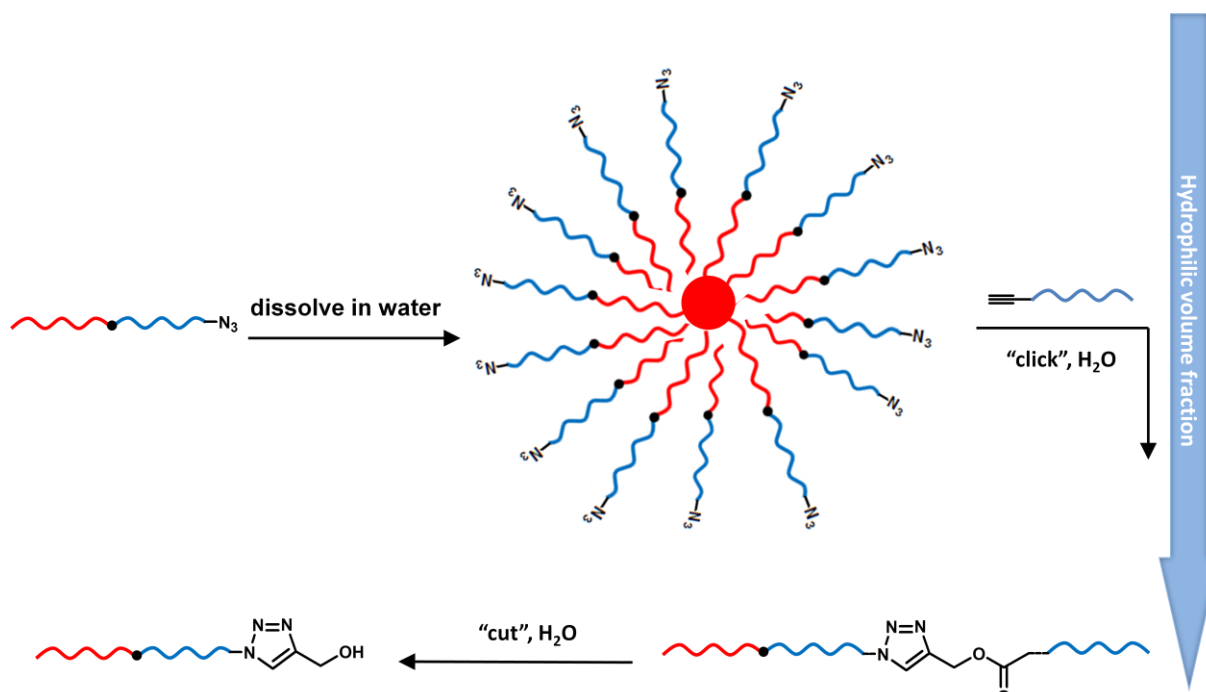
Here, click cycloaddition reaction was used as a ligation tool to couple an AB type macrosurfactant with a hydrophilic homopolymer (B' type), and as a result, a more hydrophilic ABB' triblock with a different hydrophilic-hydrophobic balance is obtained. By altering the hydrophilic-hydrophobic balance of the macrosurfactants, their self-organization behavior in water changes and this might cause even morphology changes. For some applications

(encapsulation, controlled release, catalysis, etc.), it is of interest to change *in situ* the morphology of block copolymer aggregates.

Amidst various parameters such as concentration, temperature, pH and sample preparation that influence the aggregation behavior of macrosurfactants, the most determining factor is the hydrophilic volume fraction f . Generally, for low f values ($\approx 35\%$), block copolymers form large vesicles, but for higher f values ($f > 45\%$), spherical micelles are generated, whereas for $f < 25\%$, inverted microstructures are expected¹⁹³. So, in order to induce morphology changes, different methods are applied, such as incorporating stimuli-responsive segments as blocks of block copolymers, which go through rapid conformational changes when exposed to pH, temperature, ionic strength changes or irradiation^{207,208,209,204}. Another way to alter the morphology is through the modification of the hydrophilic-hydrophobic balance via *in situ* coupling with additional hydrophilic or hydrophobic moieties. Such coupling reactions should be possible in aqueous media and mild experimental conditions, such as moderate temperatures, in which micellar aggregates are already formed. As already discussed, one of the best reactions of this type could be copper-catalyzed 1,3-dipolar cycloaddition of azides and terminal alkynes.

Following the above-mentioned concept, a model AB amphiphilic block copolymer composed of a hydrophobic polystyrene (PS) segment (A), and a hydrophilic poly[oligo (ethylene glycol) acrylate] [POEGA] segment (B) was synthesized and dispersed in water. This AB block copolymer was designed and synthesized so that it forms micelles in water. These micelles were then clicked *in situ* with an additional hydrophilic B' segment (POEGA). The extension of the diblock copolymer (A-(B+B')) shifts the hydrophilic balance of the system to a more hydrophilic one and could lead to the appearance of unimolecularly dissolved triblock copolymers.

It is also interesting to investigate the possibility of recovery of the micelles. If in this coupling strategy a labile group is inserted between AB and B' blocks, this labile moiety can be “cut” later e.g. by hydrolysis and AB and B' segments are formed (scheme 3.3.).



Scheme 3.3. *In situ* aqueous click cycloaddition of the azide functionalities on the corona of the micellar aggregates with alkyne-functionalized large polymeric molecule. Red and blue chains represent hydrophobic and hydrophilic segments, respectively.

3.3.1. Synthesis of ω -azido-functional diblock copolymer PS-*b*-POEGA 1

First, the bromine end-functionalized hydrophobic polystyrene (PS) segment (A) was synthesized by ATRP. The initiator used for ATRP was methyl 2-bromopropionate (MBP). The polymerization of styrene was stopped at low monomer conversion (roughly 20%) in order to obtain a high degree of bromine end-functionality for the synthesis of block copolymer. The characterization of pure PS by SEC showed that a well-defined oligomeric PS was obtained ($M_n = 2300 \text{ g} \cdot \text{mol}^{-1}$, $DP_n = 20$ and $M_w/M_n = 1.17$) (Figure 3.8). However, ^1H NMR spectrum of the PS macroinitiator before polymer purification and monomer removal, gives a more exact estimation for the molecular weight ($DP_n = 28$). This PS macroinitiator initiated the polymerization of OEGA to add a second, hydrophilic block made of OEGA.

After synthesis of AB diblock the bromine functionality of this diblock was transformed to the azide functionality by nucleophilic substitution using sodium azide (figure 3.9, polymer 1). The

synthesis procedures are described in a separate chapter. After each synthesis step, the samples were characterized by SEC and ^1H NMR. After synthesis of ω -azido functional block copolymer PS-*b*-POEGA **1**, chain-end substitution was confirmed by FT-IR analysis of the pure diblock (a peak around 2100 cm^{-1} was detected in the IR spectrum after substitution reaction) (Figure 3.9.A).

From the ^1H NMR spectra of the first PS block the average degree of polymerization of the PS is calculated to be 28. In figure 3.6, ^1H NMR spectrum of the PS block before purification and monomer removal is shown. By comparing the signals of styrene monomer remained in the reaction solution and PS signals, one can calculate the conversion of the styrene monomer. As shown in figure 3.6, two characteristic protons of styrene monomer are recognized at around 5.2 and 5.7 ppm (H_d and H_e). On the other hand, the magenta region represents 6 protons of styrene monomer (H_b and H_c) and 5 protons of PS (H_a). By comparing the integrals of H_d and H_e with the protons shown in magenta area, conversion is calculated: Share of protons of PS in magenta region is 12.26 ($18.26-6$) and this value is correlated with 5 protons of PS (share of each proton of PS is therefore 2.45 ($12.26/5$)). Conversion is calculated around 71% according to the ratio of polymer/(monomer+polymer) of the integral shares or ($2.45/(2.45+1)$). Since the initial molar ratio of styrene monomer to initiator is 40, the average degree of polymerization is calculated as 28 ($0.71*40$).

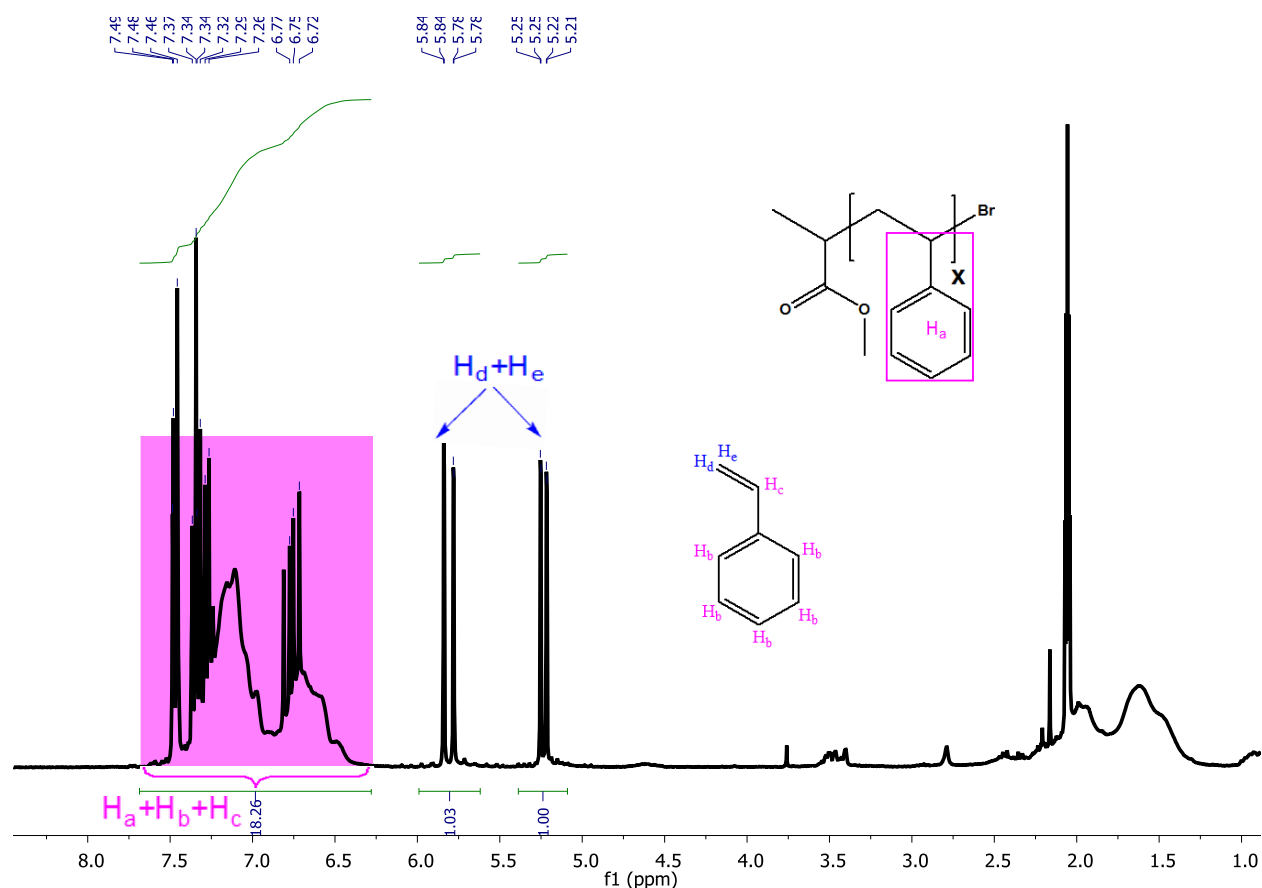


Figure 3.6. ^1H NMR spectrum of the first PS block before purification and monomer removal, measured at room temperature in acetone.

From the ^1H NMR measurements of the diblock PS-*b*-POEGA, conversion of the second monomer, OEGA, is calculated to be around 25%. The average degree of polymerization of the POEGA block was estimated to be around 13 by comparing the integration of distinct PS and POEGA signals in ^1H NMR. For example in figure 3.7, the integral of two regions is shown: 1) the integral in the magenta region is related to 5 protons of styrene in PS block. Since the average DP of PS block is 28, in the integrated region of PS, 140 protons should be present ($28 \times 5 = 140$), and 2) the integral of the blue highlighted area (at 4.25 ppm) which is related to two characteristic protons in the α position of the ester group of POEGA side chains. The integral ratio of these two regions is around 140/28 as shown in figure 3.7. Therefore the average degree of polymerization of the POEGA block could be easily estimated ($28 \div 2$ or around 14).

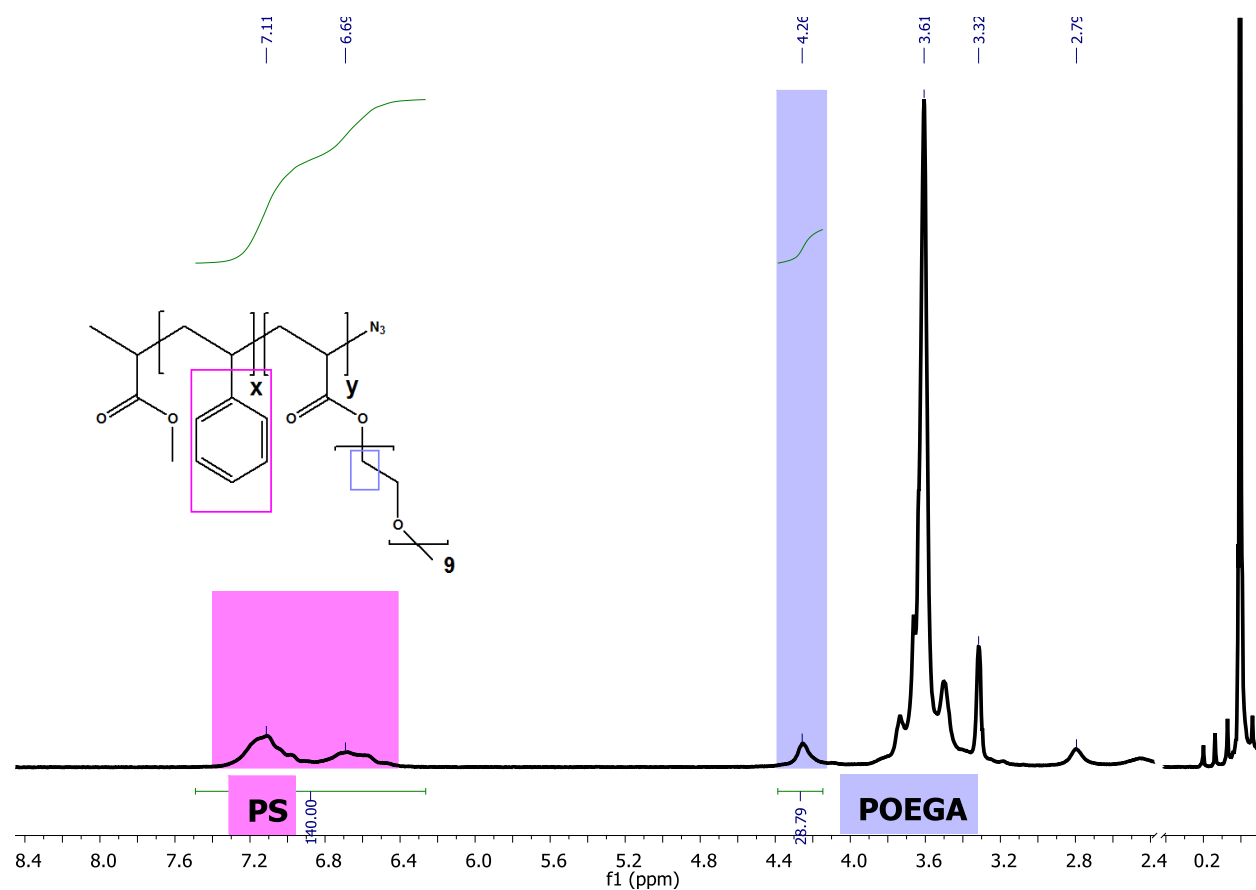


Figure 3.7. ^1H NMR spectrum of the diblock copolymer PS-*b*-POEGA **1** measured at room temperature in acetone.

SEC measurements confirmed the synthesis of the first PS block and the subsequent synthesis of a well-defined diblock copolymer ($M_n = 6300 \text{ g}\cdot\text{mol}^{-1}$, $M_w/M_n = 1.22$) (Figure 3.8).

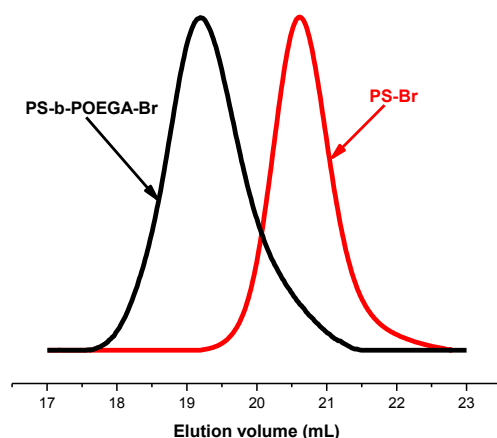


Figure 3.8. SEC chromatograms in THF for a well-defined PS macroinitiator synthesized by ATRP (red line) and the corresponding diblock PS-*b*-POEGA (black line). The latter chromatogram was recorded prior to sodium azide treatment.

After synthesis of diblock PS-*b*-POEGA **1**, its self-aggregation behavior in water was studied by DLS and Transmission Electron Microscopy (TEM). Since PS block has a high T_g and forms “frozen” aggregates in aqueous solution, stepwise dialysis from THF (a good solvent for both PS and POEGA) to water is performed to prepare solutions for DLS and TEM studies. Diblock is dissolved first in water (2 and 10 g·L⁻¹) and dialysed against gradient solutions of THF/water starting from 75/25 volume ratio to pure water. After preparing these solutions of block copolymer in deionized water, DLS and TEM measurements were performed. For TEM measurements, the solutions were deposited on the TEM grid and after removal of water by suction, images of the block copolymer micelles were obtained (negative staining with phosphotungstic acid) (Figure 3.9.B). Both TEM and DLS measurements show that the formed macrosurfactants self-assemble into compact spherical micelles in dilute aqueous solutions. The average diameter of the micelles was evidenced by both measurements to be approximately 30 nm.

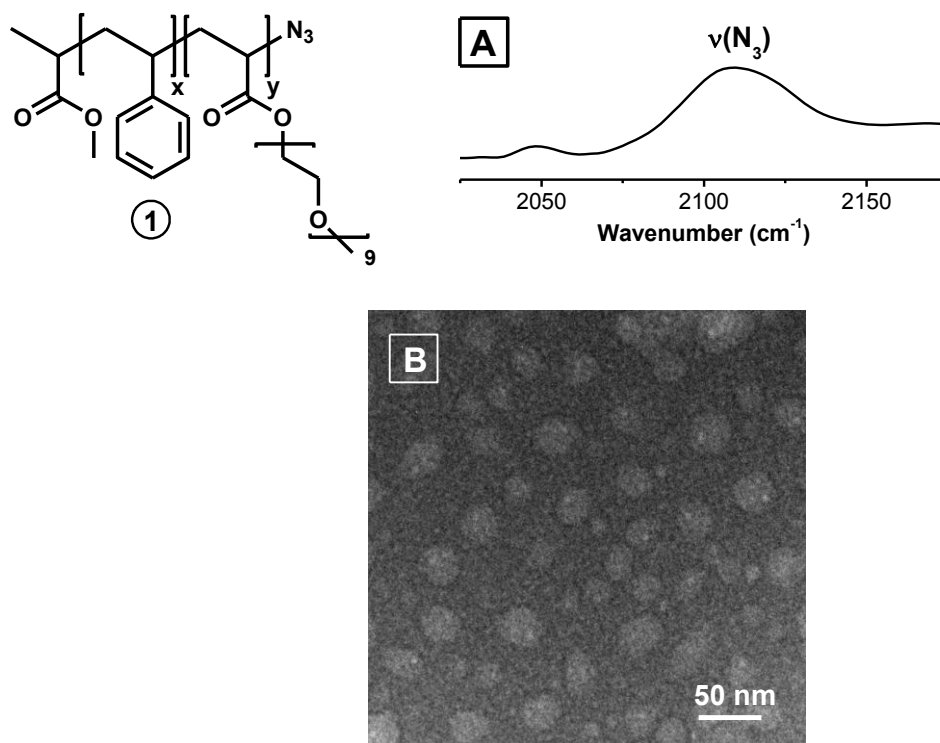


Figure 3.9. Characterization of the ω -azido-functional diblock copolymer PS-*b*-POEGA **1**: (A) IR spectrum (zoom of the region 2025–2175 cm⁻¹) of **1** recorded at room temperature. (B) TEM images of spherical aggregates of **1** formed in dilute aqueous solution. Preparation: block copolymer solutions (2 g·L⁻¹ in deionized water) were deposited on the TEM grid and water was subsequently removed by suction (Staining: negative staining with phosphotungstic acid).

3.3.2. Synthesis of α -alkyne functional homopolymer POEGA **2**

After synthesis and characterization of ω -azido diblock PS-*b*-POEGA **1** (AB diblock), α -alkyne functional homopolymer POEGA **2** (B block) was synthesized and characterized. These two polymers were then coupled together via CuAAC.

For the synthesis of POEGA **2**, a TMS protected acetylene functionalized initiator was used.

This strategy is applied to avoid the problems caused by complexation of unprotected acetylene functionality with the copper-catalyst and catalyst deactivation during polymerization.

Nevertheless, in some test experiments some α -alkyne functionalized POEGA with unprotected α -alkyne initiator “propargyl 2-bromoisobutyrate” were synthesized. After click reaction of PS-POEGA diblock with the POEGA synthesized with unprotected initiator, some evidences from SEC and ^1H NMR analysis of the product showed that the click reaction did not work out (For example, the characteristic ^1H NMR peak of the methylene protons next to the triazole ring and the main-chain ester around 5.3 ppm was not observed). One of the reasons could be the probability of some side reactions during polymerization of OEGA with unprotected alkyne initiator, such as complexation with copper or dissociation of the terminal alkyne protons and formation of radicals which could start side reactions. Any of these side reactions would eventually lead to the loss of some alkyne end-groups and therefore unsuccessful click.

In order to make sure that the alkyne end functionality remained on the polymers, a trimethylsilyl (TMS) protected initiator was chosen to polymerize OEGA, this POEGA **2** was then clicked to the PS-*b*-POEGA diblock in the next step.

The trimethylsilyl (TMS)-protected POEGA was characterized by SEC and ^1H NMR. Two characteristic peaks for TMS-protected alkyne chain-ends were observed in ^1H NMR (Figure 3.10). The signal at 4.73 ppm represents the methylene protons in the α -position of the alkyne and the peak at 0.12 ppm is due to the methyl groups of TMS. By integration of these signals and comparing them to the integration of some of the signals of the POEGA side chains (c protons in blue-highlighted region in figure 3.10), the average degree of polymerization of POEGA is calculated ($\text{DP}_n=18$).

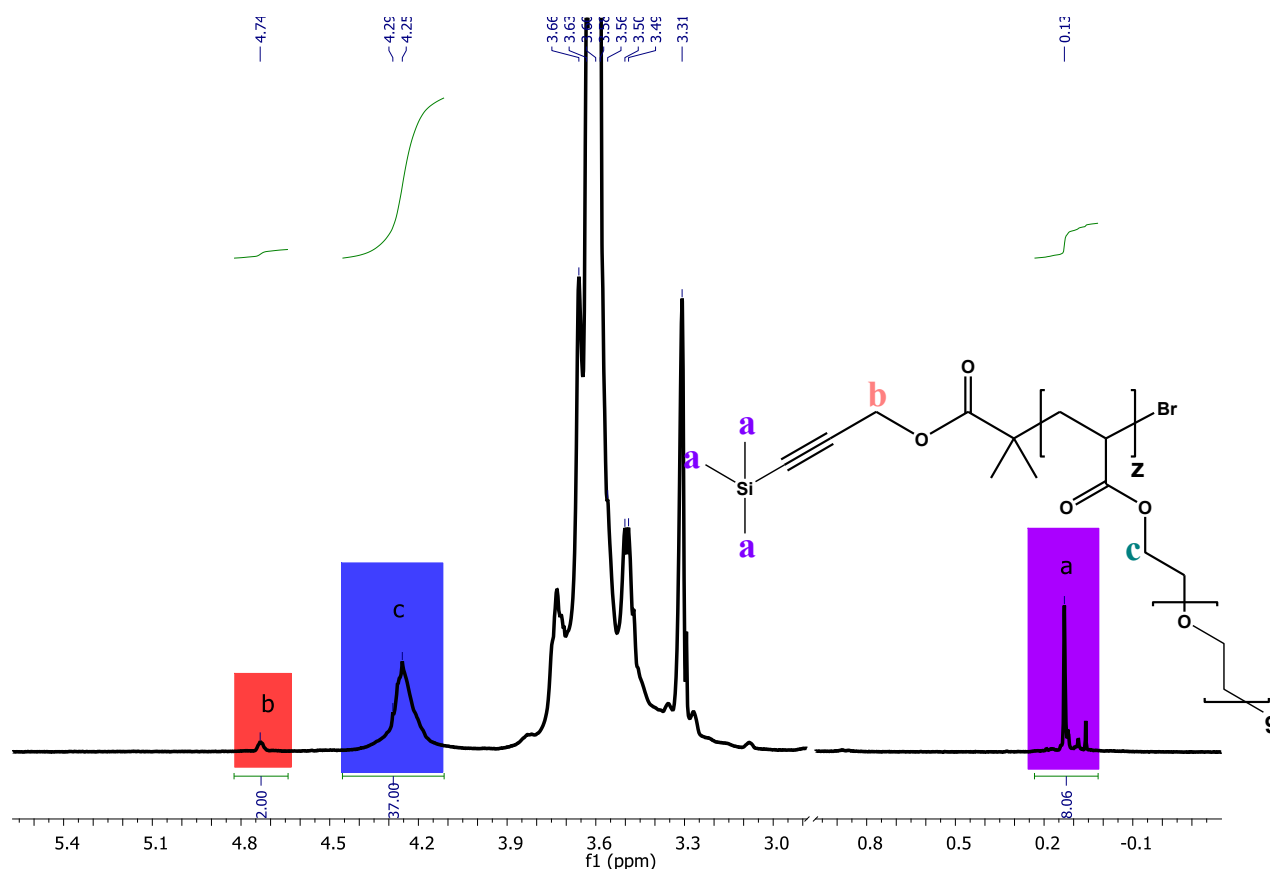


Figure 3.10. ^1H NMR spectrum of the TMS-protected POEGA recorded at room temperature in acetone- d_6 .

After characterization of the protected POEGA, TMS was deprotected for the next click reaction. TMS-deprotection was performed in THF (0.01 M solution) in the presence of tetrabutylammonium fluoride (TBAF), as previously described⁶³. The α -alkyne functional homopolymer POEGA **2** was characterized with SEC and ^1H NMR after purification ($M_n=6900 \text{ g}\cdot\text{mol}^{-1}$ and $M_w/M_n=1.15$ obtained by SEC) (Figure 3.11.A). As observed in Figure 3.11 TMS-protecting groups were quantitatively removed after treatment with TBAF in THF solution⁶³.

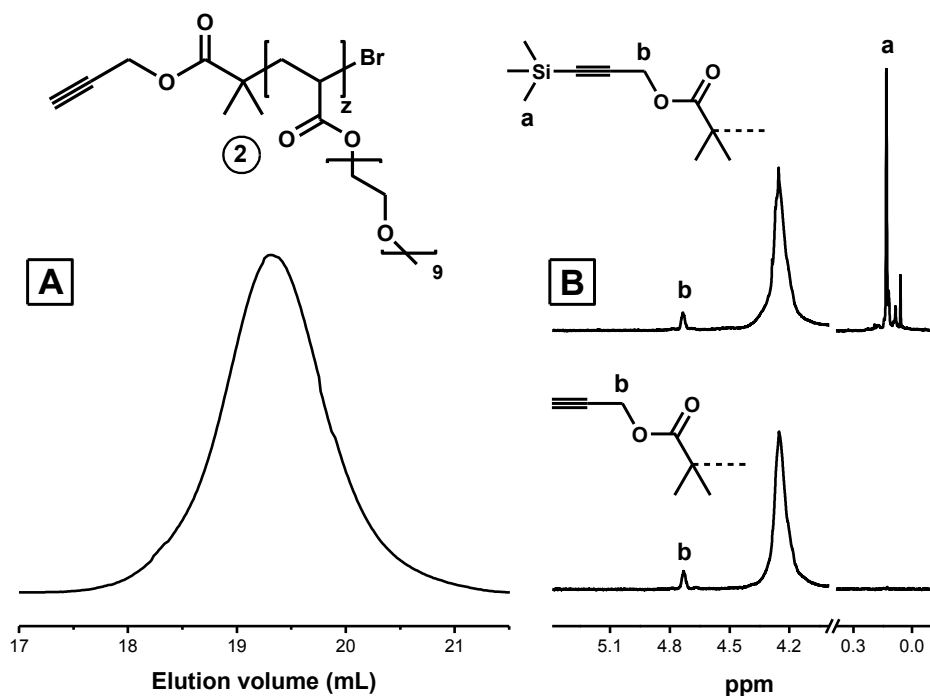


Figure 3.11. Characterization of the α -alkyne-functional homopolymer POEGA **2**: (A) SEC chromatograms measured in THF; (B) ^1H NMR spectra (zooms of regions 0.1-0.4 and 4.0-5.4 ppm) recorded at room temperature in acetone- d_6 for POEGA **2** before (top) and after (bottom) treatment with TBAF.

3.3.3. CuAAC of diblock copolymer PS-*b*-POEGA **1** and homopolymer POEGA **2**

After synthesis and characterization of diblock copolymer PS-*b*-POEGA **1** and homopolymer POEGA **2**, ω -azido functional block copolymer PS-*b*-POEGA **1** was dissolved in deionized water (concentration: $50 \text{ mg}\cdot\text{ml}^{-1}$) and was coupled *in situ* with α -alkyne functional homopolymer POEGA **2** via CuAAC. The procedure for click cycloaddition is described in chapter 7 (section 7.2.4).

3.3.4. Optimization of the click reaction conditions

After integration of the ^1H NMR signals of the POEGA homopolymer **2**, it was concluded that all POEGA chains possessed alkyne-end functionalities, whereas only 85-90% of the diblocks PS-POEGA **1** had a terminal azide functionality due to the side reactions during ATRP process (termination, transfer, elimination). These side reactions lead to the formation of dead chains without bromine end-groups that could not be transformed into azide functionalities^{203,76}. So, for an optimized click reaction, using a molar excess of diblock **1** (1.15 equiv.) to homopolymer **2** is expected to give better results.

Various experimental conditions were screened for the click cycloaddition of **1** and **2** in water. For the first trial click reaction the conditions were chosen as room temperature and 24 h of reaction time and the stoichiometric ratio (1/1) of diblock **1** to homopolymer **2** was selected. After purification and characterization of the product, SEC chromatogram and ^1H NMR spectrum showed the formation of click product (e.g. appearance of the characteristic ^1H NMR peak at around 5.2 ppm related to methylene protons between triazole ring and ester group of the main chain^{67,210}). However, the click efficiency was low. So, for the next click reactions a molar excess of diblock **1** (1.15 equiv.) to homopolymer **2** was chosen and different temperature and time ranges for the click were applied.

Temperature range was chosen from room temperature (25°C) up to 40 °C and reaction time was selected between 24 h and 4 days. Since click cycloaddition was supposed to occur between two large molecules (polymers), reaction required elevated temperatures or/and extended reaction times.

There is another limitation for increasing time and temperature which is the risk of hydrolysis of POEGA side-chains in water. Polymers made from oligo(ethylene glycol) methacrylates were reported to be relatively insensitive to hydrolysis in acidic and basic conditions^{211,147}. However, their acrylate-counterparts seem to be more easily hydrolyzable. In order to investigate this issue, different click reaction conditions were investigated. For example, reaction temperature around 40-50 °C resulted in the hydrolysis of POEGA side chains. Increasing the reaction time to around 3-4 days caused the same problem of hydrolysis. The optimized experimental conditions

for performing the stoichiometric ligation of **1** and **2** in water were found to be 48 h at 25 °C. To investigate if the side-chain hydrolysis has happened, ^1H NMR integration of the side-chains signals should correlate with the backbone signals.

The click product was characterized by 500 MHz ^1H NMR and FT-IR after purification. FT-IR analysis of the triblock confirmed that click reaction was successful; since the characteristic signal of the azide, which was detected in diblock PS-b-POEGA **1** (a peak around 2112 cm^{-1}), had disappeared.

Characterization of the pure product after click reaction with 500 MHz ^1H NMR confirmed that the click ligation of **1** and **2** was successful. Due to the relatively high molecular weight of the formed polymer, high field NMR is required to observe the junction protons (Figure 3.12). A broad characteristic signal was observed at 5.10-5.45 ppm (e proton in Figure 3.12), which is due to the methylene protons located between the formed triazole ring and the main-chain ester. This observation is in good agreement with previous reports^{67,210}. However, a weak signal around 4.73 ppm is also observed, which is due to the methylene protons of unreacted alkyne. The latter signal indicates that the click reaction was not quantitative. The integration of both signals at 5.10-5.45 ppm and 4.73 ppm confirmed a yield of coupling of almost 80%. This yield is indeed high considering the fact that homopolymer **2** and diblock copolymer **1** are both large molecules and their click ligation is not as easy as click reaction between two small molecules (or a small molecule and a macromolecule as discussed in the first part of this chapter).

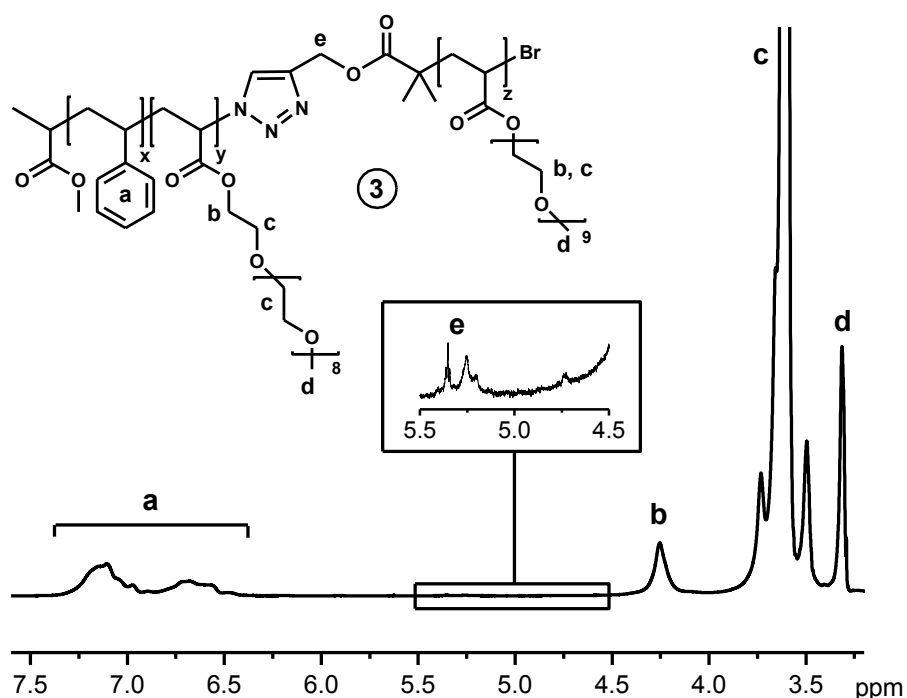
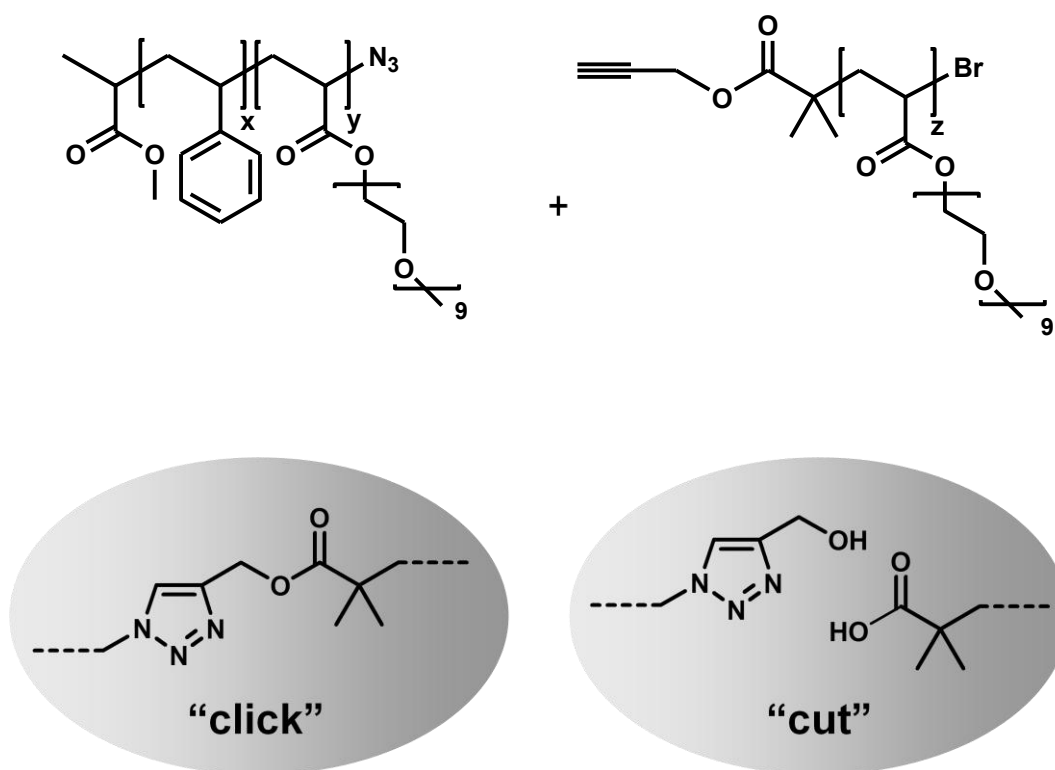


Figure 3.12. 500 MHz ^1H NMR spectrum of the triblock copolymer PS-*b*-POEGA-*b*-POEGA **3** obtained through click ligation of PS-*b*-POEGA **1** and POEGA **2**. The inset shows an intensity zoom of the region 4.5-5.5 ppm. The spectrum was recorded at room temperature in acetone- d_6 .

3.3.5. Investigation of the main-chain hydrolysis of the formed triblock copolymer **3**

As already discussed, click chemistry was used as a ligation tool to couple *in situ* an amphiphilic AB diblock with a hydrophilic B homopolymer in water. In this way the hydrophilic-hydrophobic balance of the AB amphiphiles is changed and a more hydrophilic triblock ABB' is formed. This change in hydrophilic-hydrophobic balance could result even in morphology changes. Nevertheless, for some applications it is interesting to go back to the initial morphology. This was the motivation to introduce an ester group at the junction between AB and B' segments

from the early stages of synthesis (initiator for POEGA **2** contained this ester group). This labile moiety may be “cut” on demand by hydrolysis (see scheme 3.4).



Scheme 3.4. Click coupling strategy between PS-b-POEGA **1** and POEGA **2** blocks and a hydrolysis process to cut the ester junction between **1** and **2** and obtaining the initial diblock and homopolymer.

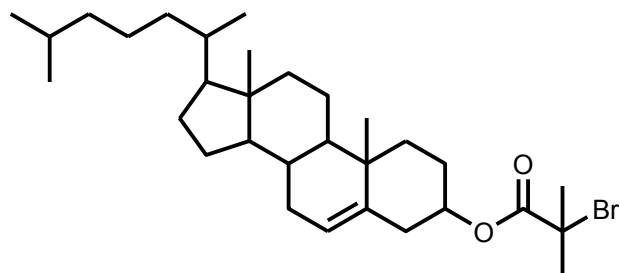
In the last step of this project, the main-chain hydrolysis of the formed triblock copolymer PS-b-POEGA-b-POEGA **3** was studied. For the hydrolysis basic condition (1% and 5% KOH solution in water (w/v)) was chosen. pH values measured for the two latter basic solutions were 11.8 and 13, respectively. The obtained results indicated that the main-chain esters could be cleaved in basic conditions. For example, ^1H NMR signal at 5.10-5.45 ppm which is characteristic of the methylene protons next to the triazole ring was disappeared after hydrolysis. However, the hydrolysis of the main-chain ester competes with the hydrolysis of the side-chain esters of

OEGA, and partial POEGA degradation may also occur. This result was confirmed when the side-chain signals were integrated and their correlation with the backbone signals was studied.

3.4. Synthetic Procedures

3.4.1. *In situ* CuAAC of the pre-formed micelles in water with propargyl alcohol

3.4.1.1. Synthesis of the ATRP initiator cholesteryl-2-bromoisobutyrate



The cholesterol-based ATRP initiator cholesteryl-2-bromoisobutyrate (CBI) was synthesized by esterification of cholesterol and 2-bromoisobutyryl bromide: Freshly distilled toluene (300 ml) and cholesterol (4.1 g, 10.6 mmol) were added in a dried flask. After full dissolution of the cholesterol, triethylamine (3.2 ml) was added and the reaction mixture was cooled in a dry ice/ethanol bath. Subsequently, 2-bromoisobutyryl bromide (5.6 g, 24 mmol) was added dropwise over a period of 90 min. The experimental mixture was slowly allowed to warm to room temperature and stirred overnight. After reaction, the mixture was washed with hydrochloric acid and sodium hydrogen carbonate solutions, dried over magnesium sulfate and concentrated *in vacuo*. The crude material was purified by column chromatography using hexane/diethyl ether (v/v 6:4) as eluent. The final product appeared as a white powder and was characterized by ^1H NMR.

3.4.1.2. General procedure for the bulk atom transfer radical copolymerization of EEO₂A and OEGA

Oligo (ethylene glycol) acrylates generally polymerize rather slowly if the conditions are the same as ones chosen for methacrylates. Thus, as previously optimized, acrylate monomers are polymerized at 90°C, in bulk and in the presence of Cu(I)Br and Bipy as catalyst^{169, 204}. Cholesteryl-2-bromoisobutyrate, copper bromide (CuBr), and Bipy were added into a dry flask. The flask was sealed with a septum and subsequently purged with dry argon for several minutes. Then a thoroughly degassed mixture of EEO₂A and OEGA was added with a degassed

syringe [the reaction medium turned dark brown, indicating complexation of Cu(I)Br and Bipy]. The mixture was heated at 90°C in an oil bath for several hours. The experiment was stopped by opening the flask and exposing the catalyst to air. The final mixture was diluted with deionized water and subsequently purified by dialysis against pure water (Roth, ZelluTrans membrane, molecular weight cut-off: 4000-6000).

3.4.1.3. General procedure for the atom transfer radical copolymerization of MEO₂MA and OEGMA

The ATRP of methacrylate monomers (OEGMA and MEO₂MA) was optimized and reported before¹¹⁵. Cholesteryl-2-bromoisobutyrate, copper chloride, and 2,2'-bipyridyl (Bipy) were added to a Schlenk tube sealed with a septum. The tube was purged with dry argon for a few minutes. Then, a degassed mixture of 2-(2-methoxyethoxy) ethyl methacrylate, OEGMA, and ethanol (monomers/ethanol~1:1.25 v/v) was added through the septum with a degassed syringe. The mixture was heated at 60°C in an oil bath for several hours. The experiment was stopped by opening the flask and exposing the catalyst to air. The final mixture was diluted with deionized water and purified by dialysis against pure water (Roth, ZelluTrans membrane, molecular weight cut-off:4000-6000).

3.4.1.4. Preparation of azide end functionalized polymers

The procedure for preparing azide-functionalized polymers was optimized and described in details in previous publications^{89,169}. In brief, the copolymers prepared by ATRP were dissolved in dimethyl formamide and reacted with a small excess of sodium azide (room temperature, 3h). The final mixture was diluted with deionized water and subsequently purified by dialysis against pure water (Roth, ZelluTrans membrane, molecular weight cut-off: 4000-6000). Finally, water was removed by rotary evaporation.

3.4.1.5. General procedure for the aqueous “click” functionalization of the amphiphilic copolymers

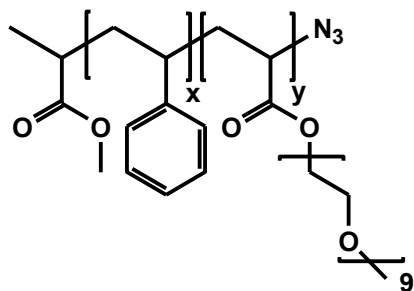
In a flask, an azide-functionalized polymer (1 equiv. of azide functions), copper (II) sulfate pentahydrate (1 equiv.), sodium L-ascorbate (2 equiv.), and deionized water were added. The flask was capped with a septum and the solution was purged with dry argon for 10 min. The mixture turned to a homogeneous yellow solution. Last, propargyl alcohol (10 equiv.) was added via a microliter syringe. The reaction mixture was stirred for 2 days at room temperature. After reaction, the final mixture was diluted with water and purified by dialysis against pure water (Roth, ZelluTrans membrane, molecular weight cut-off: 4000-6000). Small copper aggregates, which could not be removed by dialysis, were separated by centrifugation. Finally, water was removed by rotary evaporation.

3.4.2. *In situ* aqueous click cycloaddition of the corona of micellar aggregates with POEGA 2

3.4.2.1. Synthesis of polystyrene macroinitiator via atom transfer radical polymerization

Copper (I) bromide (156 mg, 1.09 mmol) and styrene (10 mL, 87.2 mmol) were added to a flask, which was afterwards sealed with a septum. The suspension was purged with dry argon for 20 min. Then, N,N,N',N'',N''-pentamethyldiethylenetriamine (PMDETA) (187 mg, 1.09 mmol) was added through the septum with a syringe and the mixture was homogenized by stirring. Last, methyl 2-bromopropionate (MBP) (364 mg, 2.18 mmol) was added with a microliter syringe. The mixture was heated at 90°C in an oil bath. After 4 h of polymerization, the experiment was stopped by opening the flask and exposing the catalyst to air. The final mixture was diluted in THF and passed through a short silica column in order to remove copper catalyst. The THF solution was concentrated by rotary evaporation and subsequently precipitated in methanol. The precipitated PS was filtered and dried under vacuum.

3.4.2.2. Synthesis of the ω -azido functional block copolymer PS-*b*-POEGA 1



4,4'-dinonyl-2,2'-dipyridyl (178 mg, 0.436 mmol) and copper (I) bromide (31.24 mg, 0.218 mmol) were added to a Schlenk tube. The flask was sealed with a septum and purged with dry argon for some minutes. Then, degassed OEGA (3.63 ml, 8.71 mmol) and a degassed toluene solution of the PS macroinitiator (500 mg, 0.218 mmol dissolved in 3 mL toluene)

were successively added through the septum with degassed syringe. The mixture was heated at 90°C in an oil bath for 30 min. The experiment was stopped by opening the flask and exposing the catalyst to air. The final mixture was diluted with deionized water, purified by dialysis against pure water (Roth, ZelluTrans membrane, molecular weight cut-off: 4000-6000), and finally dried using rotary evaporation.

The procedure for preparing azide-functionalized polymers is described in detail in previous publications^{89,169}. In brief, the diblock PS-*b*-POEGA was dissolved in N,N-dimethylformamide (DMF) and reacted with a small excess of sodium azide (room temperature, 3 h). The final mixture was diluted with deionized water and subsequently purified by dialysis against pure water.

3.4.2.3. Procedure for the synthesis of the α -alkyne functional homopolymer POEGA 2

3- (1,1,1-trimethylsilyl)-2-propynyl 2-bromo-2-methylpropanoate (166.8 mg, 0.6 mmol), copper bromide (86.07 mg, 0.6 mmol), and bipy (187.4 mg, 1.2 mmol) were added into a dry flask. The flask was sealed with a septum and subsequently purged with dry argon for several minutes. Then, thoroughly degassed OEGA (10 mL, 24 mmol) was added with a degassed syringe. The mixture was heated at 90°C in an oil bath for 3h. The experiment was stopped by opening the flask and exposing the catalyst to air. The final mixture was diluted with deionized water,

purified by dialysis against pure water (Roth, ZelluTrans membrane, molecular weight cut-off.4000-6000), and finally dried by rotary evaporation.

The trimethylsilyl (TMS)-protected POEGA was characterized by SEC and ^1H NMR. TMS-deprotection was performed in THF (0.01 M solution) in the presence of tetrabutylammonium fluoride (TBAF), as previously described⁶³. The reaction mixture was stirred overnight at room temperature. The final mixture was diluted with deionized water and subsequently purified by dialysis against pure water.

3.4.2.4. Procedure for the aqueous click ligation of PS-*b*-POEGA 1 and POEGA 2

In a flask, the ω -azido functional block copolymer PS-*b*-POEGA **1** (1.15 equiv.) was dissolved in deionized water (concentration of diblock polymer in water: $50\text{ g}\cdot\text{L}^{-1}$). Then copper (II) sulfate pentahydrate (1 equiv.), sodium L-ascorbate (2 equiv.), and the α -alkyne functional homopolymer POEGA **2** (1 equiv.) were added. The flask was capped with a septum and the solution was purged with dry argon for 20 min. The reaction mixture was stirred for 2 days at room temperature. After reaction, the final mixture was diluted with water and purified by dialysis against pure water (Roth, ZelluTrans membrane, molecular weight cut-off 4000-6000). Small copper aggregates, which could not be removed by dialysis, were separated by centrifugation. Finally, water was removed by rotary evaporation.

Chapter 4

Functionalization of polymer chain ends through methods other than CuAAC

4.1. Introduction

In the first parts of the present thesis, *in situ* copper-catalyzed azide-alkyne cycloaddition was used as a useful synthetic tool for functionalization of the chain ends of the synthetic polymers. However, other cycloaddition methods, especially metal-free ones have been developed to functionalize polymers. Some of these approaches were described in the theoretical chapter of this work. This brought a motivation to start two projects in collaboration with Frances Heaney research group in the National University of Ireland, Maynooth. In the present chapter, the results of these two approaches are discussed.

In the first project, metal-free nitrile oxide-alkyne cycloaddition (NOAC) was used as an efficient synthetic tool to functionalize the α -chain ends of well-defined biocompatible homo/copolymers of OEGMA and MEO₂MA.

In the second project, the orthogonal combination of nitrile oxide-alkyne and copper-catalyzed azide-alkyne cycloadditions (sequential NOAC and CuAAC) was employed to modify both α and ω chain ends of well-defined polystyrene.

Moreover, in the last part of this chapter, synthesis and characterization of two other α -functionalized co/polymers of P(OEGMA-*co*-MEO₂MA) are described. First example is tert-butoxycarbonyl (t-Boc) protected α -amino functionalized co/polymer which has a latent α -amino chain-end and could be deprotected in a post-polymerization step to give α -amino functionalized co/polymer. Second end-functionalized polymer is α -aldehyde functionalized copolymer of P(OEGMA-*co*-MEO₂MA).

After deprotection of the t-Boc protected polymers, α -amino functionalized polymers are reactive towards carboxylic acid groups of other polymers. The idea was to couple α -amino functionalized polymers with carboxylic acid end functionalities of other polymers, which have nitrile oxide functionalities on the other chain end. In the second step, these PEG-based nitrile oxide functionalized polymers could react with alkyne-functionalized oligonucleotide-based drugs (bioconjugation).

Since the aldehyde functionality of synthetic polymers can react with amine groups on the proteins²¹², α -aldehyde terminally functionalized copolymers of P(OEGMA-co-MEO₂MA) were synthesized to react with oligonucleotides in another project with collaboration with Frances Heaney research group in Ireland (bioconjugation), that is interested in the development of coupling methods for oligonucleotide bioconjugation¹⁰⁵.

4.2. Chain-end modification of biocompatible polymers via a “metal-free” cycloaddition of nitrile oxides and alkynes

Well-defined α and ω telechelic model homo/copolymers were synthesized by ATRP of oligo (ethylene glycol methacrylate)s. The α -alkyne functionality was introduced in polymers **P1** and **P2** (Figure 4.1, top) by using a trimethylsilyl-protected alkyne ATRP initiator, which is subsequently deprotected. Polymer synthesis and deprotection procedure is described in the end of this chapter (See sections 4.5.1 and 4.5.2). After characterization of the polymers, they were functionalized with some low molecular weight nitrile oxide model molecules (Figure 4.1, molecules **1-5**) via 1,3-dipolar cycloaddition of nitrile oxides and alkynes. In all cases, the nitrile oxide was prepared *in situ* from the oxime precursor (Figure 4.1, bottom) and (N-chloro-N-sodio-4-methylbenzene sulfonamide (chloramine T) was selected as the dipole generating agent²¹³. It should be mentioned that nitrile oxides are unstable and dimerize easily, so they are usually generated *in situ* from their oxime precursors.

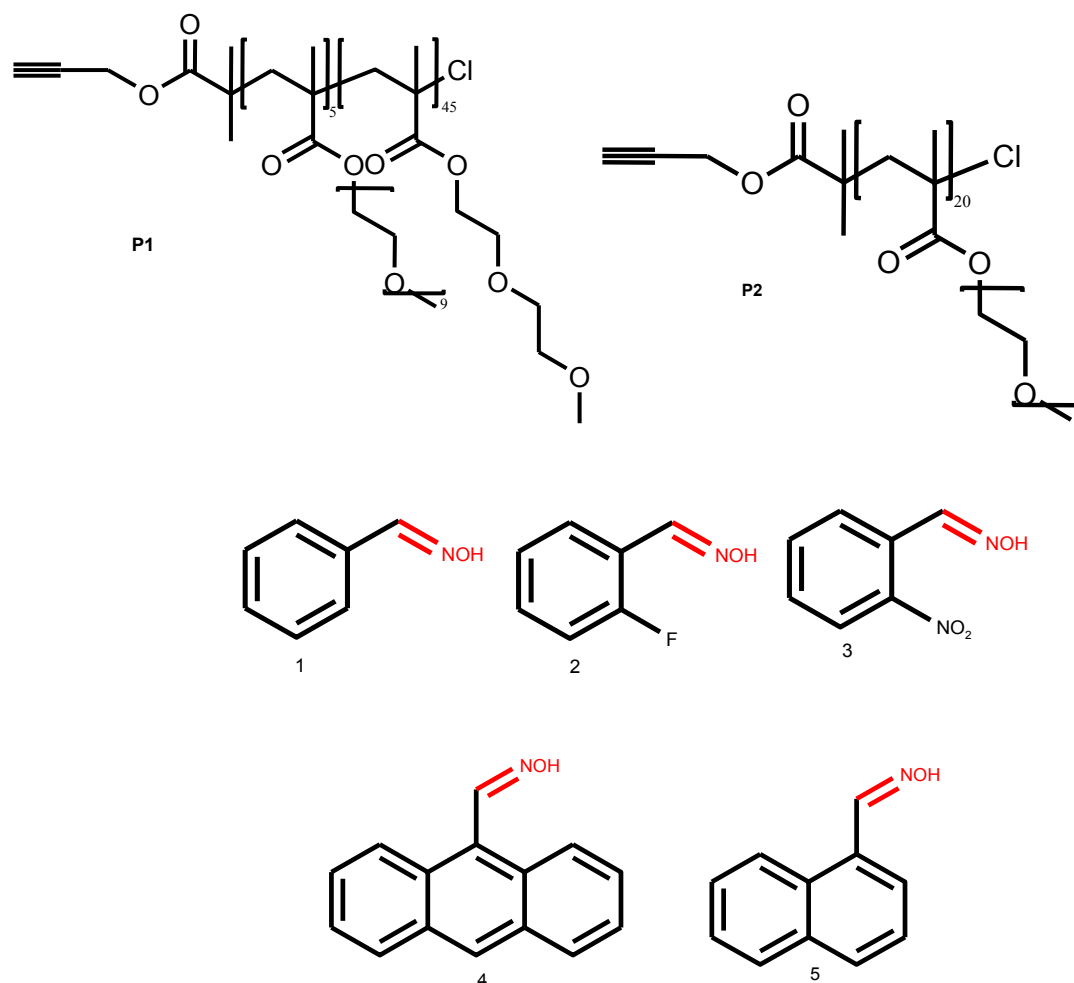


Figure 4.1. Molecular structures of the alkyne-functionalized homo/co polymers used for cycloaddition with some model nitrile oxides (top) and of the oximes used as nitrile oxide precursors (bottom).

The trimethylsilyl (TMS)-protected copolymer P(OEGMA-*co*-MEO₂MA) (**P1** in Figure 4.1 is the structure of OEGMA-*co*-MEO₂MA after TMS-deprotection) was synthesized via ATRP and characterized by SEC and ¹H NMR spectroscopy. **P1** was characterized by ¹H NMR, SEC and turbidimetry. From SEC chromatogram, $M_n=15000 \text{ g}\cdot\text{mol}^{-1}$, $M_w/M_n= 1.18$ was calculated. ¹H NMR spectrum of **P1** is shown in Figure 4.2. Characteristic α -alkyne proton (proton a) around 2.5 ppm and methylene protons in the α of the alkyne functionality (b protons) around 4.6 ppm are highlighted in Figure 4.2. Turbidimetry measurements showed that cloud point in pure water was 39 °C (transmittance of polymer solutions in water at concentration of $3 \text{ g}\cdot\text{L}^{-1}$ was measured).

TMS-protected P(OEGA) homopolymer **P2** was also synthesized by ATRP. After purification and characterization, this homopolymer was deprotected (**P2** in Figure 4.1). **P2** was characterized by ^1H NMR, SEC and turbidimetry and exhibited a well-defined molecular structure ($M_n = 100 \text{ g}\cdot\text{mol}^{-1}$; $M_w/M_n = 1.12$).

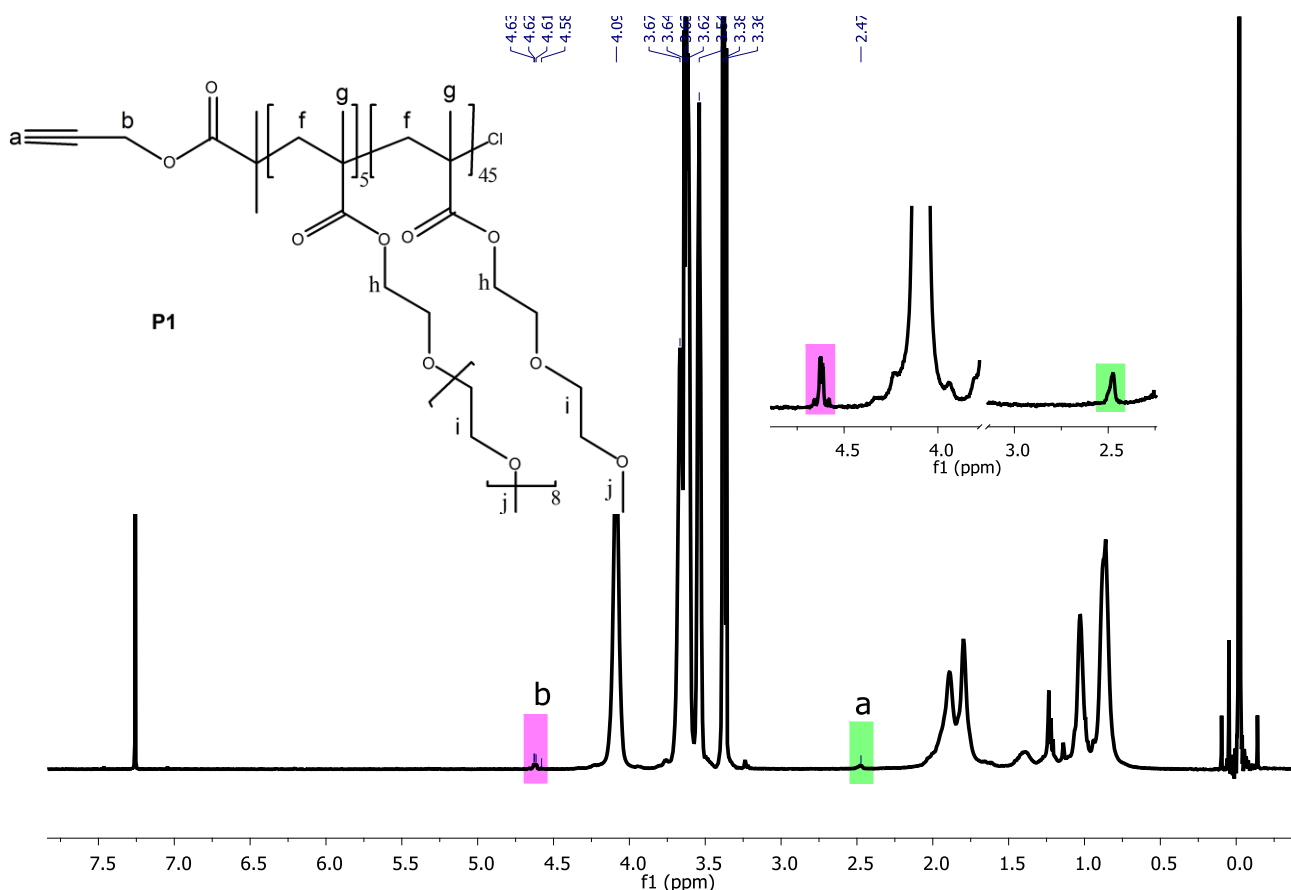


Figure 4.2 ^1H NMR spectrum of the α -alkyne functionalized P(OEGMA-*co*-MEO₂MA) **P1** recorded in CDCl_3 at room temperature.

4.2.1. Nitrile oxide-alkyne cycloaddition (NOAC) reactions on α -alkyne-functionalized polymers

After purification and characterization of α -alkyne functionalized **P1** and **P2**, nitrile oxide click reactions were performed on these two polymers. These functionalization reactions were done by Frances Heaney research group in the National University of Ireland, Maynooth. The nitrile

oxide-alkyne cycloaddition (NOAC) procedure is described in the end of this chapter (see sections 4.5.3 and 4.5.4). The procedures of the cycloaddition reactions of both polymers with all of the five oximes were almost the same with the exception of the NOAC of 2-nitrobenzo nitrile oxide on polymer alkyne **P1**. 2-nitrobenzo nitrile oxide dimerizes itself, so it has to be added in portions to drive the reaction to completion.

P1 is functionalized through NOAC with all of the five nitrile oxide precursors shown in Figure 4.1, whilst **P2** was reacted only with the oxime **1**. In Table 4.1 yields of these NOAC reactions and type of the produced regioisomers is shown.

Table 4.1 “Click” functionalization of poly(oligo ethylene glycol methacrylates) by 1,3-dipolar cycloaddition of nitrile oxides and alkynes^a

alkyne-polymer	nitrile oxide precursor	functionalized polymer	yield ^b (%)	formed isomer
P1	1	P1-1	>99	3,5
P2	1	P2-1	95	3,5
P1	2	P1-2	99	3,5
P1	3^c	P1-3	95	3,5
P1	4	P1-4	95	3,5
P1	5	P1-5	98	3,5

^a Experimental conditions: room temperature, chloramines-T, EtOH: 4%aqueous NaHCO₃ 1:1, 16h. ^b Estimated from the ¹H NMR spectra of the purified polymers. ^c A second dose of oxime and chloramine-T was added after the first 12h, total reaction time 24 h.

In almost all cases, nearly quantitative yields were obtained (Table 4.1). Additionally, the cycloaddition reaction is regioselective as evidenced by ¹H NMR and signals of 3,5-disubstituted isoxazole could be observed almost exclusively in all cases. Two possible isomers generated from NOAC are 3,4 and 3,5-disubstituted isoxazoles, which are shown in Figure 4.4 for polymer **P1-1** in Table 4.1.

In fact from ^1H NMR spectra of the polymers after cycloaddition it is clear that the characteristic signal of the alkyne function (2.5 ppm) disappeared in all NMR spectra and was replaced by new α -chain-end signals originating from the attached nitrile oxides. For all of the modified polymers, some new ^1H NMR characteristic signals of the 3,5-disubstituted isoxazole moiety are detected. For example, a signal around 6.50 ppm is the characteristic of the 4-H ring proton and neighbouring methylene protons of the isoxazole ring resonate at around 5.20 ppm²¹⁴. In Figure 4.3 the ^1H NMR spectrum of **P1-1** functionalized polymer is demonstrated.

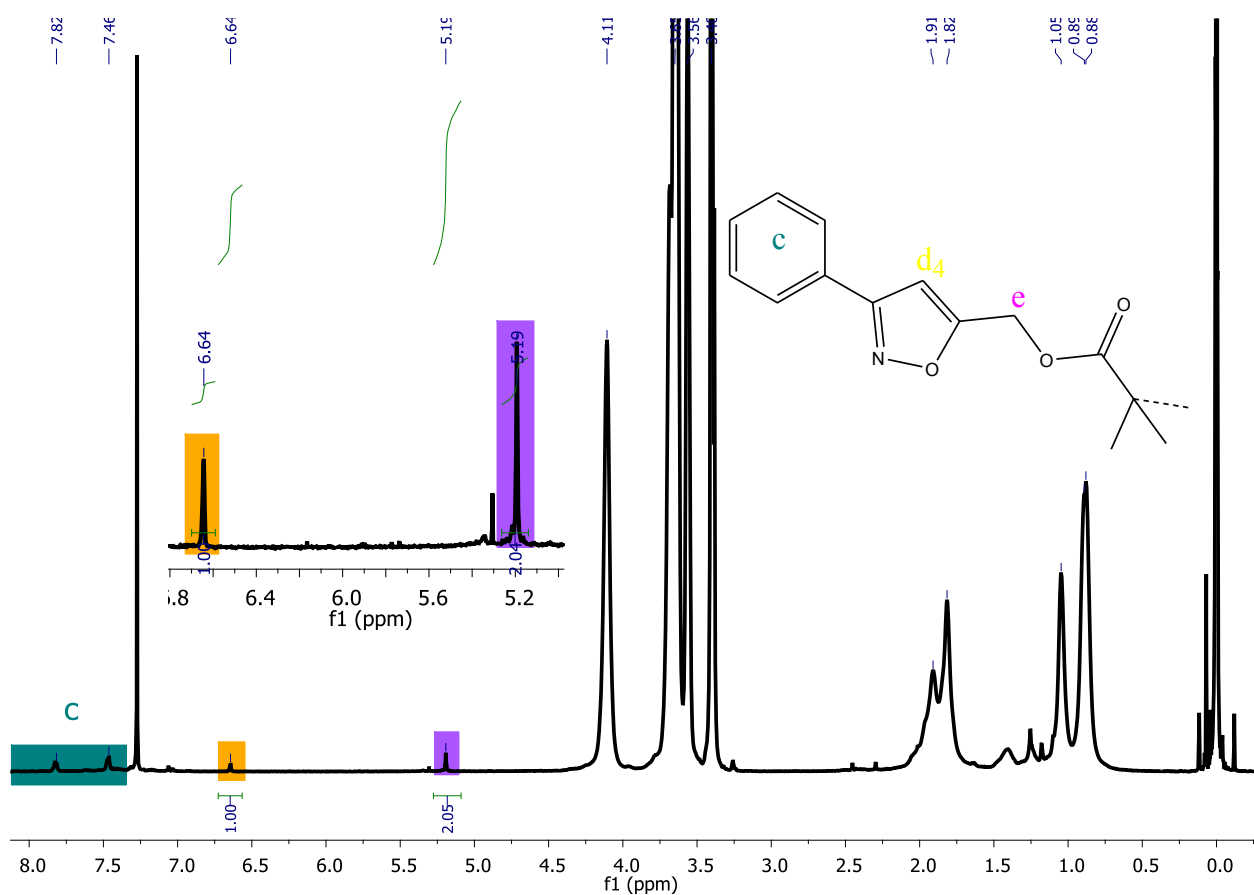


Figure 4.3. 500 MHz ^1H NMR spectrum recorded in CDCl_3 for the polymer **P1** after reaction with the nitrile oxide derived from oxime **1** (Polymer **P1-1** in Table 4.1).

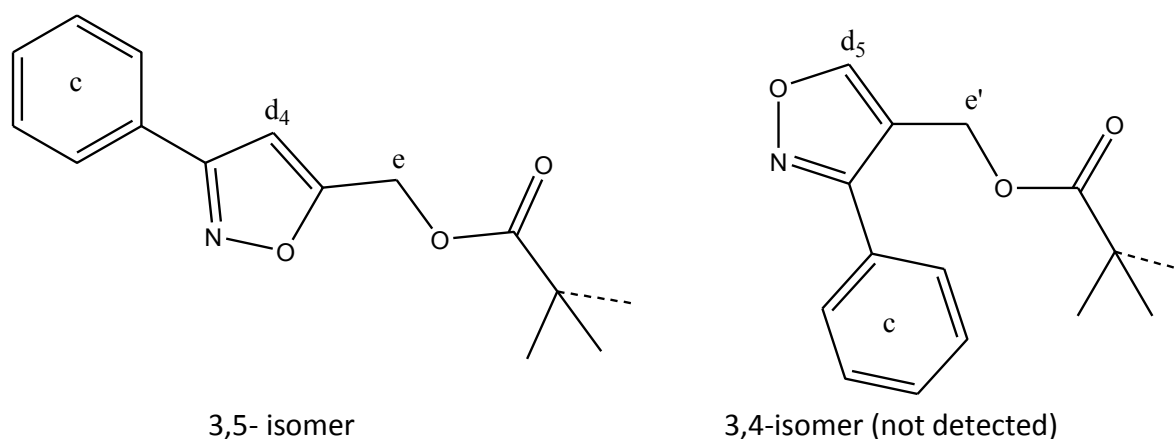


Figure 4.4. Structures of two possible regio-isomers generated from cycloaddition of α -alkyne functionalized polymer with a model nitrile oxide molecule. ^1H NMR analysis demonstrated that only 3,5-isomer was detected as product.

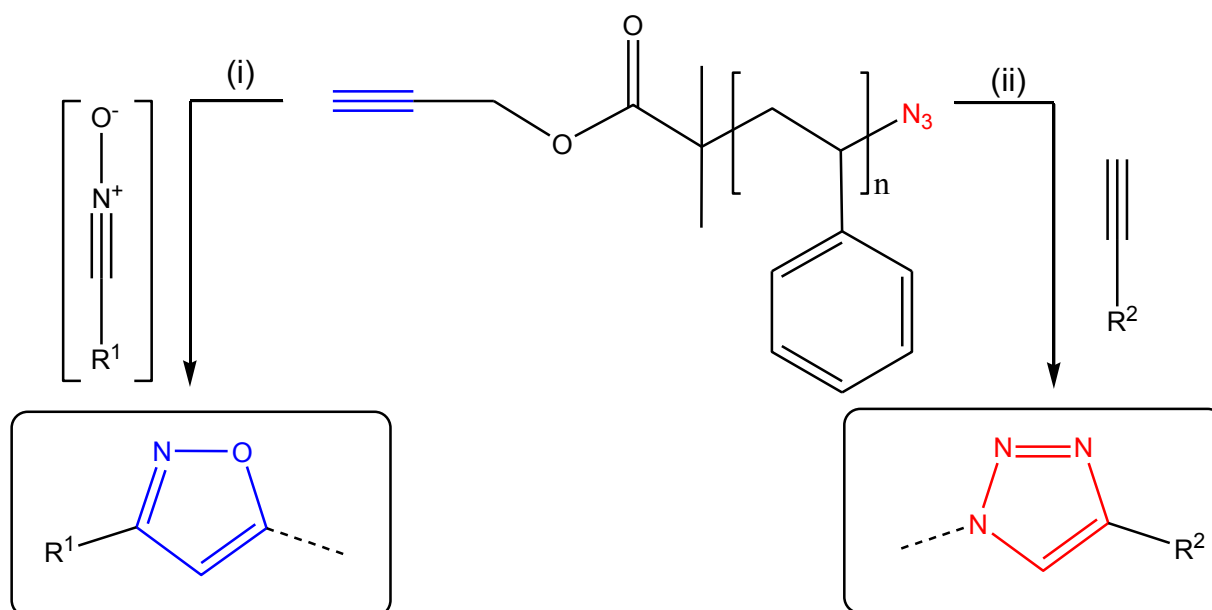
By further interpretation of the ^1H NMR signals, no evidence of the other regio-isomer, 3,4-disubstituted isoxazole is detected. It could be argued that if 3,4-isomer might exist also as the product, its methylene protons next to the isoxazole ring (e' protons in Figure 4.4) would resonate at the same region as the 3,5-isomer's methylene protons (e protons in Figure 4.4) resonate, i.e. around 5.20 ppm. To check this hypothesis, the relative integrals of the signals representing the 4-H-isoxazole proton (d_4 in Figure 4.4) and the methylene protons were investigated, which gave a ratio of 1H/2H. This confirms the formation of only 3,5-isomer as the product, since if 3,4-isomer had been also generated and its methylene protons had been expected to resonate around 5.20 ppm as well, this integration ratio would have been expected to be 1H/4H but not 1H/2H. It should be noted that 5-H isoxazole ring proton of the 3,4-isomer (d_5 in Figure 4.4) would have been expected to resonate in the region of 7.50-8.50 ppm^{215,216,217} and therefore this signal could have been probably masked by other aromatic signals (c protons in Figure 4.4). However, a small fraction of the 3,4-regioisomer might be produced in this click cycloadditions. If so, these structures could not be detected by standard polymer analysis techniques.

Both modified polymers of **P1** and **P2** were also characterized by SEC and turbidimetry after 1,3-dipolar cycloaddition of nitrile oxides and alkynes. SEC measurements showed no change in

molecular weight and molecular weight distribution of the polymers after modification. Also, the cloud points observed in pure water for the modified polymers remained almost unchanged after cycloaddition. However, depending on the nature (hydrophobicity) of the chain ends, a slight change of ($\pm 1^\circ\text{C}$) was observed for different modified polymers obtained from **P1**. For example, for **P1-4** and **P1-5** modified polymers cloud points in pure water were shifted to 38°C compared to the cloud point of **P1** before modification (39°C). This phenomenon results from higher hydrophobicity of the oximes **4** and **5** used for NOAC.

4.3. Orthogonal modification of polymers chain-ends via sequential nitrile oxide-alkyne and azide-alkyne Huisgen cycloadditions

A model polystyrene chain bearing α -alkyne and ω -azido end-groups was modified first by nitrile oxide-alkyne cycloaddition (NOAC) and then by copper-catalyzed azide-alkyne cycloaddition (CuAAC) (Scheme 4.1). The mentioned project was a collaboration with the research group of professor Heaney in Ireland. The two mentioned methods appear as efficient complementary tools in polymer design in a sequential orthogonal approach. Sequential orthogonal approaches have been recently shown to be interesting pathways for functionalization and multiple labeling of materials^{218,219,220,221}. The ‘click’ type methods generally have been demonstrated to be very versatile and efficient reactions for post-modification or functionalization of polymers prepared by controlled radical polymerization techniques^{151,6,80,89,169,222,223}. Nitrile oxide-alkyne cycloaddition (NOAC), evidenced as a very efficient tool in polymer chemistry, is regioselective and proceeds in high yields in the absence of metal catalyst^{5,105, 214,224, 225,226,227,228}.



Scheme 4.1. General strategy for the synthesis of well-defined heterotelechelic polystyrene. Experimental conditions: (i) $R_1CH=NOH$ (precursor oxime), NCS (N-chlorosuccinimide), NEt_3 , CH_2Cl_2 , RT; (ii) CuBr, HMTETA, THF, RT.

4.3.1. Synthesis of well-defined α -alkyne, ω -azido heterotelechelic polystyrene

The α -alkyne, ω -azido heterotelechelic polystyrene, **Q** was synthesized in three steps. First, bromine end-functionalized polystyrene was synthesized by bulk ATRP in the presence of a radical initiator bearing a trimethylsilyl-protected alkyne initiator⁶³. The procedure for bulk ATRP of styrene is described in a separate chapter (bulk ATRP of styrene is performed in the presence of (1,1,1-trimethylsilyl)-2-propynyl 2-bromo-2-isobutyrate as protected initiator, and copper bromide and pentamethyldiethylenetriamine as catalyst).

It has been reported that unprotected alkyne-containing initiators can be used in ATRP of styrene^{70,71}. However, there is always a risk of unwanted side reactions, such as radical addition to the triple bond in radical polymerizations^{229,230,231}. Hence, in the present study, a TMS-protected alkyne-functionalized initiator was used in order to minimize chain-end functionality losses. Such a TMS-protecting group can be easily cleaved after polymerization in the presence

of TBAF. After polymerization and purification, SEC and ^1H NMR spectral analysis confirmed that a well-defined heterotelechelic precursor was synthesized ($M_n = 3700 \text{ g}\cdot\text{mol}^{-1}$; $M_w/M_n = 1.2$). Afterwards, in the second step, the bromine chain-end of this precursor was transformed to azide by sodium azide mediated nucleophilic substitution. In the third step, TMS deprotection was done using tetrabutylammonium fluoride (TBAF). ^1H NMR spectrum of the α -alkyne, ω -azido heterotelechelic polystyrene **Q** is shown in figure 4.5.

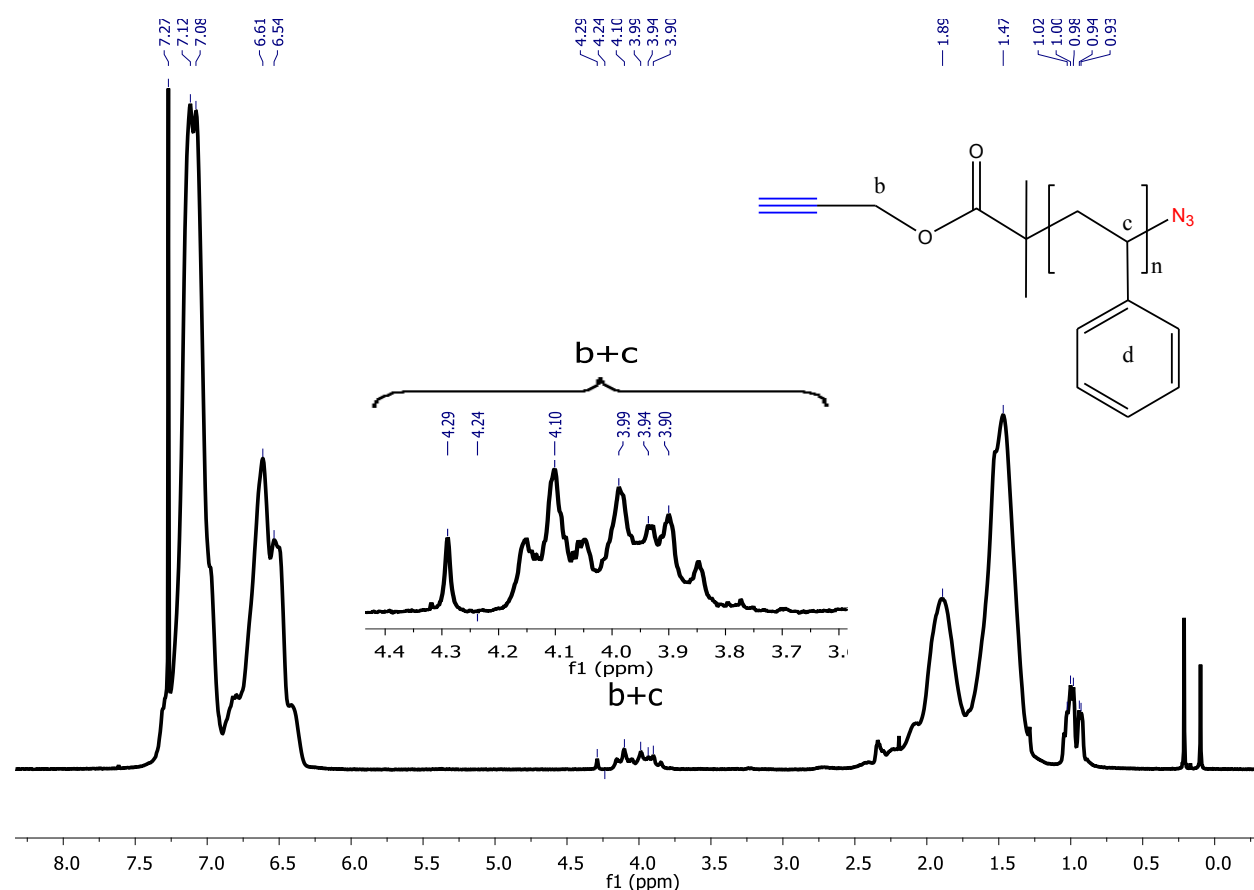


Figure 4.5. ^1H NMR spectrum of the α -alkyne, ω -azido heterotelechelic polystyrene **Q** recorded in CDCl₃.

In ^1H NMR spectrum of the polystyrene **Q** as it is shown in Figure 4.5, a broad signal is observed at 3.75-4.25 ppm, which is the characteristic of two types of protons located on the both chain ends, i.e. the signal corresponding to the methylene protons located in the α position of the

alkyne function (proton b in Figure 4.5) and a signal due to the proton neighboring the azide function which resonates around 4.0 ppm (proton c in Figure 4.5). These two signals overlap with each other and are therefore shown as 'b+c' protons as a broad signal.

It should be emphasized that the sequence of transformation to azide and TMS deprotection is important. Even though, in theory, the deprotection step can be performed directly after ATRP polymerization or after the nucleophilic substitution with NaN_3 , some experimental results obtained in the research group of J.F.Lutz showed that the sequence of azide transformation and TMS deprotection can not be interchanged²³². According to this study, two sequences of reactions can be considered for preparing α -alkyne, ω -azido heterotelechelic polystyrene: ATRP, deprotection, and substitution (approach **a**) or ATRP, substitution, and deprotection (approach **b**) (see Figure 4.6 and 4.7 for approaches **a** and **b**, respectively). Both approaches were evaluated with model polystyrene samples ($M_n \approx 2000 \text{ g}\cdot\text{mol}^{-1}$; $M_w/M_n \approx 1.2$).

Figure 4.6 shows the ^1H NMR spectra of a polystyrene sample in different stages of approach **a**. This sample was first synthesized by ATRP in the presence of 3-(1,1,1-trimethylsilyl)-2-propynyl 2-bromo-2-methylpropanoate. After purification and isolation, the corresponding NMR spectrum displayed characteristic signals of the initiator moiety at 0.17, 0.80 to 1.05, and 3.65 to 4.2 ppm (Figure 4.6.A, protons c, d, and a, respectively). In addition, a clear signal due to the methine proton located in the α position of the terminal bromine atom can be observed at 4.30 to 4.65 ppm (Figure 4.6.A. proton b). The integration of these chain-end signals indicated a degree of bromine functionality above 95%. This well-defined polymer was subsequently reacted with TBAF to deprotect the alkyne moieties. As expected, the signal of the methyl groups of TMS (c protons) vanished almost quantitatively at 0.17 ppm (as observed in Figure 4.6.B and 4.6.C, around 5% of the c protons were still remained after deprotection), and a new signal due to the alkyne terminal proton appeared at 2.31 ppm (Figure 4.6.B, e protons). This NMR spectrum indicates an efficient deprotection process. However, the chain-end peak at 4.30 to 4.65 ppm also disappeared after TBAF treatment. The peaks around 0.03-0.1 ppm originate from impurities (e.g., grease) on the glassware joints.

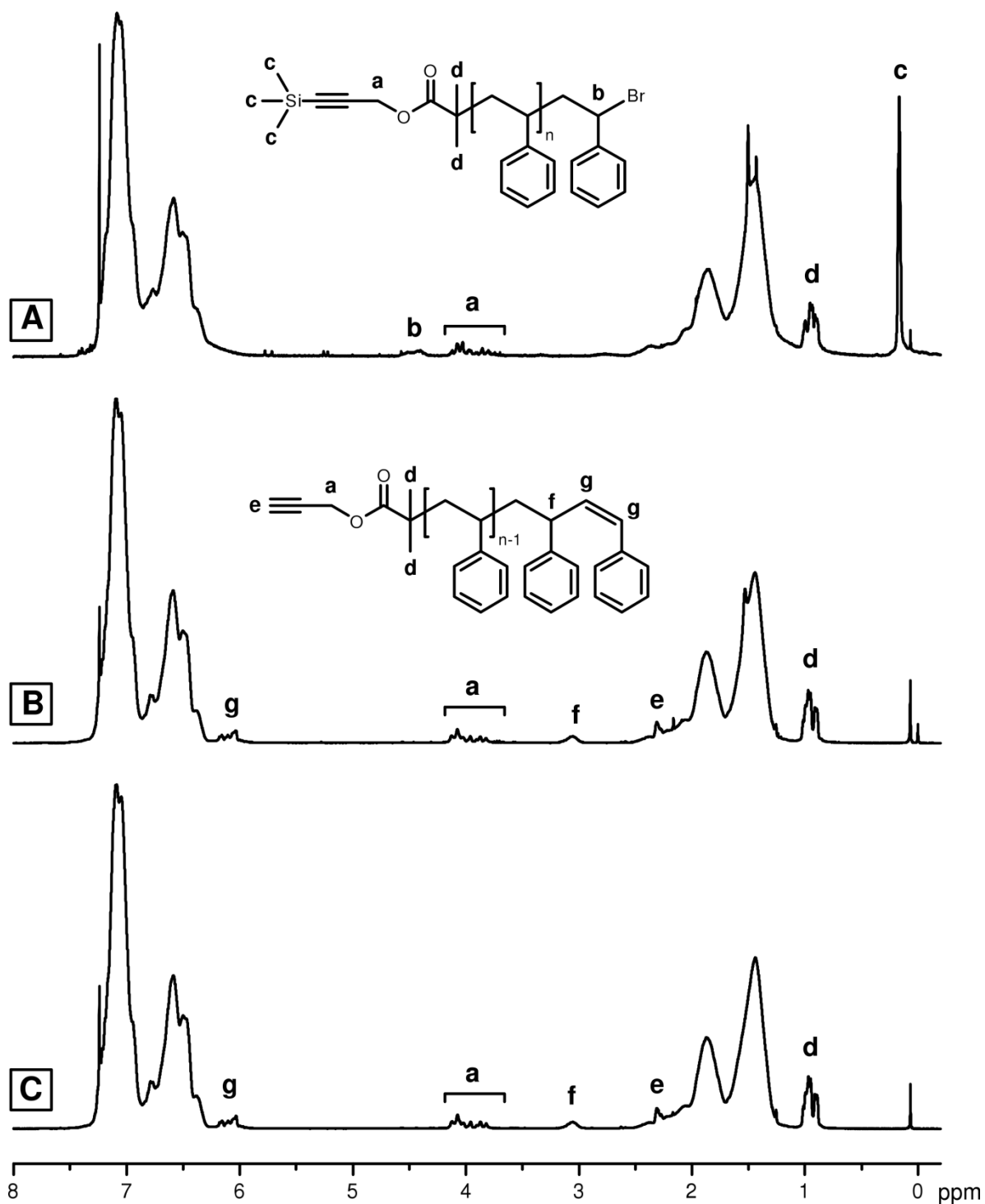


Figure 4.6. ^1H NMR spectra recorded in CDCl_3 for a α -alkyne functional polystyrene sample: (A) after ATRP synthesis and purification; (B) after TBAF treatment and (C) after NaN_3 treatment (approach a).

This seems to indicate that the bromine chain ends were modified during this deprotection step. In fact, two new peaks can be observed in this spectrum at 5.90 to 6.25 ppm and 3.05 ppm (Figure 4.6.B, protons g and f). The first signal is typical for a polystyrene terminal unsaturation, whereas the latter probably corresponds to the methine proton located in the α position of this double bond. These experimental observations suggest that HBr elimination occurred in the presence of TBAF. As a consequence, bromine atoms are not available for nucleophilic substitution after this step. Indeed, after NaN_3 treatment, no significant change could be observed in the NMR spectrum (Figure 4.6.C). Furthermore, only a weak azide signal could be observed in the FT-IR spectrum of the final polymer (data not shown). Therefore, it seems that approach **a** can not be used to prepare α -alkyne, ω -azido heterotelechelic polystyrene.

Figure 4.7 shows the ^1H NMR spectra of a polystyrene sample in different stages of approach **b**. In this case, NaN_3 nucleophilic substitution was performed directly after the ATRP step. Both FT-IR and NMR spectroscopy evidenced the successful formation of azide chain ends. In the IR spectrum, an intense absorption band at 2094 cm^{-1} , corresponding to the asymmetric stretching vibration of the azide function, was observed. In addition, a signal due to the methine proton located in α of the azide function could be observed in the NMR spectrum (Figure 4.7.B, proton h). This peak overlaps with another signal because of the initiator moiety but can be distinguished around 4.0 ppm. Afterwards, this polystyrene sample was treated with TBAF, thus leading to the almost quantitative removal of the TMS protecting group (around 5% of the c protons were still in the purified sample after deprotection) (Figure 4.7.C). After purification and isolation, the final polystyrene exhibited clear NMR and IR signals corresponding to both alkyne and azide chain ends. Therefore, approach **b** is a reliable strategy for synthesizing α -alkyne, ω -azido heterotelechelic polystyrene. In Figure 4.7., the peaks around 0.03-0.1 ppm originate from impurities (e.g., grease) on the glassware joints.

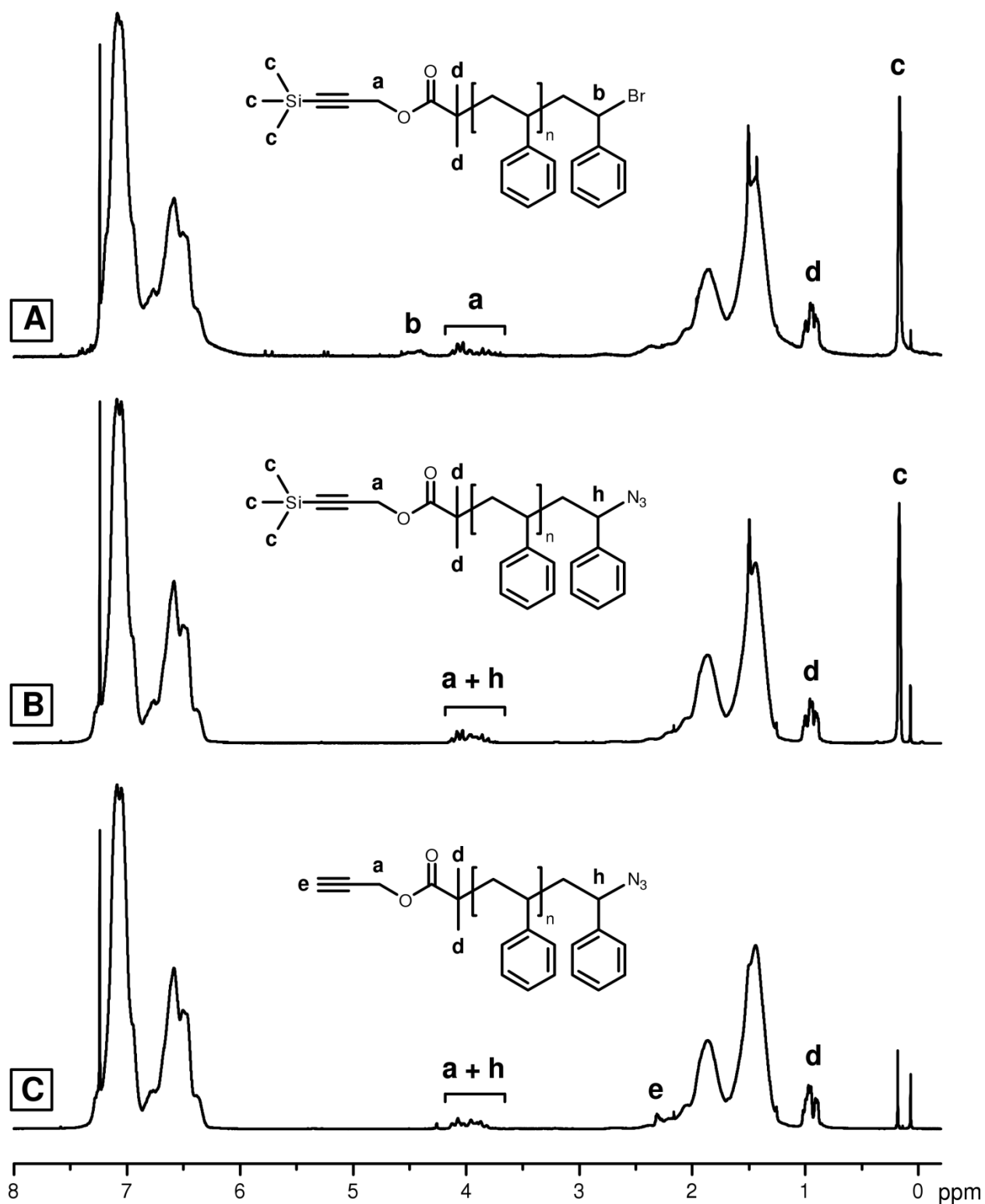
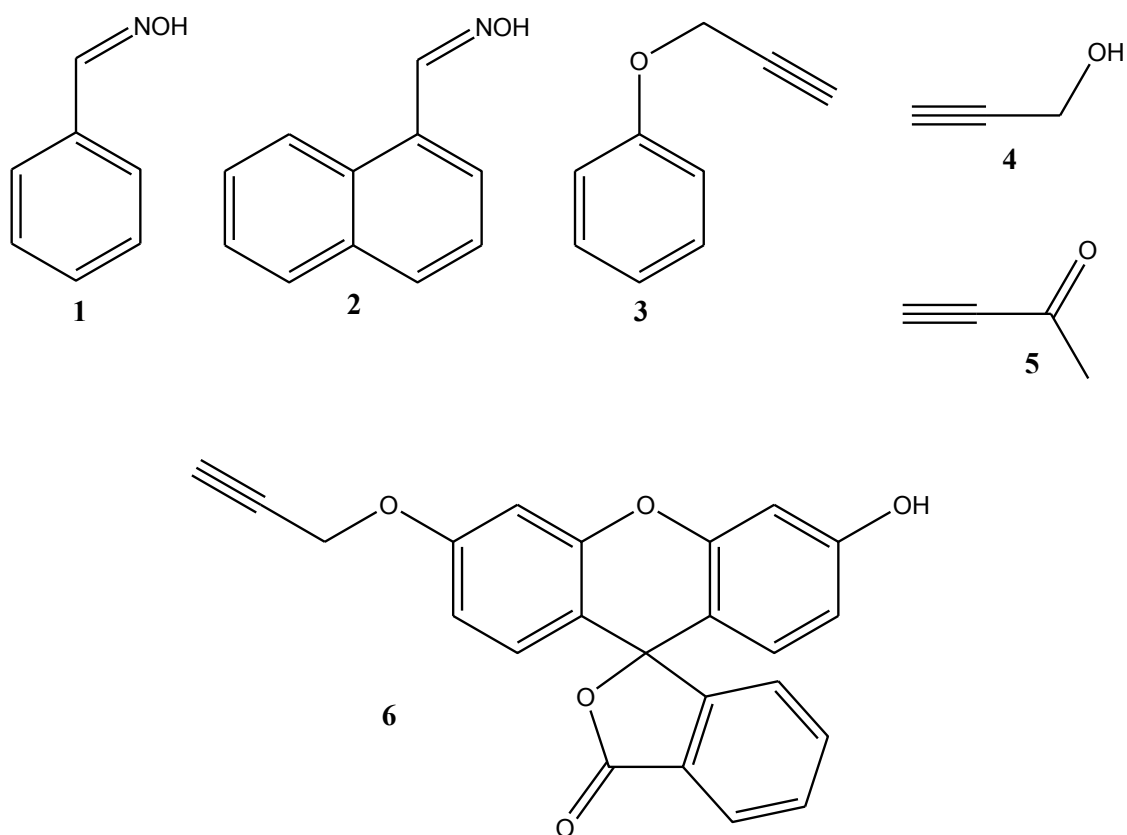


Figure 4.7. ^1H NMR spectra recorded in CDCl_3 for a α -alkyne functional polystyrene sample: (A) after ATRP synthesis and purification; (B) after NaN_3 treatment and (C) after TBAF treatment (approach b).

After α -alkyne, ω -azido heterotelechelic polystyrene **Q** was synthesized and characterized, the α -alkyne chain-end of this precursor was first modified *in situ* from the oxime precursors via hydroxyimoyl chloride intermediates (Table 4.2). Two model oximes were used in this study:

benzaldehyde oxime **1** and 1-naphthaldehyde oxime **2** (structures **1-2** in Scheme 4.2), the ω -chain ends of the resulted functionalized polystyrene molecules, **Q1** and **Q2** were then functionalized by CuAAC in a second step (Table 4.2). Four different alkyne models were investigated in this study (structures **3-6** in scheme 4.2).



Scheme 4.2. Molecular structure of the model compounds used for chain-end modification

Table 4.2. Sequential functionalization of polystyrene chain-ends

Polymer precursor	Nitrile oxide precursor ^a	Functional alkyne ^b	Functionalized polymer	Yield ^c (%)
Q	1	-	Q1	>99%
Q	2	-	Q2	>99%
Q1	-	3	Q13	>99%
Q1	-	4	Q14	>99%
Q1	-	5	Q15	>99%
Q2	-	4	Q24	>99%
Q2	-	5	Q25	>99%
Q2	-	6	Q26	>99%

^a Modification of the α -chain end via nitrile oxide-alkyne cycloaddition. ^b Modification of the ω -chain end via copper-catalyzed azide-alkyne cycloaddition. ^c Estimated from the ¹H NMR spectra of the purified polymers.

4.3.2. Nitrile oxide-alkyne cycloaddition (NOAC) step

The nitrile oxide-alkyne cycloadditions of polymer **Q** with nitrile oxides derived from precursors **1** and **2** were done in the research group of Professor Heaney in Ireland (see section 4.5.5). From the ¹H NMR spectra of the purified polymers after reaction with nitrile oxides derived from both **1** and **2**, it was evidenced that functionalization proceeded in very high yields in all cases. For example, ¹H NMR spectrum of a purified polymer after reaction with the nitrile oxide derived from **1** is shown in Figure 4.8. As it is observed, after the NOAC step several new chain-end signals due to the clicked phenyl moiety appeared in the characteristic aromatic region (a protons in Figure 4.8). Furthermore, the methylene protons b in the α - to the alkyne functionality were significantly shifted downfield (4.25-4.85 ppm), which confirmed the

formation of an isoxazole ring. Moreover, the signal due to the proton neighboring the azide function (proton c resonating at 3.8-4.1 ppm) still remained after NOAC, which confirmed that azide functionality stayed chemically inert during the NOAC step.

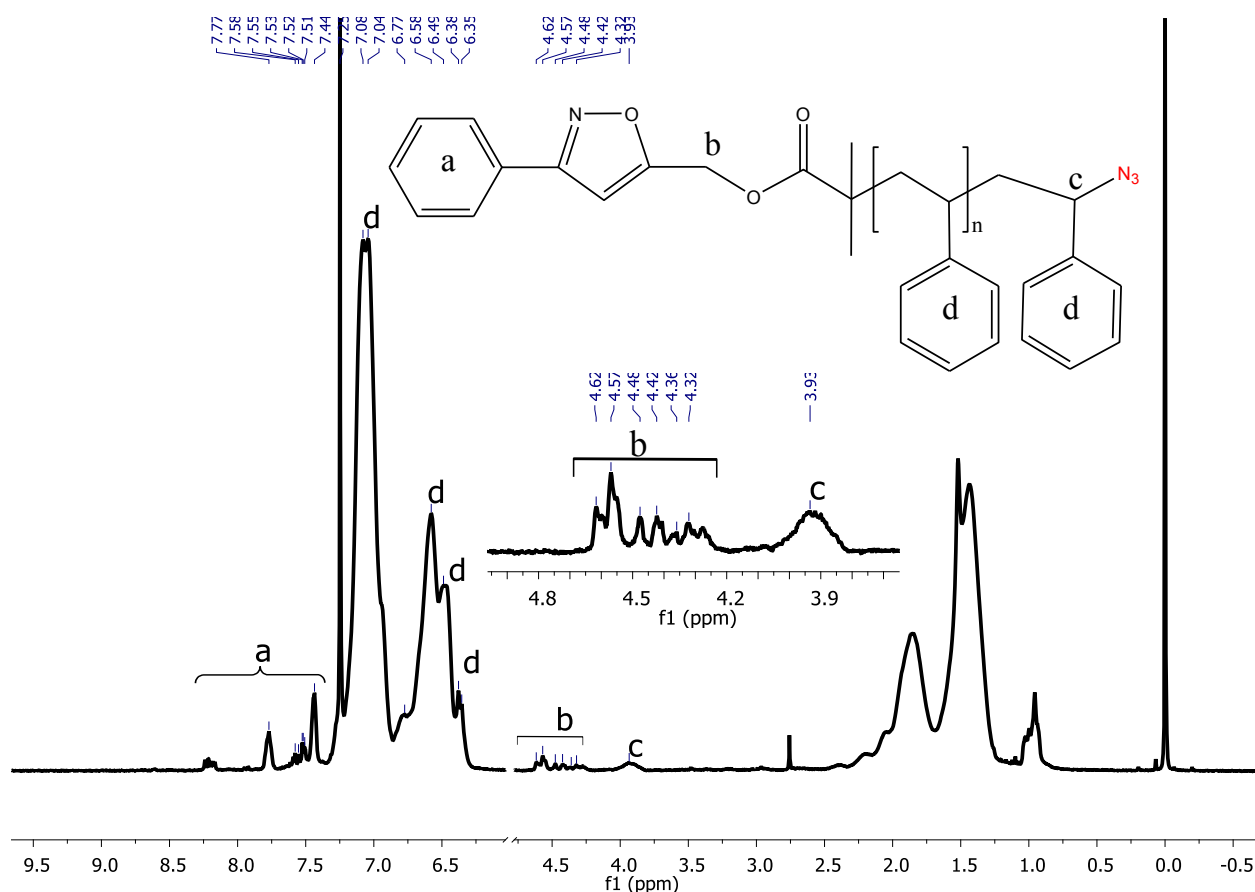


Figure 4.8. ^1H NMR spectrum of a purified PS after reaction with the nitrile oxide derived from **1**

4.3.3. Copper-catalyzed azide-alkyne cycloaddition (CuAAC) step

The CuAAC reactions were done in the research group of Professor Heaney in Ireland (see section 4.5.6). From the ^1H NMR spectra of the purified polymers after the CuAAC step, it was obvious that nearly quantitative chain-end modification were obtained in all cases (^1H NMR

spectrum is not shown). For all model alkynes after click cycloaddition, the quantitative shift of methine proton in the α position of the azide end-group (c proton resonating at 3.8-4.1) to the characteristic peak of the methine proton in the α of the formed triazole ring (at 4.95-5.25 ppm) was observed.

4.4. Inducing some other α -functionalities in co/polymers synthesized by ATRP

4.4.1. Synthesis of protected α -amino functionalized co/polymer P(OEGMA-co-MEO₂MA)

Amine terminated polymers were another group of functionalized polymers which were synthesized and investigated in the present thesis. During ATRP process, aliphatic primary amines can react with the halogen chain ends and after polymerization they might act as nucleophiles and replace halogens by other functional groups²³³. Because of these side reactions, in order to get α -amino polymers by ATRP, it is suggested that the amino group of the ATRP initiator be protected and later be deprotected in a post-polymerization step. After deprotection, this amino end group could react for example through amidification with carboxyl group of another polymeric molecule and generate a new chain end-functionality which can further go through modular reactions to couple different blocks.

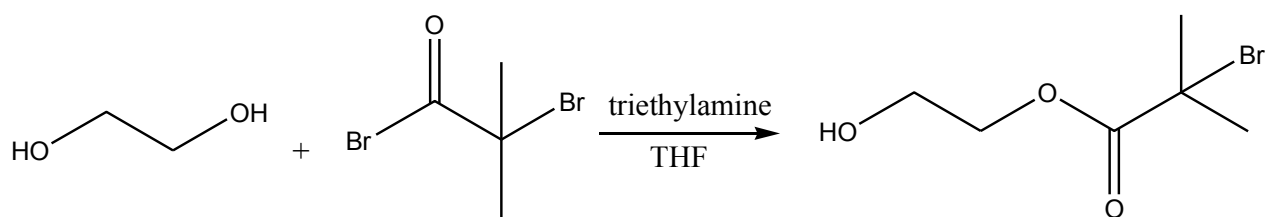
Here, a tert-butoxycarbonyl (t-BOC) protected initiator, t-Boc-2-aminoethyl-2-bromoisobutyrate was synthesized and characterized by ¹H NMR (Figure 4.7, top)²³⁴. This initiator was then used for the synthesis of homopolymer, P(OEGMA) and copolymer, P(OEGMA-co-MEO₂MA). Characterization of these co/polymers by SEC and ¹H NMR showed well-defined structures: homopolymer ($M_n=9400\text{ g}\cdot\text{mol}^{-1}$; $M_w/M_n=1.09$) and copolymer ($M_n=13080\text{ g}\cdot\text{mol}^{-1}$; $M_w/M_n=1.22$).

^1H NMR spectrum of the purified homopolymer of POEGMA is shown in figure 4.7, bottom. A characteristic signal due to the 9 protons of the methyl groups of initiator is observed at around 1.46 ppm in the spectrum of the homopolymer (**a** protons in figure 4.7, bottom). By comparing the integrations of these methyl protons and of the methylene protons in the α position of the ester group of the side chains of the homopolymer (**e** protons in figure 4.7, bottom), the average degree of polymerization is calculated ($\text{DP}_n = 20$).

4.4.2. Synthesis of the α -aldehyde functionalized copolymer P(OEGMA-co-MEO₂MA)

In order to synthesize an α -aldehyde functionalized polymer, oxidation of the terminal hydroxyl functionality of the polymer into the aldehyde functionality was done²³⁵. In this method, the hydroxyl-functionalized polymer was added to acetic anhydride in DMSO and stirred for 30 h at room temperature²³⁵. At the end of the reaction and after product purification, the Schiff test was done to estimate the conversion of the hydroxyl groups to the aldehyde functionalities. So, as the previous step to this oxidation step, a copolymer of P(OEGMA-co-MEO₂MA) with a hydroxyl-functionalized initiator was synthesized via ATRP. The initiator used was 2-hydroxyethyl bromoisobutyrate (HEBB) which was synthesized according to the literature²³⁶.

The hydroxyl functionalized initiator was synthesized from ethylene glycol and 2-bromoisobutyryl bromide according to the literature²³⁶ (scheme 4.3). After characterization of the purified initiator with ^1H NMR, three characteristic peaks of the purified initiator were detected (spectrum not shown).



Scheme 4.3. Schematic synthesis of ATRP initiator, 2-hydroxyethyl bromoisobutyrate.

After synthesis and characterization of the initiator, the α -functionalized copolymer of P(OEGMA-co-MEO₂MA) was synthesized and characterized by ¹H NMR and SEC ($M_n=12300$ g·mol⁻¹; $M_w/M_n=1.34$). This well-defined copolymer was then oxidized to make an α -aldehyde copolymer of P(OEGMA-co-MEO₂MA). Hydroxyl groups were oxidized by dimethylsulfoxide (DMSO) which was activated with acetic anhydride which acted as activating electrophilic reagent²³⁷.

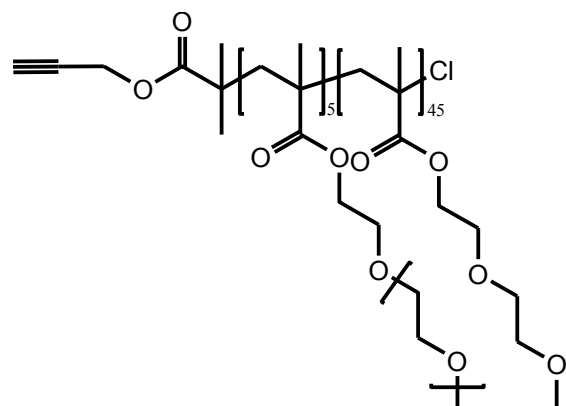
For the analysis of the aldehyde groups formed after the oxidation reaction, Schiff's reagent for aldehydes was used (see section 4.5.8). After addition of the Schiff's reagent to the aldehyde-functionalized product and shaking of the vial, a magenta (purple)-colored product was formed. Indeed, after attachment of the Schiff's reagent to the PEG-based polymer an absorption is expected to be observed ($\lambda_{max}=560$ nm). This estimated value for wavelength is extracted from literature for absorption of the Schiff's reagent attached to the PEG-aldehyde samples [33].

To investigate if the development of the magenta color is due to the attached Schiff's reagent to the aldehyde group on the polymer, some GPC/UV measurements were done. Two samples were prepared for the measurements (wavelength adjusted at $\lambda_{max}=560$ nm). The first sample was a mixture of polymer and Schiff's reagent and second sample was polymer without Schiff's reagent. For the polymer/Schiff's reagent mixture, a UV signal was detected but for the pure polymer no signal was detected. This result was expected since the pure polymer without Schiff's reagent has no absorption at this wavelength. This experiment confirms that aldehyde functionality existed on the polymer and conversion of the hydroxyl functionality to aldehyde was successful.

4.5. Synthetic procedures

4.5.1. Chain-end modification of biocompatible polymers via a “metal-free” cycloaddition of nitrile oxides and alkynes

4.5.1.1. TMS-protected copolymer P(OEGMA-co-MEO₂MA) P1 by ATRP



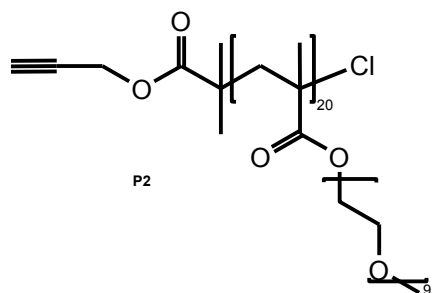
Copper (I) chloride (62.5 mg, 0.63 mmol) and 2,2'-bipyridyl (197.3 mg, 1.26 mmol) were added to a Schlenk tube sealed with a septum. The tube was purged with dry argon for a few minutes. Then, a degassed mixture of oligo(ethylene glycol) methyl ether methacrylate (1.5 g, 3.16 mmol), 2-(2-methoxyethoxy) ethyl methacrylate (5.35 g, 28.4

mmol), 3-(1,1,1-trimethylsilyl)-2-ropynyl 2-bromo-2-methylpropanoate (175.6 mg, 0.63 mmol), and 7 mL of ethanol was added through the septum with a degassed syringe. The mixture was heated at 60 °C in an oil bath for 1 day. The polymerization was stopped by opening the flask and exposing the catalyst to air. The solution was diluted with deionized water and subsequently purified by dialysis against water (Roth, ZelluTrans membrane, molecular weight cutoff: 4000-6000). Last, water was removed by rotary evaporation.

TMS-deprotection was performed in THF (0.01 M solution) in the presence of TBAF, as previously described⁶⁸. The reaction mixture was stirred overnight at room temperature. The final mixture was diluted with deionized water and subsequently purified by dialysis against pure water.

P1: ¹H NMR (500 MHz, CDCl₃): δ 0.85-1.13 ppm (br. m, -CH₃), 1.75-2.25 (br. m, CH₂- backbone), **α-alkyne end group: 2.46 (m, 1H, -C≡CH)**, 3.35- 3.50 (br. s, CH₃-O), 3.50-3.70 (m, CH₂-CH₂-O), 4.00-4.25 (br. s, CH₂-O-CO), **4.61 (m, 2H, CH₂-C≡CH)**.

4.5.1.2. Synthesis of the homopolymer P2 by ATRP



Copper (I) chloride (20.8 mg, 0.21 mmol) and 2,2'-bipyridyl (65.76 mg, 0.42 mmol) were added to a Schlenk tube sealed with a septum. The tube was purged with dry argon for a few minutes. Then, a degassed mixture of poly(ethylene glycol) methyl ether methacrylate (2 g, 4.21 mmol), 3- (1,1,1-trimethylsilyl)-2-propynyl 2-bromo-2-methylpropanoate (58.5 mg, 0.21 mmol) and 1.85 mL of ethanol was added through the septum with a degassed syringe. The mixture was heated at 60 °C in an oil bath for 1 day. The experiment was stopped by opening the flask and exposing the catalyst to air. The solution was diluted with deionized water and subsequently purified by dialysis against water. Last, water was removed by rotary evaporation. At this stage, the trimethylsilyl (TMS)-protected POEGMA was characterized by SEC and ¹H NMR. TMS-protected POEGMA (1600 mg, 0.198 mmol) was dissolved in 19.8 mL THF (0.01 M solution) and 518 mg of TBAF. The reaction mixture was stirred overnight at room temperature. The final mixture was diluted with deionized water and subsequently purified by dialysis against pure water.

P2: ¹H NMR (500 MHz, CDCl₃): δ 0.70-1.25 ppm (br. m, -CH₃), 1.75-2.25 (br. m, CH₂- backbone), **α-alkyne end group: 2.53 (m, 1H, -C≡CH)**, 3.35-3.50 (br. s, CH₃-O), 3.50-3.70 (br. m, CH₂-CH₂-O), 4.00-4.25 (br. s, CH₂-O-CO), **4.61 (m, 2H, CH₂-C≡CH)**.

4.5.1.3. Nitrile oxide click reactions on polymer alkynes P1 and P2

To the polymer alkyne (mg) (**P1** or **P2**) in a round bottom flask, ethanol (1 mL) and 4% aqueous NaHCO₃ (1 mL) were added, followed by oxime (1-2, 4-5 in Figure 4.1, 0.50 mmol) and chloramine-T monohydrate (0.98 mmol, 224 mg). The mixture was stirred at room temperature for 16 h. The reaction mixture was diluted with ethanol (5 mL) and purified by dialysis first

against water and subsequently against ethanol (Roth, ZelluTrans membrane, molecular weight cutoff: 4000-6000). Finally, solvent was removed by rotary evaporation.

P1-1: ^1H NMR (500 MHz, CDCl_3): δ 0.85-1.13 ppm (br. m, $-\text{CH}_3$) , 1.75-2.25 (br. m, CH_2 backbone), 3.20-3.50 (br. s, $\text{CH}_3\text{-O}$), 3.50-3.70 (br. m, $\text{CH}_2\text{-CH}_2\text{-O}$), 4.00-4.25 (br m., $\text{CH}_2\text{-O-CO}$), 5.19 (s, 2H, $-\text{CH}_2\text{-isoxazole}$), 6.64 (s, 1H, isoxazole 4-H), 7.46 (s, 3H, ArH), 7.82(s, 2H, ArH). **P2-1:** ^1H NMR (500 MHz, CDCl_3): δ 0.85-1.13 ppm (br. m, $-\text{CH}_3$) , 1.75-2.25 (br. m, CH_2 backbone), 3.20-3.50 (br. s, $\text{CH}_3\text{-O}$), 3.50-3.70 (br. m, $\text{CH}_2\text{-CH}_2\text{-O}$), 4.00-4.25 (br. m, $\text{CH}_2\text{-O-CO}$), 5.18 (s, 2H, $\text{CH}_2\text{-isoxazole}$), 6.64 (s, 1H, isoxazole 4-H), 7.44 (s, 3H, ArH), 7.81 (s, 2H, ArH). **P1-2:** ^1H NMR (500 MHz, CDCl_3): δ 0.70-1.25 ppm (br. m, $-\text{CH}_3$) , 1.75-2.25 (br. m, CH_2 backbone), 3.35-3.50 (br. s, $\text{CH}_3\text{-O}$), 3.50-3.70 (br. m, $\text{CH}_2\text{-CH}_2\text{-O}$), 4.00-4.25 (br m., $\text{CH}_2\text{-OCO}$), 5.18 (s, 2H, $-\text{CH}_2\text{-isoxazole}$), 6.73 (s, 1H, isoxazole 4-H), 7.43 (s, 2H, ArH), 7.96 (s, 2H, ArH). **P1-4:** ^1H NMR (500 MHz, CDCl_3): δ 0.85-1.13 ppm (br. m, $-\text{CH}_3$) , 1.75-2.25 (br. m, CH_2 backbone), 3.20-3.50 (br. s, $\text{CH}_3\text{-O}$), 3.50-3.70 (br. m, $\text{CH}_2\text{-CH}_2\text{-O}$), 4.00-4.25 (br m., $\text{CH}_2\text{-O-CO}$), 5.28 (s, 2H, $-\text{CH}_2\text{-isoxazole}$), 6.55 (s, 1H, isoxazole 4-H), 7.48 (m, 4H, ArH), 7.80 (m, 2H, ArH), 8.04 (m, 2H, ArH), 8.59 (m, 1H, ArH). **P1-5:** ^1H NMR (500 MHz, CDCl_3): δ 0.85-1.13 ppm (br. m, $-\text{CH}_3$) , 1.75-2.25 (br. m, CH_2 backbone), 3.20-3.50 (br. s, $\text{CH}_3\text{-O}$), 3.50-3.70 (br. m, $\text{CH}_2\text{-CH}_2\text{-O}$), 4.00-4.25 (br m., $\text{CH}_2\text{-O-CO}$), 5.18 (s, 2H, $-\text{CH}_2\text{-isoxazole}$), 6.73 (s, 1H, isoxazole 4-H), 7.54 (m 3H, ArH), 7.70 (m 1H, ArH), 7.80-7.95 (m, 2H, ArH), 8.30-8.40 (m, 1H, ArH).

4.5.1.4. 2-nitrobenzo nitrile oxide click reactions on polymer alkyne P1

As 2-nitrobenzo nitrile oxide dimerizes spontaneously, it has to be added in portions to drive the reaction to completion. To the polymer alkyne **P1** (mg) in a round bottom flask, ethanol (1 mL) and 4% aqueous NaHCO_3 (1 mL) were added, followed by 2-nitrobenzaldehyde oxime (42 mg) and chloramine-T monohydrate (110 mg). The mixture was stirred at room temperature for 12 h, a second portion of 2-nitrobenzaldehyde oxime (42 mg) and chloramine-T monohydrate (110 mg) was then added and the resulting mixture stirred for further 12 h. Due to the steric hinderance of the 2-nitrobenzo nitrile oxide, the cycloaddition reaction could be slow, so the reaction time is increased to 24 h in the case of this nitrile oxide. The reaction mixture was

diluted with ethanol (5 mL) and subsequently purified by dialysis first against water and second against ethanol (Roth, ZelluTrans membrane, molecular weight cutoff: 4000-6000). Last, solvent was removed by rotary evaporation. **P1-3**: ^1H NMR (500 MHz, CDCl_3): δ 0.85-1.13 ppm (br. m, - CH_3), 1.75-2.25 (br. m, CH_2 backbone), 3.20-3.50 (br. s, $\text{CH}_3\text{-O}$), 3.50-3.70 (br. m, $\text{CH}_2\text{-CH}_2\text{-O}$), 4.00-4.25 (br. m., $\text{CH}_2\text{-O-CO}$), 5.18 (s, 2H, $-\text{CH}_2\text{-isoxazole}$), 6.42 (s, 1H, isoxazole 4-H), 7.46 (m, 1H; ArH), 7.71-7.74 (m, 2H, ArH), 8.00 (m, 1H, ArH).

4.5.2. Orthogonal modification of polymer chain ends via sequential nitrile oxide-alkyne and azide-alkyne Huisgen cycloadditions

4.5.2.1. Nitrile oxide-alkyne cycloaddition (NOAC) step

The nitrile oxide was generated *in situ*. A stock solution of the required hydroxyimoyl chloride was prepared by dissolving the parent oxime (0.826 mmol) in dichloromethane (6 mL) to which pyridine (20 μL) and N-chlorosuccinimide (0.826 mmol) were added. The mixture was allowed to stir at room temperature. After 1h, a 2 mL portion of this solution was added to a second flask containing a solution of polymer **Q** (~200 mg) dissolved in dichloromethane (6 mL). Triethylamine (150 μL) was added and the mixture stirred at rt for 8 h. Further portions of the stock solution (2 mL) were added following 8 and 16 h stirring at rt. The reaction was terminated after a total of 24 h stirring, the solvent was evaporated to ~1 mL and the product precipitated by addition of chilled MeOH, filtered, washed and dried under vacuum.

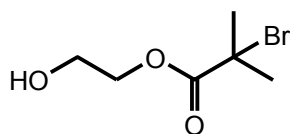
4.5.2.2. Copper-catalyzed azide-alkyne cycloaddition (CuAAC) step

To a flask containing the isoxazole modified azido polystyrene (**Q1** or **Q2**, ~50 mg) hexamethyltriethylenetetraamine (0.136 mmol) and copper (I) bromide (0.066 mmol) were added. The flask was capped with a septum and purged with argon for 2 minutes. In a second flask, a solution of the alkyne (0.066 mmol) in THF (4 mL) was degassed prior to transfer, via a degassed syringe, to the mixture containing the polymer. The mixture was allowed to stir

overnight at room temperature under argon. The solvent was concentrated to approximately 1 mL. Dichloromethane was added and all precipitating salts removed by filtration. Following evaporation of the filtrate to a volume of ~1 mL, the final product was precipitated by addition of chilled methanol, filtered and dried under vacuum.

4.5.3. Inducing some other α -functionalities in co/polymers synthesized by ATRP

4.5.3.1. Synthesis of ATRP initiator, 2-hydroxyethyl bromoisobutyrate (HEBB)



Ethylene glycol (31 g, 0.5 mol), 75 mL of anhydrous THF, and 6.96 mL (0.05 mol) of triethylamine (TEA) were charged into a 250-mL, three-necked, round-bottom flask, which was cooled at 0°C in ice water. To this solution, 11.48 g (0.05 mol) of 2-bromoisobutyryl bromide and 50 mL of THF were added dropwise under argon environment. The mixture was stirred overnight, warming up to room temperature. Solids were removed by filtration, and the solvent was evaporated. The remaining liquid was redissolved in 150 mL of deionized water and extracted with dichloromethane. The organic phase was dried over anhydrous MgSO_4 , and the solvent was removed. A colorless liquid HEBB was obtained (5.9 g, yield 51%). ^1H NMR of $\text{HOCH}_2\text{CH}_2\text{OCOC}(\text{CH}_3)_2\text{Br}$ (300 MHz, CDCl_3): δ 1.95 (s, 6H, 2- CH_3), 3.94 (t, 2H, $-\text{OCH}_2\text{CH}_2\text{OH}$), 4.31 (t, 2H, $-\text{COOCH}_2\text{CH}_2-$).

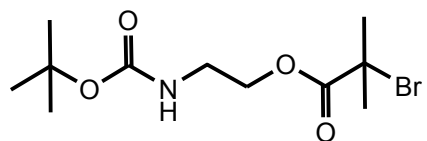
4.5.3.2. α -aldehyde copolymer of P(OEGMA-co-MEO₂MA)

In order to introduce the α -aldehyde functionality in the P(OEGMA-co-MEO₂MA) copolymer, α -hydroxyl functionalized P(OEGMA-co-MEO₂MA) was oxidized by activated DMSO²³⁷. The procedure was taken from the literature²³⁵. α -Hydroxyl-functionalized copolymer of P(OEGMA-co-MEO₂MA) (2 g, 0.18 mmol) was added to 395 mg (3.87 mmol) acetic anhydride in 3 mL dimethylsulfoxide and stirred for 30 h at room temperature. The reaction mixture was then

diluted with deionized water and subsequently purified by dialysis against pure water. (Roth, ZelluTrans membrane, molecular weight cutoff: 4000-6000). Last, water was removed by rotary evaporation.

For the analysis of the aldehyde groups formed after the oxidation reaction, Schiff's reagent for aldehydes was used. Schiff's reagent was bought from Sigma-Aldrich (84655) and had the following composition: water (97.93%), potassium disulfite (0.97%), pararosaniline base (0.56%), and hydrochloric acid (0.54%).

4.5.3.3. t-Boc protected α -amino functionalized co/polymer P(OEGMA-co-MEO₂MA)



The procedure was taken from literature²³⁴. In a 3-neck round-bottom flask, N-Boc-ethanolamine (5 g, 0.031 mol) and triethylamine (4.7 g, 0.046 mol) in 40 mL anhydrous dichloromethane was cooled in an ice bath. 2-bromoisobutyryl bromide (5.75 mL, 0.046 mol) was added dropwise into the solution. The reaction was slowly warmed to room temperature and stirred overnight. The salt was filtered off and the reaction mixture was extracted sequentially with water and saturated sodium bicarbonate solution (5 times). Organic phase was concentrated with rotary evaporation and precipitated in cold hexane. The product is precipitated as a white solid (12.5 g). ¹H NMR (CDCl₃) δ (ppm): 1.46 (s, 9H), 1.95 (s, 6H), 3.45-3.47 (m, 2H), 4.24-4.26 (t, 2H).

Chapter 5

Activated ester-functionalized polymers

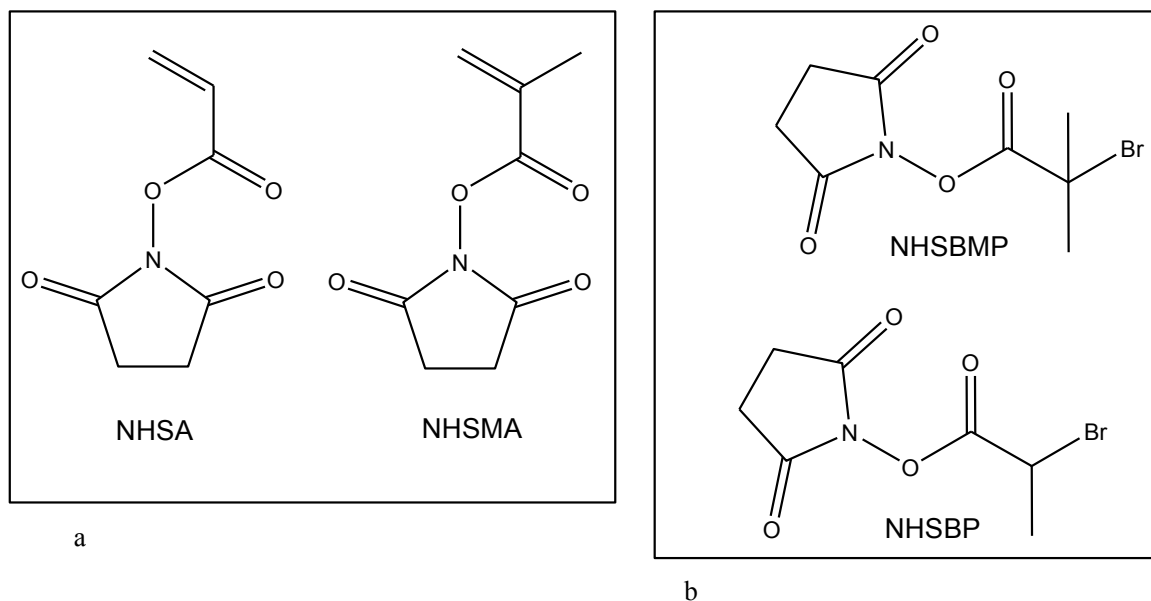
5.1. Activated ester derivatives as ATRP initiators

In the present chapter the reaction of activated esters with amines is proposed as an alternative reaction to 'Huisgen 1,3 dipolar cycloaddition' or 'metal-free nitrile oxide-azide cycloaddition' employed in the previous chapters of this thesis. These click-type reactions were used as efficient methods to functionalize or modify macromolecules synthesized by ATRP. Each of these approaches has their own advantages/drawbacks. However all of them can be used in combination with CRP methods, especially ATRP, to give highly functionalized macromolecular structures. The reaction of activated-ester with amine proceeds under mild conditions, such as room temperature, and does not need the use of metal catalyst as in the case of CuAAC.

Activated esters are suitable derivatives for covalently linking amines and carboxylic acids to obtain amides⁵⁹. Polymeric activated esters could be synthesized for example from activated ester vinyl monomers such as N-hydroxy succinimide meth/acrylates (NHSA or NHSMA) (Scheme 5.1.a). The resulting polymers (poly (N-hydroxy succinimide meth /acrylate)s contain active ester groups on each monomer which might go through post-polymerization modification reactions with amine groups of another molecule. In this way functionalized polyacrylamides or polymethacrylamides are obtained. Furthermore, activated ester initiators are used to synthesize polymers with active sites on α and ω chain ends (scheme 5.1.b). These polymer precursors can react in the next steps with other amine-bearing species (surfaces, polymers, biomolecules, etc.) to generate functionalized surfaces, block copolymers, bioconjugates or any other highly functionalized macromolecular architecture.

This alternative coupling method was the motivation of different projects. First, thermoresponsive polymers with reactive ester chain ends were synthesized and characterized and in a further step grafted onto amino-functionalized silica monoliths to build thermoresponsive stationary phases for chromatography. This project was a collaboration with the Max Planck Institute of Colloids and Interfaces¹⁶². In the second project, the reactive ester chain ends of thermoresponsive oligo (ethylene glycol)-based copolymers were coupled

(conjugated) with amino groups of the lysine residues on the surface of trypsin (polymer bioconjugation).



Scheme 5.1. Structures of some a. activated ester monomers: NHSA(N-hydroxy succinimide acrylate); NHSMA(N-hydroxy succinimide methacrylate) and b. activated ATRP initiators: NHSBMP (N-hydroxy succinimide-2-bromo-2-methylpropionate or *N*-Succinimidyl 2-bromo-bromoisobutyrate); and NHSBP (N-hydroxy succinimidyl-2-bromopropionate).

5.2. PEGylated chromatography: Thermoresponsive stationary phases for bioseparation

In a project in collaboration with the Max Planck Institute of Colloids and Interfaces in Potsdam, copolymers of MEO₂MA and OEGMA were used for modification of silica monoliths for chromatography to separate proteins and some steroids. A series of P(OEGMA-*co*-MEO₂MA) copolymers with variable chain lengths and compositions were synthesized by ATRP in the presence of an activated ester-containing initiator, *N*-Succinimidyl 2-bromo-bromoisobutyrate (Table 5.1). ATRP initiator *N*-succinimidyl 2-bromoisobutyrate was synthesized and characterized by ¹H NMR (see section 5.5.2., spectrum is not shown). In the ¹H NMR spectrum

of the initiator, two characteristic peaks were recognized: a signal at 2.05 ppm related to the six protons of two methyl groups and the second peak at 2.83 ppm related to the four methylene protons of the succinimidyl ester part of the initiator (see section 5.5.2). After co/polymerization, the formed copolymers were characterized by SEC, ^1H NMR, and turbidimetry (Table 5.1). All of these techniques confirmed the formation of well-defined copolymers with controlled chain lengths, chain end functionalities and cloud points in water. The reactive N-succinimidyl ester chain ends of the polymers were reacted with amino-functionalized silica monoliths via standard amide coupling chemistry.

Table 5.1. Characterization of the copolymers P(MEO₂MA-co-OEGMA) and of the corresponding modified silica monoliths.

	[OEGMA] ₀ /[MEO ₂ MA] ₀	DP ^a _{n,th}	M _n ^b	M _w /M _n ^b	cloud point ^c (°C)	Grafting density ^d (μg/m ²)	Grafting density(chains/nm ²)
a	10:90	100	18100	1.3	41	230	0.0071
b	10:90	75	15700	1.4	38	400	0.018
c	10:90	50	12300	1.3	39	370	0.025
d	10:90	25	6200	1.4	40	300	0.039
e	5:95	100	18100	1.7	33	250	0.0093
f	15:85	100	17000	1.4	43	230	0.0072

^aTheoretical degree of polymerization $D_{Pn,th} = ([\text{OEGMA}]_0 + [\text{MEO}_2\text{MA}]_0) / [\text{initiator}]_0$. ^bMeasured by SEC. ^cMeasured by turbidimetry. ^dIn a typical reaction, approximately 0.05 g of polymer was dissolved in 1 mL of DMF (1 mL/cycle). Parallel to the grafting of the copolymer, grafting was also performed on a free-standing piece of aminated monolith. Grafting densities were calculated from elemental analysis data²³⁸.

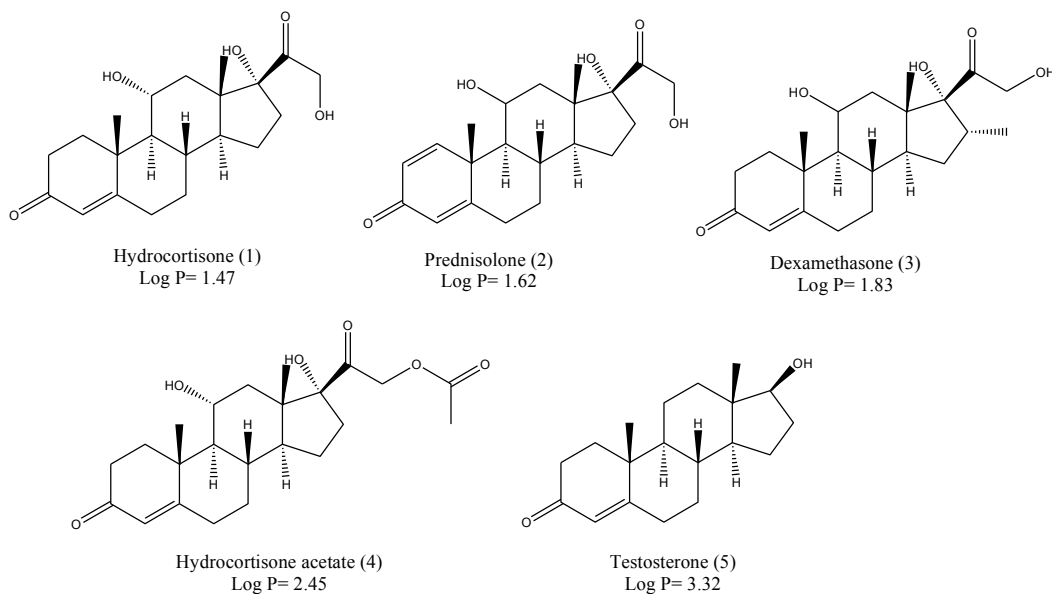
5.2.1. Functionalization of the Silica monoliths

Before and after modification with copolymers, silica monoliths were analyzed by elemental analysis and FT-IR spectroscopy. FT-IR of the modified monolith showed new adsorption bands

corresponding to the amide functionality. Grafting densities of grafted polymers were calculated from elemental analysis results (Table 5.1). This part of the work was done in Max-Planck Institute of Colloids and Interfaces in collaboration with the research group of Dr. M. Titirichi. Experiments were done in the same research group by Irene Tan.

5.2.2. Chromatographic performance of the P(OEGMA-*co*-MEO₂MA)-grafted stationary phases

a. Steroid chromatography. To investigate the chromatographic performance of the P(OEGMA-*co*-MEO₂MA)-grafted stationary phases a mixture of five steroids in aqueous media under isocratic conditions was run into the columns packed with different composites of grafted polymers (scheme 5.2). These five steroids have different hydrophobicities (log P values), which increase as (1) ~ (2) < (3) < (4) < (5). Therefore, they exhibit different interactions with the thermoresponsive stationary phase as it changes its hydrophobicity with temperature.



Scheme 5.2. Chemical structures of the steroids used as bioanalytes for separation investigation and their partition coefficients (log P).

Since the thermoresponsive polymers used to make composites ‘a’ to ‘f’ in Table 5.1 have different molecular weights and molecular weight compositions, they have different cloud

points and grafting densities on silica monoliths. The effect of some molecular parameters of the grafted polymers (molecular weight, comonomer composition) and also temperature below and above LCST on the elution profiles and retention times of the aqueous solution of the five steroids is investigated.

a) Molecular weight: compared to polymers with lower molecular weights, polymers with higher molecular weights require smaller grafting densities on the silica support in order to achieve the similar performance in the separation of five steroids at the same temperature above the LCST of both polymers. So for an efficient separation process, higher molecular weight polymers are preferred, since in this case a hydrophobic column would require a lower grafting density, considering that overgrafting might lead to the blocking of mesopores.

b) Comonomer composition: One of the advantages of the copolymer P(OEGMA-co-MEO₂MA) is the possibility to tune its cloud point by adjusting the comonomer composition. So, in the present research, separation efficiency of copolymers with different comonomer compositions and LCSTs are investigated. Polymers with lower LCST are more hydrophobic and can separate more hydrophobic steroids at lower temperatures, on the other hand, polymers with higher LCST values require higher temperatures to separate the same hydrophobic analytes and the elution profiles show a lower resolution. Therefore, separation temperature is closely correlated to the LCST of the polymer, which could be adjusted by changing the comonomer composition of the P(OEGMA-co-MEO₂MA) thermoresponsive copolymers.

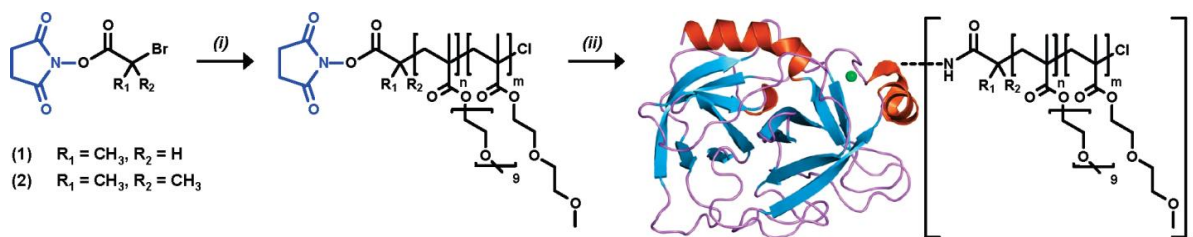
c) Temperature: For the same composite, if the steroids mixture is run at two different temperatures below and above LCST of the column, at temperatures above LCST, the less hydrophobic steroids (1 and 2) are eluted together, however if the temperature is below LCST, the less hydrophobic analytes could be separated as well and show two peaks in the elution profiles. However below LCST, more hydrophobic analytes (3,4) elute as a single peak. So, a switch in temperature leads to the successful separation of all hydrophilic and hydrophobic bioanalytes.

b. Protein chromatography. The efficiency of the P(OEGMA-co-MEO₂MA)-grafted stationary phases was tested for protein chromatography. The most hydrophobic column (Table 5.1. entry

e) was chosen for separation of the two proteins with relatively close hydrophobicities, lysozyme and myoglobin. At the temperature below the LCST of column, two proteins were eluted as a single peak, whereas above LCST a near base-line separation occurred. Also, the elution times were short in contrast to the pure PNIPAM analogue. A reason for this observation may be the nonspecific interaction of the amide bond of PNIPAM with the proteins which extends the retention time on the column. In the case of P(OEGMA-*co*-MEO₂MA) copolymers the absence of such interactions led to the fast elution of proteins.

5.3. Smart PEGylation of trypsin

A series of well-defined copolymers of MEO₂MA and OEGMA₄₇₅ with variable chain lengths and comonomer compositions were synthesized and tested for trypsin bioconjugation. These oligo (ethylene glycol)-based thermoresponsive copolymers were prepared via atom transfer (co)polymerization of MEO₂MA and OEGMA₄₇₅ in ethanol. The formed conjugates were characterized by SDS-PAGE, turbidimetry, and enzyme activity tests. The coupling strategy for trypsin conjugation is a grafting-onto method (grafting-onto technique is one of the main strategies to synthesize graft copolymers by coupling the pre-made polymeric side chains to a functional backbone). In this approach, P(MEO₂MA-*co*-OEGMA₄₇₅) copolymers containing N-hydroxysuccinimide (NHS) active ester α -chain ends were reacted with the surface lysine residues of trypsin (scheme 5.3)²³⁹. The NHS active ester α -chain ends were introduced in the copolymers by using NHS active ester-containing ATRP initiators. In order to compare the coupling efficiency of different substituted NHS-active ester α -chain ends, two slightly different ATRP initiators were used for ATRP of two comonomers (Scheme 5.3)²³⁹.



Scheme 5.3. General strategy for preparing P(MEO₂MA-*co*-OEGMA₄₇₅)-trypsin conjugates

Two ATRP initiators, **1** (N-hydroxy succinimidyl-2-bromopropionate) and **2** (N-Succinimidyl 2-bromo-bromoisobutyrate) (Scheme 5.3) were synthesized. The synthesis procedures for initiators **1** and **2** were adapted from literature^{240, 55, 58}.

5.3.1. Characterizaion of P(MEO₂MA-*co*-OEGMA₄₇₅) copolymers

Characteristic properties of a series of P(MEO₂MA-*co*-OEGMA₄₇₅) copolymers synthesized by ATRP are shown in table 5.2. For the copolymerization, two different ATRP initiators containing succinimidyl ester moieties were tested (initiators **1** and **2** in Scheme 5.3). Haddleton *et al.* demonstrated that polymers initiated by **1** are much more reactive towards nucleophiles such as amines, than polymers initiated by **2** and consequently the rate of protein conjugation was faster with polymers initiated by **1**, as they showed in a study in their group⁵⁸. As it is observed in Table 5.2, copolymers with various chain lengths and MEO₂MA/OEGMA₄₇₅ compositions were synthesized, but the chain lengths targeted were rather short ($25 < DP < 50$), because the molecular weight and length of the conjugated polymer is a determining factor in grafting onto strategies. It can influence the final biological activity and stability of the conjugate, as well as number of polymer molecules grafted on the biomolecule. Moreover, the comonomer composition was adjusted so that the LCST values of the copolymer were located in the range of 30-35°C in physiological buffer. Indeed, trypsin should be handled very carefully since it is a self-digestive enzyme. In the lab, trypsin should be stored at -20 °C and in an optimized media. Therefore, temperature cycles above 35 °C could potentially degrade trypsin.

Table 5.2. Properties of the copolymers of MEO₂MA and OEGMA₄₇₅ prepared by ATRP^a

Polymer	I	I/MEO ₂ MA/OEGMA ₄₇₅	Conv. ^b	M _n ^c [g·mol ⁻¹]	M _w /M _n ^c	M _{n,th} ^d [g·mol ⁻¹]	f ^e	Cloud point ^f [°C]
Poly1	1	1:25:0	0.70	7400	1.2	3290	0.44	30
Poly2	1	1:24.25:0.75	0.62	7080	1.2	3050	0.43	33
Poly3	1	1:22.5:2.5	0.80	7700	1.2	4330	0.56	43
Poly4	2	1:22.5:2.5	0.99	8100	1.2	5360	0.66	41
Poly5	2	1:45:5	0.86	13400	1.2	9320	0.69	40

^a Experimental conditions: 60°C; overnight; in ethanol solution (monomer/ethanol=1:1.25 (v/v)); [I]₀/[CuCl]₀/[Bipy]= 1/1/2, I stands for initiator. ^b Overall monomer conversion measured by ¹H NMR from the crude reaction products. ^c Measured by SEC in THF. ^d M_{n,th}= conversion (188 [MEO₂MA]₀+475[OEGMA]₀)/[I]₀. ^e Initiator efficiency estimated from the SEC data. For calculation of f: f= M_{n,th}/M_{n,SEC}. ^f Measured in pure deionized water at a concentration of 3 g·L⁻¹

SEC analysis of the copolymers after purification shows that well-defined macromolecules with low polydispersities were obtained (Table 5.2). Nevertheless, the experimental molecular weights measured by SEC deviate from the theoretical molecular weights estimated from ¹H NMR. The SEC results showed much higher molecular weights than estimated. These large deviations could not be merely explained by probable drawbacks of calibration method of SEC using polystyrene standards. In fact, it was demonstrated previously that the molecular weights of P(MEO₂MA-co-OEGMA) could be estimated relatively accurately using polystyrene as standard^{118, 152}. Moreover, in the present case using polystyrene and poly(methyl methacrylate) as standard resulted in the comparable molecular weight values. Haddleton and co-workers investigated previously the initiation efficiency *f* of these two initiators. They reported low initiation *f* values and thus remarkable molecular weight deviations for the polymers synthesized with two initiators, **1** and **2**^{58,240}. For example, they investigated the ATRP of OEGMA₄₇₅ in toluene and obtained initiation efficiencies of 40-55% for initiator **1** and 65% for initiator **2**⁵⁸. The results we obtained regarding the efficiencies of the two initiators (43-56%

and 66-69% for **1** and **2** respectively) are in good agreement with the studies of Haddleton and co-workers.

For the trypsin bioconjugation in the next step, synthesized macromolecules should contain enough active ester end groups. From the ^1H NMR spectra it is observed that all of the polymers still contain succinimidyl ester end groups. This indicates that no significant hydrolysis of the active ester has happened during the purification process. The chain end signal which is clearly recognized in all ^1H NMR spectra is around 2.77 ppm which corresponds to the four methylene protons of the succinimidyl ring (protons **a** in Figure 5.1). By comparing the integration of this chain-end signal and some side chain protons (e.g. protons **b** or **d** in Figure 5.1), the average molecular weight of the formed co(polymers) could be calculated. The molecular weights calculated from ^1H NMR of the pure polymers and by comparing chain-end to side- chain integration matched the deviated molecular weights obtained by SEC.

All of the (co)polymers showed a LCST in pure deionized water (Table 5.2). The cloud points depended closely on the MEO₂MA/OEGMA composition of the (co)polymers as it was studied in the previous studies^{118,151,152}. So, transition temperatures between 30 and 43 °C were obtained (Table 5.2). It should be mentioned that the cloud points observed in pure water are usually 3-4 °C higher than in physiological buffer^{150,152,204}.

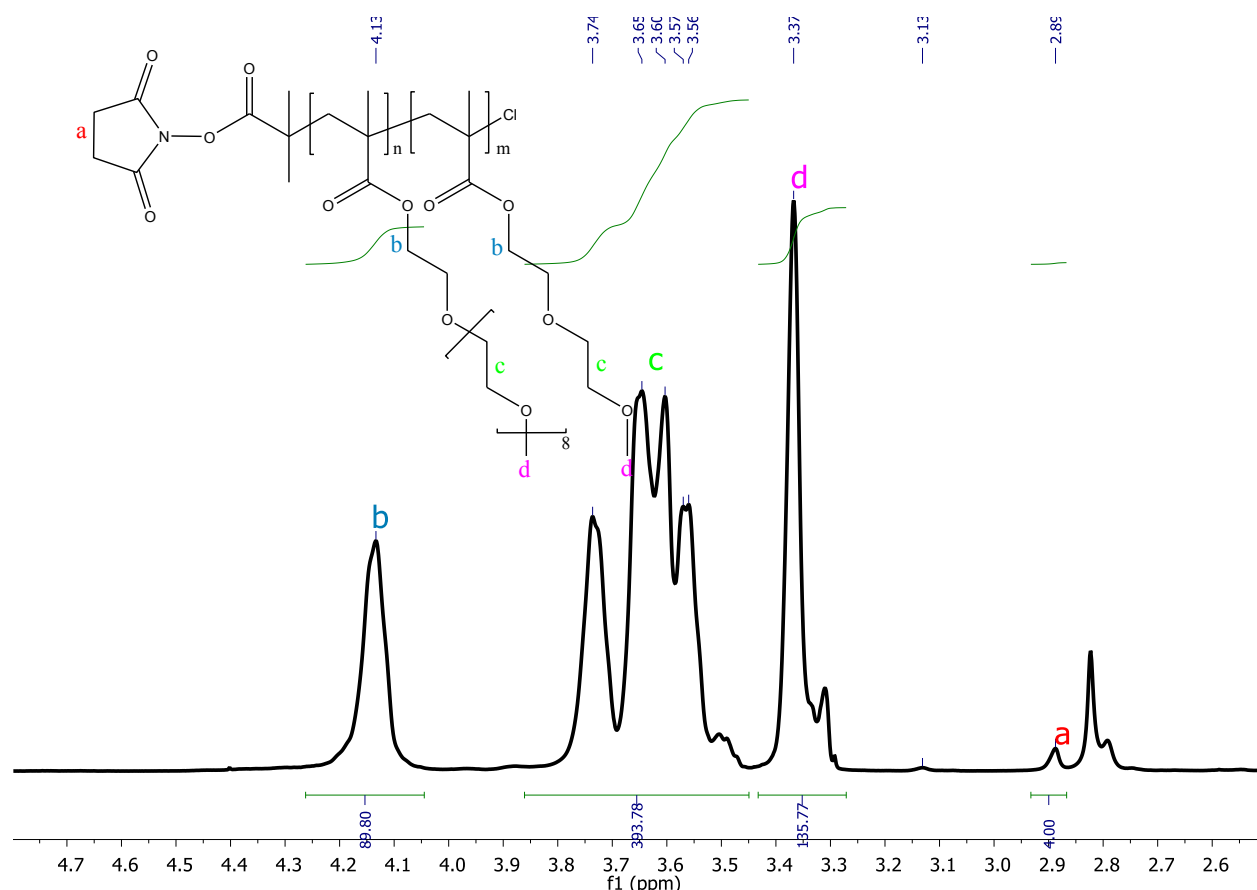


Figure 5.1. ^1H NMR spectrum of the α -N-hydroxy succinimidyl functional copolymer **Poly4** in Table 5.2 [P(MEO₂MA-co-OEGMA₄₇₅)] in acetone- d_6 .

5.3.2. Polymer Conjugation of Trypsin

Trypsin has 15 lysine residues (including the N-terminus), which can potentially react with the N-hydroxy succinimidyl end groups of the synthesized (co)polymers. Nevertheless, it was previously reported that a maximum of 11 lysine sites can be reacted with synthetic polymer chains¹⁷⁹.

In this study, a mild degree of bioconjugation (i.e., approximately five polymer chains per enzyme) was targeted.

The conjugation procedure was adapted from the literature¹⁷⁹. NHS-functionalized copolymer (**Poly1-Poly5** in Table 5.2) was dissolved in a small amount of DMF (polymer concentration ~

200 g·L⁻¹). Trypsin was dissolved in buffer (borax/HCl, pH = 9 at 20 °C) at 4 °C (trypsin concentration ~ 40 g·L⁻¹). The two solutions were then mixed and gently shaken at 4 °C for 4 h and then at room temperature for 2 h to allow the conjugation to proceed. Various molar ratios polymer/ trypsin were tested ranging from 3/1 to 11/1. After reaction, the conjugation solution was dialyzed in Tris/HCl buffer (pH 8.2, 0.05 M Tris containing 0.02 M CaCl₂) for 2 weeks at 4 °C. Dialysis membranes with a molecular weight cutoff of 25000 g·mol⁻¹ were used to selectively separate unreacted polymer (7080 < M_n < 13400) and unreacted trypsin (23.8 kDa) from the formed conjugates. The buffer solution was renewed two times per day. It was previously demonstrated that trypsin conjugates should be stable for approximately 30 days under these dialysis conditions¹⁸⁵.

After dialysis, different isolation procedures were used depending on the type of polymer used for conjugation. For polymers having a low LCST in buffer (i.e., cloud point around 30 °C), the dialysis solution was heated up to 33 °C and centrifuged for 30 min at 14000 rpm speed. This step allows separation of the thermoresponsive conjugate from the rest of the unreacted trypsin. After 30 min, the supernatant was removed and the white precipitate was stored at -18 °C. For polymers with a higher LCST (i.e., cloud point above 33 °C), a saturated aqueous solution of ammonium chloride was added to the dialysis solution to reduce the LCST of the solution to 30 °C. Indeed, at temperatures above 33 °C, the risk of autodigestion and denaturation of trypsin is non-negligible. The modified solution was then heated up at 30 °C and centrifuged for 30 min at a speed of 14000 rpm. After 30 min, the supernatant was removed and the white precipitate was stored at -18 °C.

5.4. Characterization of the conjugates of MEO₂MA-OEGMA₄₇₅ copolymers with trypsin

The corresponding synthesized and purified bioconjugates of **Poly1-Poly5** copolymers with trypsin are called **C1-C5** in the following parts of the text. Formed conjugates were characterized by SDS-PAGE, turbidimetry, and enzyme activity tests.

5.4.1. SDS-PAGE

SDS-PAGE (Sodium Dodecyl Sulfate Poly(acrylamide) Gel Electrophoresis) was performed according to Laemmli with a 12.5% separating gel ²⁴¹. Protein concentrations were determined by the method of Bradford using Bio-Rad Protein Assay kit (Bio-Rad,CA) with bovine serum albumin as a standard ²⁴². Samples were loaded into each well to get 30 µg of protein. Protein solution was mixed with SDS-PAGE sample buffer (250 mM Tris pH6.8, 40% glycerol, 8% SDS, 20% 2-mercaptoethanol, and 0.01% bromophenol blue) with a ratio of 3:1 and heated at 95 °C for 10 min. The slab gel was composed of 2 cm of concentrating gel (5% acrylamide, 62.5 mM Tris pH6.8, 0.1% SDS) and 6 cm of separating gel (12.5% acrylamide, 375 mM Tris pH8.8, 0.1% SDS) with 1.5 mm thickness. Slab gel electrophoresis was performed by SE 250 mini vertical unit (Hoefer, Holliston, MA) for about 100 min with maximum current and voltage of 20 mA and 150 V, respectively. Proteins were visualized by blue silver staining ²⁴³. Gels were incubated in staining solution (0.12% Coomassie brilliant blue G250, 10% ammonium sulfate, 10% phosphoric acid, and 20% methanol) overnight with gentle shaking, and washed once with methanol. Gels were further incubated in water for several days to remove background. Different gel and protein concentrations were tested. In all measurements, raw conjugation product (i.e. immediately after reaction), conjugate solutions after dialysis, and conjugates redissolved in buffer after thermally induced precipitation were compared. P(MEO₂MA-co-OEGMA) copolymers were also loaded as a negative control to get 750 µg in a lane but did not give any band (data not shown).

It should be mentioned that SDS-PAGE analysis of the conjugates was run after each step of purification (i.e. after dialysis and after thermo-precipitation) to monitor the formation of bioconjugates and investigate the isolation process of bioconjugates from the polymer and trypsin in the solution. This study was done in order to estimate the efficiency and applicability of thermo-precipitation in the case of our thermoresponsive polymers. Since as highlighted before, one of the most important advantages of thermoresponsive polymer/enzyme conjugates is the possibility to isolate them via thermoprecipitation. However, in the case of trypsin conjugates, another aspect should be taken into account, i.e. the precipitation

temperature should be under 35 °C to prevent autodigestion. The bioconjugation mixtures (**C1'** and **C2'**) which were obtained immediately after dialysis step were analyzed by SDS-PAGE (Figure 5.2). In both of these mixtures it is possible to see that high molecular weight bioconjugates were formed, although the contrast of the images is rather low. However, in the mixtures of **C1'** and **C2'** a small amount of unreacted trypsin is still detected (compared to the unmodified trypsin band in Figure 5.2). These results indicate that although the molecular weight cutoff of the dialysis membranes was chosen carefully higher than both the molecular weights of unreacted polymer and unreacted trypsin in order to selectively separate them from the bioconjugates, all of the unreacted trypsin could not be separated after this dialysis procedure and for the complete removal of the trypsin from the conjugates further purification step was required. Nevertheless, dialysis step allows the complete removal of the unreacted polymer, since the molecular weights of the (co)polymers are far below the cutoff of the membrane, yet the membrane cutoff is not much higher than molecular weight of trypsin. So, these bioconjugation mixtures of **C1'** and **C2'** were purified by thermoprecipitation, centrifuged, and analyzed by SDS-PAGE (samples **C1''** and **C2''** in figure 5.2).

The conjugate **C1''** could be easily precipitated out and isolated since the LCST of the homopolymer **Poly1** is 30 °C and enough lower than 33 °C which is the thermoprecipitation process temperature. So, the quantitative precipitation of the conjugate **C1''** occurs after this step. However, conjugate **C2''** prepared from the copolymer **Poly2** with LCST around 33 °C could not be quantitatively precipitated in the same conditions. So, in that case a saturated salt solution was used to lower the LCST of the polymer/enzyme conjugate. This approach was previously used to precipitate PNIPAM/trypsin conjugates^{185, 179}. SDS-PAGE images (Figure 5.2) clearly show that the rest of the unreacted trypsin was removed after this thermoprecipitation and centrifugation step. Moreover, the SDS-PAGE images indicate the formation of P(MEO₂MA-co-OEGMA₄₇₅)-trypsin conjugates with a molecular weight of roughly 60000 g·mol⁻¹. This value suggests a conjugation degree of approximately five polymer chains per enzyme (a polymer/enzyme ratio of 6.5 was used in these two experiments). It should be noted that molecular weight values obtained from SDS-PAGE for polymer bioconjugation are not accurate and therefore should be rather considered as estimation. Nevertheless, this SDS-PAGE results -

although not quantitatively % reliable- confirm well that polymers **Poly1** and **Poly2** could modify trypsin efficiently.

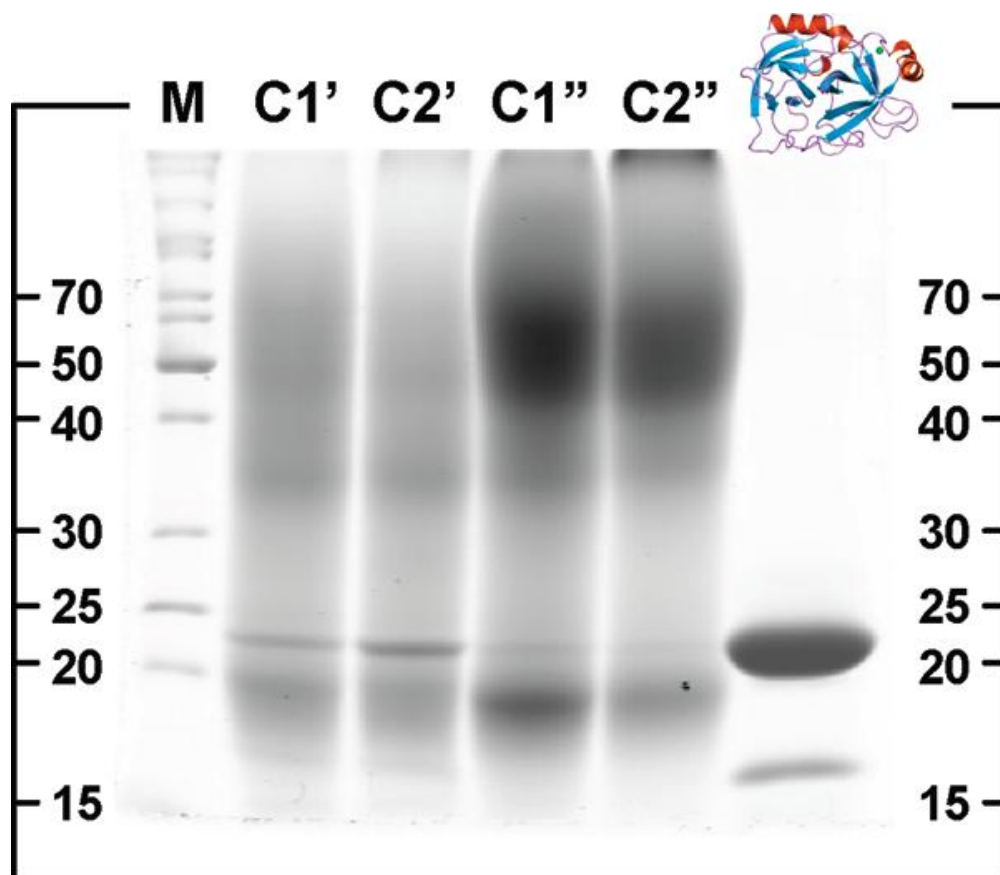


Figure 5.2. SDS-PAGE image obtained for unmodified trypsin (right) and various P(MEO₂MA-co-OEGMA₄₇₅)-trypsin conjugates. The conjugates **C1** and **C2** were obtained with polymers **Poly1** and **Poly2** (Table 5.2), respectively. A polymer/enzyme ratio of 6.5 was used in both cases. The samples **C1'** and **C2'** were isolated after conjugation and dialysis. The samples **C1''** and **C2''** are the final conjugates after reaction, dialysis, thermo-induced precipitation, and centrifugation. The acronym M represents protein molecular weight markers.

It should be also mentioned that via this bioconjugation method, it is not possible to control the degree of modification and to obtain a uniform distribution of the conjugates per trypsin molecules. Indeed, each trypsin has multiple sites for bioconjugation and it is reasonable that some of the trypsin molecules are coupled with less, and some with more polymers than the average value of five polymer chains/trypsin. This might be also the reason of some pale bands

around 35kDa in the SDS-PAGE image (Figure 5.2). However, these bands are considerably “pale” compared to the bands observed around 60kDa and this reflects that majority of enzymes have been modified with five polymer chains.

In comparison, polymers **Poly3-Poly5** were found to be less appropriate for bioconjugation. Overall, the LCST values of these polymers were too high and risky for trypsin handling (see cloud points in Table 5.2). Moreover, polymers prepared in the presence of initiator **2** are usually not very efficient for protein bioconjugation^{166,58}. Haddleton *et al.* performed hydrolytic stability experiments (under basic conditions) on the polymers prepared by initiators **1** and **2**⁵⁸. These experiments showed that polymers initiated by **1** were much more reactive towards water and consequently other nucleophiles such as amines compared to polymers prepared by initiator **2**. Therefore, initiator **1** is a more suitable initiator than initiator **2** for reaction with amine groups of protein and trypsin bioconjugation. For example, in the present case, it was observed that polymers P4 and P5 led to relatively low degrees of conjugation (i.e., approximately one polymer chain per enzyme).

5.4.2. Turbidimetry

The purified polymer/enzyme conjugates **C1** and **C2** were characterized by turbidimetry measurements, which indicated that both bioconjugates were thermoresponsive. The phase transitions of these biohybrids were roughly comparable to those of their thermoresponsive precursors, **Poly1** and **Poly2**. For example, Figure 5.3 shows the cloud point measurements obtained for the bioconjugates **C1** and **C2** and their parent polymers **Poly1** and **Poly2**, respectively. The measured cloud points of conjugates and their precursor polymers were approximately the same. However, in the case of **C2** and its parent polymer **Poly2**, the cloud point of the conjugate was found to be approximately 2 °C higher than that of the polymer.

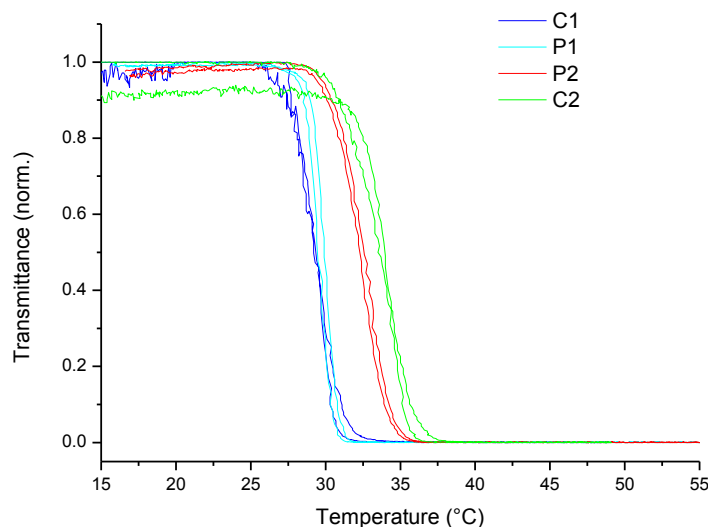


Figure 5.3. Plots of transmittance as a function of temperature measured by turbidometry in aqueous solution ($3 \text{ g} \cdot \text{L}^{-1}$) for homopolymer **Poly1** (Table 5.2) and its corresponding conjugate **C1** and for copolymer **Poly2** and the corresponding P(MEO₂MA-co-OEGMA₄₇₅)-trypsin conjugate **C2**.

5.4.3. Enzyme activity tests

The amidase activity of unmodified trypsin, P(MEO₂MA)-trypsin conjugate (**C1**) and P(MEO₂MA-co-OEGMA₄₇₅)-trypsin (**C2**) was studied at 25°C. N $_{\alpha}$ -benzoyl-L-arginine 4-nitroanilide hydrochloride (BAPNA) was chosen as a model substrate for these enzymatic tests. When hydrolyzed, this compound releases *p*-nitroaniline, which can be monitored spectrophotometrically (maximum absorbance at 410 nm, extinction coefficient = $8800 \text{ M}^{-1} \text{ cm}^{-1}$). The enzymatic activity of **C1** and **C2** was compared to that of unmodified trypsin.

The tests were performed with a solution of polymer/trypsin conjugates in Tris/HCl buffer (pH=8.2) according to the method of Erlanger *et al.*²⁴⁴. Prior to each measurement, the exact concentration of protein in the solution was determined by a Bradford assay²⁴².

For the enzyme kinetics investigation, a series of tubes containing graded concentrations of BAPNA was prepared. Initial concentration of BAPNA is shown as [BAPNA]. At time zero, a fixed amount of the polymer-enzyme conjugate was added in the tubes. The

absorption/concentration of p-nitroaniline formed was measured in the early stages of the enzymatic reaction (i.e., 2-3 min after addition of the enzyme) and the change in absorbance was plotted against time. From the initial slope of these plots the initial reaction rate (V_i) for different substrate dilutions was determined. These data were then used to draw a Lineweaver-Burk plot, from which the maximum velocity (V_{\max}) and the Michaelis-Menten constant (K_m) were extracted (Figure 5.4) ²⁴⁵.

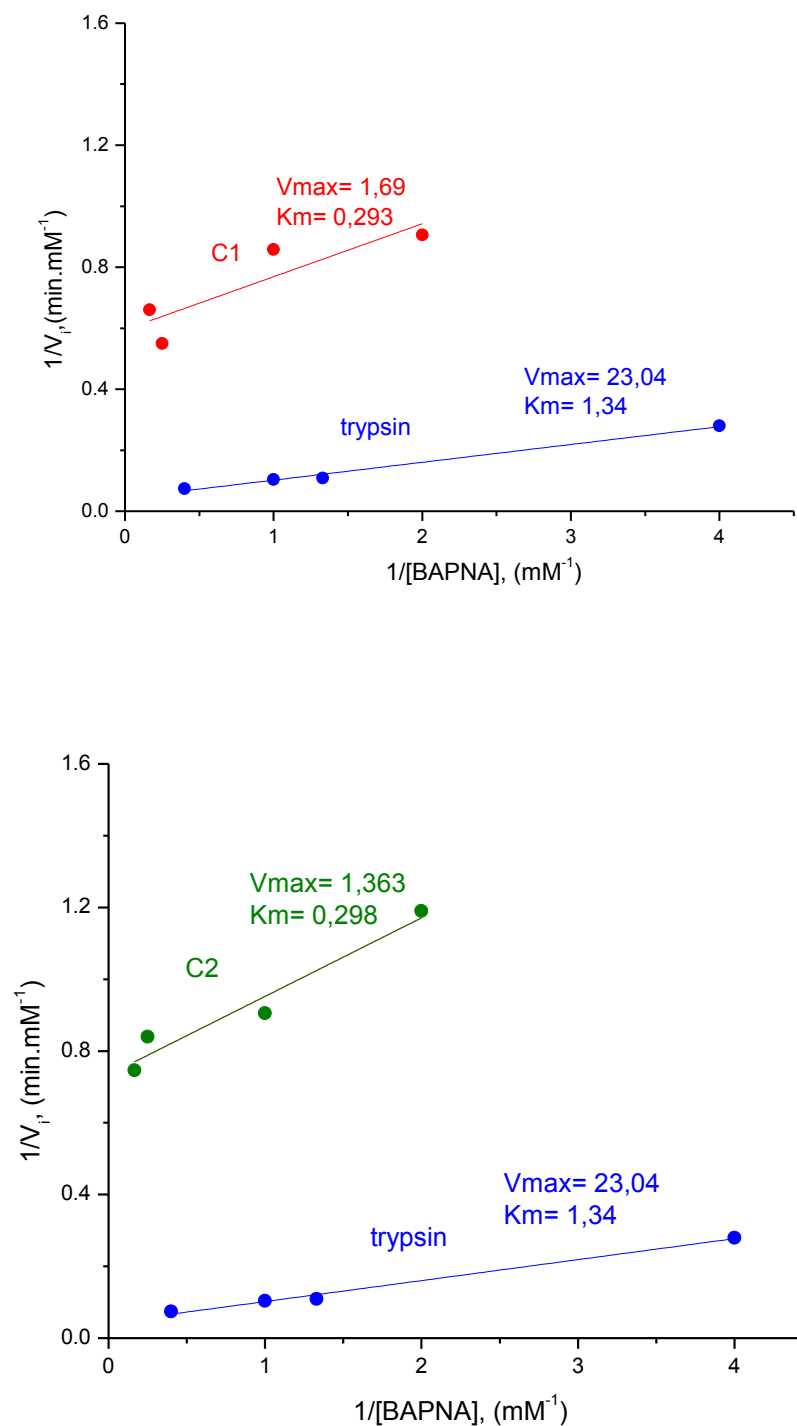


Figure 5.4. Lineweaver-Burk plots obtained for BAPNA hydrolysis assays in the presence of unmodified trypsin (blue dots and the corresponding linear fit) and P(MEO₂MA)-trypsin conjugate **C1** (red dots and corresponding linear fit) or P(MEO₂MA-co-OEGMA₄₇₅)-trypsin conjugate **C2** (green dots and the corresponding linear fit).

The slopes of these graphs allow calculation of the Michaelis-Menten constant (K_m), which reflects the enzyme-substrate affinity. Values of 1.34, 0.29 and 0.3 were found for the enzyme and the conjugates **C1** and **C2**, respectively. These results indicate that amidase activity of the conjugates is higher than that of unmodified trypsin (low K_m values reflect a high enzyme-substrate affinity). It was previously reported that PNIPAM or PEG conjugation increases the enzymatic activity of trypsin^{181,183,184, 185, 187}.

Indeed, previous studies demonstrated that K_m values decreased for PNIPAM-trypsin conjugates compared to native trypsin and also with increasing the number of polymer chains attached to trypsin¹⁸⁷. Similar results were already observed for poly (N-vinylpyrrolidone (PVP))-trypsin, PEG-trypsin and PEG-chemotrypsin conjugates. This phenomenon was explained by the hypothesis that conjugate increases the local substrate concentration by interaction with hydrophobic substrate. However, this interesting effect was never clearly explained. Nevertheless, it was proposed that generally the polymer modification may either influence the microenvironment of the enzymatic site or lead to allosteric changes in the enzyme conformation.

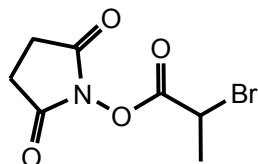
On the other hand, according to previous studies, enzyme modification stabilizes self-digestive enzymes such as trypsin against probable autolysis, since conjugate activity increases towards low molecular weight substrates, but decreases towards high molecular weight substrates such as polypeptides or the enzyme itself²⁴⁶. These results could be explained by the repulsion properties of the PEG chains against proteins due to PEG's low interfacial free energy with water, unique solution properties and molecular conformation in aqueous solution, hydrophilicity, high surface mobility and steric stabilization effects²⁴⁷.

All the present data obtained from characterization of conjugates confirm that polymer conjugation has an apparent beneficial effect on the *in vitro* enzymatic behavior of trypsin.

5.5. Synthetic procedures

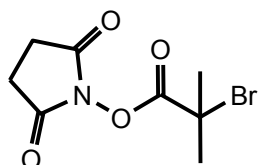
5.5.1. NHS-containing or activated ester initiators for ATRP

5.5.1.1. Synthesis of ATRP initiator N-succinimidyl-2-bromopropionate



The mixture was stirred, allowed to reach room temperature, and then stirred overnight at room temperature. Then the reaction mixture was extracted three times with water, and the organic phase was evaporated under reduced pressure to give a brownish solid. This solid was dissolved in isopropanol at 70-80 °C and a few drops of dichloromethane were added. By cooling the solution with liquid nitrogen, a white product was recrystallized from the solution. The process of recrystallization was repeated three times and a white pure product was formed. ^1H NMR (CDCl_3) δ (ppm) 1.95 (d, 3H, CH_3), 2.83 (s, 4H, CH_2), 4.60 (q, 1H, CH).

5.5.1.2. Synthesis of the ATRP initiator N-Succinimidyl 2-bromo-bromoisobutyrate



This initiator was synthesized according to a procedure reported by Pan and co-workers⁵⁵. 2-Bromoisobutyric acid (6.68 g, 40 mmol) and *N*-hydroxysuccinimide (5.52 g, 48 mmol) were dissolved in 200 mL of anhydrous dichloromethane. DCC was added into the solution. The reaction mixture was stirred at room temperature for 24 h. A white byproduct was separated by filtration. The filtrate was washed with distilled water three times for removal of the unreacted *N*-hydroxysuccinimide and then dried over anhydrous sodium sulfate overnight. After removal of the solvent under reduced pressure, the residue was crystallized from hexane. ^1H NMR (CDCl_3) δ (ppm) 2.05 (s, 6H, CH_3), 2.83 (s, 4H, CH_2).

5.5.2. Functionalization of Silica monoliths

The synthetic procedure was adapted from literature ²⁴⁸. A 1 ml volume of (3-amino propyl) triethoxysilane (APS) (Fluka, 98%) was dissolved in 50 ml dry toluene. 10 ml of the solution was pumped to the cladded rehydroxylated silica monolithic column (Merck, Darmstadt, mm x 4.6 mm), using an HPLC pump, equipped with a degasser. The column was closed and heated up to 65 °C for 24 h. After the reaction, the column was washed with 10 ml of toluene and methanol respectively. 5 ml of the copolymer solution dissolved in DMF (0.05 g per ml) was then pumped through the column with the same procedures. The column was closed and left overnight at room temperature. For characterization, the same reaction was done on free standing monoliths.

Chapter 6

Summary and Outlook

Taking advantage of ATRP and using functionalized initiators, different functionalities were introduced in both α and ω chain-ends of synthetic polymers. These functionalized polymers could then go through modular synthetic pathways such as click cycloaddition (copper-catalyzed or copper-free) or amidation to couple synthetic polymers to other synthetic polymers, biomolecules or silica monoliths. Using this general strategy and designing these co/polymers so that they are thermoresponsive, yet bioinert and biocompatible with adjustable cloud point values (as it is the case in the present thesis), the whole generated system becomes smart and potentially applicable in different branches. The applications which were considered in the present thesis were in polymer post-functionalization (*in situ* functionalization of micellar aggregates with low and high molecular weight molecules), hydrophilic/hydrophobic tuning, chromatography and bioconjugation (enzyme thermoprecipitation and recovery, improvement of enzyme activity). Different α -functionalized co/polymers containing cholesterol moiety, aldehyde, t-Boc protected amine, TMS-protected alkyne and NHS-activated ester were designed and synthesized in this work. All of these functionalities were induced by suitable ATRP initiators. Some examples of functionalized polymers synthesized in this work and their potential applications are explained.

In the first chapter of this thesis, high and low molecular weight molecules were clicked *in situ* with pre-formed micellar aggregates in aqueous solutions. The click strategy applied was “copper-catalyzed click cycloaddition of azides and alkynes (CuAAC)”.

First, a low molecular weight model alkyne was used for clicking on the micelle coronas: Cholesterol-based azide functionalized surfactants were synthesized by atom transfer radical (co)polymerization of oligo (ethylene glycol) (meth) acrylates and subsequent nucleophilic substitution reaction of the bromide end-functionality with azide end group. Depending on their hydrophilic-hydrophobic balance, these macrosurfactants formed either unimolecularly soluble random coils or self-organized into micellar aggregates in pure water. This phenomenon was studied by DLS and measuring hydrodynamic volume of the objects formed in water. ($D_h \sim 5$ nm for random coils and ~ 100 nm for micelles). Also, the formation of aggregates was confirmed by ^1H NMR measurements in D_2O , in which the protons of the hydrophobic cholesterol-based core were shielded and therefore not detected in this solvent. The micellar

aggregates were characterized and showed thermoresponsive behavior with a LCST around 45°C in pure water. After micellization process, the outer coronas of these macrosurfactants were successfully “functionalized” with a model alkyne (propargyl alcohol) via a copper catalyzed azide alkyne cycloaddition reaction. Alkyne functionality of the propargyl alcohol reacted with azide functions on the corona of the formed micelles. The optimized copper-based catalytic system for cycloaddition was proved to be the mixture of copper (II) sulfate and the reducing agent sodium L-ascorbate (Na-AsA) with click yields of up to 98% in water at room temperature in more than 1 day of reaction. All these results confirm that CuAAC is a very efficient and facile method to “functionalize” *in situ* micellar aggregates or any type of colloidal objects in water under mild conditions.

After optimization of the click reaction, CuAAC was applied to couple *in situ* a hydrophilic homopolymer with micellar aggregates of an amphiphilic diblock copolymer in water. This could be a potential strategy for *in situ* “tuning” of hydrophilic-hydrophobic balance of AB type macrosurfactants: ω -azido functionalized model AB amphiphilic block copolymer composed of a hydrophobic polystyrene (PS) segment (A), and a hydrophilic poly[oligo (ethylene glycol) acrylate] [POEGA] segment (B) was synthesized via ATRP and subsequent nucleophilic substitution reaction of the bromide end-functionality with azide end group. The hydrophilic/hydrophobic balance of AB block copolymer was adjusted so that it forms micelles in water. The formation of micelles was studied by DLS and TEM (average diameter estimated around 30 nm). These micelles were then clicked *in situ* with an additional hydrophilic B segment (POEGA). Conditions for click cycloaddition of two polymers were optimized. Characterization of the click product with 500 MHz ^1H NMR and FT-IR confirmed the efficient click reaction with a coupling yield of almost 80%. Hydrolysis of the main-chain ester group of ABB triblock copolymer was also investigated. The results showed there was a competition between the main chain esters and the side chain esters of the block copolymer.

In both cases, CuAAC was a promising reaction, showing all the advantageous features of click chemistry, such as its almost quantitative yields, easiness, tolerance to functional groups and mild reaction conditions even in pure water.

In the second chapter of this thesis, it was demonstrated that metal-free 1,3-dipolar cycloaddition of nitrile oxides and alkynes is an efficient tool for functionalization of biocompatible, thermoresponsive polymers at room temperature and in polar medium. These reactions were proved to give high yields and be regioselective generating almost exclusively 3,5-regioisomer.

Moreover, in a sequential procedure, the α -alkyne and ω -azido chain ends of well-defined polystyrene chains synthesized by ATRP were successfully modified. Modification of chain ends were performed by using consecutive Huisgen cycloadditions in two orthogonal steps: First by nitrile oxide-alkyne cycloaddition (NOAC) and then by copper catalyzed azide-alkyne cycloaddition (CuAAC). These both click-type reactions proceeded in almost quantitative yields in all cases and with all model molecules to give various heterotelechelic polymers. This stepwise method might be extended for chain-end modification of many macromolecular structures other than polystyrene.

In the third chapter of this thesis, polymers functionalized with activated ester moieties were synthesized and examined. For example, thermoresponsive oligo (ethylene glycol)-based copolymers were investigated for trypsin conjugation. Here, two N-hydroxy succinimide (NHS) based initiators were applied for ATRP. Different polymers with varying LCST values could be successfully conjugated to trypsin. Conjugates were characterized and SDS-PAGE indicated that polymer/enzyme conjugates were obtained in all cases. However, conjugation efficiency (number of conjugated polymer chains/trypsin) was higher for some polymers initiated with one of the NHS-initiators. The formed conjugates were found to be thermoresponsive and moreover exhibited a higher enzyme activity than unmodified trypsin.

As another example of a coupling reaction through complementary functionalities, thermoresponsive polymers with reactive ester chain ends (initiated from NHS-based initiators) were synthesized and characterized and in a further step grafted onto aminated silica monoliths to build thermoresponsive stationary phases for chromatography. Efficiency of these smart chromatography columns were tested for temperature-induced separation of a mixture of steroids and proteins and in both cases separation was shown to be successful.

All functionalization methods and their potential applications mentioned in this thesis are just few examples of various possible ways of functionalization. It is even possible to use other controlled radical polymerization methods and initiators to introduce functionalities. This work emphasized the important role of “functionalization” on one side and “smartness” on the other side. Nowadays, it is also important to develop efficient and easy techniques such as click chemistry to couple functionalized polymers with other polymers, biomolecules and other species such as inorganic surfaces and particles. Combination of these three aspects (functionalization, smartness and efficient coupling methodologies) gives the material scientists a lot of possibilities to design and synthesize smart materials required in different applications.

Chapter 7

Analytical methods

7.1. Nuclear Magnetic Resonance (NMR)

^1H NMR spectra were recorded on a Bruker DPX-400 (operating at 400.1 MHz) or with a Bruker Avance 300 spectrometer (operating at 300.1 MHz) or a Bruker Avance 500 spectrometer.

7.2. Size exclusion chromatography (SEC)

Molecular weights and molecular weight distributions were determined by SEC performed at 25 °C in THF (flow rate 1 mL·min⁻¹), using four 5 µ-SDV columns (one guard column and three columns of 4·10³, 3·10⁵, 2·10⁶ Å). The detection was performed with a RI (DN-0, WGE Dr. Bures) and a UV/VIS detector (UV 2000; 260 nm). For calibration, linear polystyrene standards (PSS, Germany) were used.

7.3. Cloud point measurements (Turbidimetry)

The cloud points of the polymer solutions in water were measured on a Tepper TP1 photometer (Mainz, Germany). Transmittance of polymer solutions in deionized water at 670 nm was monitored as a function of temperature (cell path length: 12 mm; one heating/cooling cycle at rate of 1°C·min⁻¹). Typical sample concentration was 3 g·L⁻¹.

7.4. FT-IR spectroscopy

IR spectra were measured using a Bruker spectrophotometer (IFS 66/S) equipped with a Deuterated Triglycerine Sulfate (DTGS) detector.

7.5. Enzyme activity tests

The enzyme activity tests were recorded on a UVIKON 941 PLUS spectrophotometer using tungsten halogen lamp (λ range: 290-900 nm) as a light source and a photomultiplier R 446 detector.

References

1. Matyjaszewski, K., *et al.*, *Nat. Chem.*, 2009, **1**, 4, 276-288.
2. Ouchi, M., *et al.*, *Chem. Rev.*, 2009, **109**, 11, 4963-5050.
3. Kolb, H. C., *et al.*, *Angew. Chem.-Int. Edit.*, 2001, **40**, 11, 2004-2021.
4. Lutz, J. F., *Angew. Chem.-Int. Edit.*, 2007, **46**, 7, 1018-1025.
5. Singh, I., *et al.*, *Macromolecules*, 2009, **42**, 15, 5411-5413.
6. Lowe, A. B., *Polym. Chem.*, **1**, 1, 17-36.
7. Hoyle, C. E., *et al.*, *J. Polym. Sci. Pol. Chem.*, 2004, **42**, 21, 5301-5338.
8. Hoyle, C. E., *et al.*, *Angew. Chem.-Int. Edit.*, **49**, 9, 1540-1573.
9. Lowe, A. B., *et al.*, *J. Mater. Chem.*, **20**, 23, 4745-4750.
10. Hoogenboom, R., *Angew. Chem.-Int. Edit.*, **49**, 20, 3415-3417.
11. Durmaz, H., *et al.*, *Macromolecules*, 2007, **40**, 2, 191-198.
12. Sinnwell, S., *et al.*, *Chem. Commun.*, 2008, 17, 2052-2054.
13. Inglis, A. J., *et al.*, *Angew. Chem.-Int. Edit.*, 2009, **48**, 13, 2411-2414.
14. Inglis, A. J., *et al.*, *Macromolecules*, 2008, **41**, 12, 4120-4126.
15. Ranjan, R., *et al.*, *Macromol. Rapid Commun.*, 2008, **29**, 12-13, 1104-1110.
16. Ranjan, R., *et al.*, *Macromol. Rapid Commun.*, 2007, **28**, 21, 2084-2089.
17. Magenau, A. J. D., *et al.*, *Macromolecules*, 2009, **42**, 21, 8044-8051.
18. Zhang, T., *et al.*, *Eur. Polym. J.*, 2009, **45**, 6, 1625-1633.
19. Ranjan, R., *et al.*, *Macromolecules*, 2007, **40**, 17, 6217-6223.
20. Zhang, T., *et al.*, *Macromol. Rapid Commun.*, 2008, **29**, 21, 1716-1720.
21. Puttick, S., *et al.*, *J. Mater. Chem.*, 2009, **19**, 18, 2679-2682.
22. Agut, W., *et al.*, *Macromolecules*, 2007, **40**, 16, 5653-5661.
23. Durmaz, H., *et al.*, *J. Polym. Sci. Pol. Chem.*, **48**, 7, 1557-1564.
24. Dag, A., *et al.*, *Polym. Chem.*, **1**, 5, 621-623.
25. Durmaz, H., *et al.*, *J. Polym. Sci. Pol. Chem.*, 2008, **46**, 21, 7091-7100.
26. Erdogan, M., *et al.*, *Polymer*, 2002, **43**, 6, 1925-1931.
27. Dag, A., *et al.*, *J. Polym. Sci. Pol. Chem.*, 2009, **47**, 1, 178-187.
28. Barner-Kowollik, C., *et al.*, *Angew. Chem.-Int. Edit.*, **50**, 1, 60-62.

29. Lutz, J.-F., *Journal of Polymer Science Part A: Polymer Chemistry*, 2008, **46**, 11, 3459-3470.
30. Lutz, J. F., *Angew. Chem.-Int. Edit.*, 2008, **47**, 12, 2182-2184.
31. Szwarc, M., *Nature*, 1956, **178**, 4543, 1168-1169.
32. Szwarc, M., *et al.*, *J. Am. Chem. Soc.*, 1956, **78**, 11, 2656-2657.
33. Fischer, H., *J. Polym. Sci. Pol. Chem.*, 1999, **37**, 13, 1885-1901.
34. Braunecker, W. A., *et al.*, *Prog. Polym. Sci.*, 2008, **33**, 1, 165-165.
35. Bertin, D., *et al.*, *Chem. Soc. Rev.*, **40**, 5, 2189-2198.
36. Tebben, L., *et al.*, *Angew. Chem.-Int. Edit.*, **50**, 22, 5034-5068.
37. Georges, M. K., *et al.*, *Macromolecules*, 1993, **26**, 11, 2987-2988.
38. Chong, Y. K., *et al.*, *Macromolecules*, 1999, **32**, 21, 6895-6903.
39. Farcet, C., *et al.*, *Macromolecules*, 2000, **33**, 23, 8559-8570.
40. Keoshkerian, B., *et al.*, *Macromolecules*, 2001, **34**, 19, 6531-6532.
41. Nicolas, J., *et al.*, *Macromolecules*, 2004, **37**, 12, 4453-4463.
42. Chiefari, J., *et al.*, *Macromolecules*, 1998, **31**, 16, 5559-5562.
43. Moad, G., *et al.*, *Polymer*, 2008, **49**, 5, 1079-1131.
44. Destarac, M., *et al.*, *Macromol. Chem. Phys.*, 2002, **203**, 16, 2281-2289.
45. Lowe, A. B., *et al.*, *Prog. Polym. Sci.*, 2007, **32**, 3, 283-351.
46. Perrier, S., *et al.*, *J. Polym. Sci. Pol. Chem.*, 2005, **43**, 22, 5347-5393.
47. Krzysztof Matyjaszewski , A. H. E. M., *Controlled and Living Polymerizations: From Mechanisms to Applications*, Wiley, 2009.
48. Braunecker, W. A., *et al.*, *Prog. Polym. Sci.*, 2007, **32**, 1, 93-146.
49. Matyjaszewski, K., *et al.*, *Chem. Rev.*, 2001, **101**, 9, 2921-2990.
50. Clark, K. B., *et al.*, *J. Am. Chem. Soc.*, 1991, **113**, 24, 9363-9365.
51. Mueller, L., *et al.*, *Macromolecules*, 2007, **40**, 18, 6464-6472.
52. Tang, W., *et al.*, *J. Am. Chem. Soc.*, 2008, **130**, 32, 10702-10713.
53. Coessens, V., *et al.*, *Prog. Polym. Sci.*, 2001, **26**, 3, 337-377.
54. Lutz, J. F., *et al.*, *Prog. Polym. Sci.*, 2008, **33**, 1, 1-39.
55. Han, D. H., *et al.*, *Polymer*, 2006, **47**, 20, 6956-6962.
56. Nicolas, J., *et al.*, *Chem. Commun.*, 2007, 17, 1722-1724.
57. Tao, L., *et al.*, *J. Am. Chem. Soc.*, 2004, **126**, 41, 13220-13221.
58. Lecolley, F., *et al.*, *Chem. Commun.*, 2004, 18, 2026-2027.

59. Theato, P., *Journal of Polymer Science Part a-Polymer Chemistry*, 2008, **46**, 20, 6677-6687.
60. Haddleton, D. M., *et al.*, *Macromolecules*, 1999, **32**, 26, 8732-8739.
61. Jankova, K., *et al.*, *Macromolecules*, 1998, **31**, 2, 538-541.
62. Matyjaszewski, K., *Macromolecules*, 1995, **32**, 20, 6526-6535.
63. Opsteen, J. A., *et al.*, *Chem. Commun.*, 2005, 1, 57-59.
64. Boyer, C., *et al.*, *Polym. Degrad. Stabil.*, 2005, **90**, 2, 326-339.
65. Vazquez-Dorbatt, V., *et al.*, *Biomacromolecules*, 2009, **10**, 8, 2207-2212.
66. Hasneen, A., *et al.*, *React. Funct. Polym.*, 2009, **69**, 9, 681-687.
67. Opsteen, J. A., *et al.*, *J. Polym. Sci. Pol. Chem.*, 2007, **45**, 14, 2913-2924.
68. Zarafshani, Z., *et al.*, *Macromol. Rapid Commun.*, 2008, **29**, 12-13, 1161-1166.
69. Urbani, C. N., *et al.*, *Macromolecules*, 2008, **41**, 1, 76-86.
70. Tsarevsky, N. V., *et al.*, *Macromolecules*, 2005, **38**, 9, 3558-3561.
71. Laurent, B. A., *et al.*, *J. Am. Chem. Soc.*, 2006, **128**, 13, 4238-4239.
72. Li, C. H., *et al.*, *Macromolecules*, 2009, **42**, 8, 2916-2924.
73. Campos, L. M., *et al.*, *Macromolecules*, 2008, **41**, 19, 7063-7070.
74. Batz, H. G., *et al.*, *Angewandte Chemie-International Edition in English*, 1972, **11**, 12, 1103-1104.
75. Ferruti, P., *et al.*, *Polymer*, 1972, **13**, 10, 462-&.
76. Lutz, J. F., *et al.*, *J. Polym. Sci. Pol. Chem.*, 2005, **43**, 4, 897-910.
77. Saxon, E., *et al.*, *Science*, 2000, **287**, 5460, 2007-2010.
78. Kalia, J., *et al.*, *Bioconjugate Chemistry*, 2007, **18**, 4, 1064-1069.
79. Kohn, M., *et al.*, *Angew. Chem.-Int. Edit.*, 2004, **43**, 24, 3106-3116.
80. Lutz, J. F., *et al.*, *Polymer*, 2008, **49**, 4, 817-824.
81. Tornøe, C. W., *et al.*, *J. Org. Chem.*, 2002, **67**, 9, 3057-3064.
82. Rostovtsev, V. V., *et al.*, *Angew. Chem.-Int. Edit.*, 2002, **41**, 14, 2596-+.
83. Zhang, L., *et al.*, *J. Am. Chem. Soc.*, 2005, **127**, 46, 15998-15999.
84. Oppiliart, S., *et al.*, *Tetrahedron*, 2007, **63**, 34, 8094-8098.
85. Collman, J. P., *et al.*, *Langmuir*, 2004, **20**, 4, 1051-1053.
86. Diaz, D. D., *et al.*, *J. Polym. Sci. Pol. Chem.*, 2004, **42**, 17, 4392-4403.
87. Helms, B., *et al.*, *J. Am. Chem. Soc.*, 2004, **126**, 46, 15020-15021.
88. Wu, P., *et al.*, *Angew. Chem.-Int. Edit.*, 2004, **43**, 30, 3928-3932.

89. Lutz, J. F., *et al.*, *Macromol. Rapid Commun.*, 2005, **26**, 7, 514-518.
90. Rodionov, V. O., *et al.*, *Angew. Chem.-Int. Edit.*, 2005, **44**, 15, 2210-2215.
91. Becer, C. R., *et al.*, *Angew. Chem.-Int. Edit.*, 2009, **48**, 27, 4900-4908.
92. van Berkel, S. S., *et al.*, *ChemBioChem*, 2007, **8**, 13, 1504-1508.
93. Seo, T. S., *et al.*, *J. Org. Chem.*, 2003, **68**, 2, 609-612.
94. Li, Z. M., *et al.*, *Tetrahedron Lett.*, 2004, **45**, 15, 3143-3146.
95. Baskin, J. M., *et al.*, *Proc. Natl. Acad. Sci. U. S. A.*, 2007, **104**, 43, 16793-16797.
96. Agard, N. J., *et al.*, *J. Am. Chem. Soc.*, 2004, **126**, 46, 15046-15047.
97. Agard, N. J., *et al.*, *ACS Chem. Biol.*, 2006, **1**, 10, 644-648.
98. Baskin, J. M., *et al.*, *QSAR Comb. Sci.*, 2007, **26**, 11-12, 1211-1219.
99. Wittig, G. K., A, *Chemische Berichte-Recueil*, 1961, **94**, 12, 3260-3275.
100. Ning, X. H., *et al.*, *Angew. Chem.-Int. Edit.*, 2008, **47**, 12, 2253-2255.
101. Jewett, J. C., *et al.*, *J. Am. Chem. Soc.*, **132**, 11, 3688-3690.
102. Jewett, J. C. B., Carolyn R, *Chem Soc Rev* 2010, **39**, 4, 1272-1279.
103. Sperry JB, *et al.*, *Current Opinion In Drug Discovery & Development*, 2005, **8**, 6, 723-740.
104. Coutouli-Argyropoulou, E., *et al.*, *Tetrahedron*, 2006, **62**, 7, 1494-1501.
105. Singh, I., *et al.*, *Chem. Commun.*, 2009, 22, 3276-3278.
106. Himo, F., *et al.*, *J. Am. Chem. Soc.*, 2004, **127**, 1, 210-216.
107. Grecian, S., *et al.*, *Angewandte Chemie International Edition*, 2008, **47**, 43, 8285-8287.
108. Gutsmedl, K., *et al.*, *Organic Letters*, 2009, **11**, 11, 2405-2408.
109. Wankhede KS, *et al.*, *Tetrahedron Lett.*, 2008, **49**, 13, 2069-2073.
110. Lutz, J.-F. o., *et al.*, *Macromolecules*, 2005, **39**, 2, 893-896.
111. Kanazawa, H., *et al.*, *Journal of Pharmaceutical and Biomedical Analysis*, 1997, **15**, 9-10, 1545-1550.
112. Kikuchi, A., *et al.*, *Progress in Polymer Science*, 2002, **27**, 6, 1165-1193.
113. Kanazawa, H., *Analytical and Bioanalytical Chemistry*, 2004, **378**, 1, 46-48.
114. Schild, H. G., *Progress in Polymer Science*, 1992, **17**, 2, 163-249.
115. Lutz, J. F., *Polym. Int.*, 2006, **55**, 9, 979-993.
116. Wu, J. Y., *et al.*, *Journal of Controlled Release*, 2005, **102**, 2, 361-372.
117. Lutz, J. F., *J. Polym. Sci. Pol. Chem.*, 2008, **46**, 11, 3459-3470.
118. Lutz, J. F., *et al.*, *Macromolecules*, 2006, **39**, 2, 893-896.

119. Jonas, A. M., *et al.*, *Macromolecules*, 2007, **40**, 13, 4403-4405.
120. Chen, G., *et al.*, *Chem. Commun.*, 2008, 9, 1097-1099.
121. Lee, H. I., *et al.*, *Chem. Commun.*, 2008, 32, 3726-3728.
122. Magnusson, J. P., *et al.*, *Journal of the American Chemical Society*, 2008, **130**, 33, 10852.
123. Chanana, M., *et al.*, *Chemistry of Materials*, 2009, **21**, 9, 1906-1914.
124. Chen, G. J., *et al.*, *Chem. Commun.*, 2009, 10, 1198-1200.
125. Pietsch, C., *et al.*, *Angewandte Chemie-International Edition*, 2009, **48**, 31, 5653-5656.
126. Veronese, F. M., *et al.*, *Farmaco*, 1999, **54**, 8, 497-516.
127. Pasut, G., *et al.*, *Prog. Polym. Sci.*, 2007, **32**, 8-9, 933-961.
128. Pasut, G., *et al.*, in *Polymer Therapeutics I: Polymers as Drugs, Conjugates and Gene Delivery Systems*, Springer-Verlag Berlin, 2006, pp. 95-134.
129. Gil, E. S., *et al.*, *Progress in Polymer Science*, 2004, **29**, 12, 1173-1222.
130. Stayton, P. S., *et al.*, *Nature*, 1995, **378**, 6556, 472-474.
131. Hoffman, A. S., *et al.*, *Macromolecular Symposia*, 2004, **207**, 139-151.
132. Chen, G. H., *et al.*, *Bioconjugate Chem.*, 1993, **4**, 6, 509-514.
133. Shimoboji, T., *et al.*, *Bioconjugate Chem.*, 2003, **14**, 3, 517-525.
134. Kulkarni, S., *et al.*, *Bioconjugate Chem.*, 2004, **15**, 4, 747-753.
135. Li, M., *et al.*, *Macromolecular Rapid Communications*, 2008, **29**, 12-13, 1172-1176.
136. Vazquez-Dorbatt, V., *et al.*, *Macromolecules*, 2009, **42**, 20, 7650-7656.
137. Heredia, K. L., *et al.*, *Polymer Chemistry*, **1**, 2, 168-170.
138. Le Droumaguet, B., *et al.*, *Polymer Chemistry*, **1**, 5, 563-598.
139. Nicolas, J., *et al.*, *Macromolecular Rapid Communications*, 2007, **28**, 10, 1083-1111.
140. Alarcon, C. D. H., *et al.*, *Journal of Materials Chemistry*, 2005, **15**, 21, 2089-2094.
141. Teeuwen, R. L. M., *et al.*, *Chem. Commun.*, 2009, 27, 4022-4024.
142. Hoogenboom, R., *et al.*, *Chem. Commun.*, 2008, 44, 5758-5760.
143. Diehl, C., *et al.*, *Macromolecular Bioscience*, 2009, **9**, 2, 157-161.
144. Han, S., *et al.*, *Macromolecules*, 2003, **36**, 22, 8312-8319.
145. Ali, M. M., *et al.*, *Macromolecules*, 2004, **37**, 14, 5219-5227.
146. Yamamoto, S. I., *et al.*, *Journal of Polymer Science Part A-Polymer Chemistry*, 2008, **46**, 1, 194-202.
147. Lutz, J. F., *et al.*, *Macromolecules*, 2007, **40**, 24, 8540-8543.

148. Chang, C. W., *et al.*, *Chem. Commun.*, 2009, 24, 3580-3582.
149. Pissuwan, D., *et al.*, *Biomacromolecules*, **11**, 2, 412-420.
150. Lutz, J. F., *et al.*, *J. Am. Chem. Soc.*, 2006, **128**, 40, 13046-13047.
151. Lutz, J. F., *et al.*, *Macromolecules*, 2007, **40**, 7, 2503-2508.
152. Lutz, J. F., *et al.*, *Designed Monomers and Polymers*, 2009, **12**, 4, 343-353.
153. Fechler, N., *et al.*, *Macromolecules*, 2009, **42**, 1, 33-36.
154. Badi, N., *et al.*, *Journal of Controlled Release*, 2009, **140**, 3, 224-229.
155. O'Lenick, T. G., *et al.*, *Langmuir*, **26**, 11, 8787-8796.
156. Hu, Z. B., *et al.*, *Soft Matter*, **6**, 10, 2115-2123.
157. Dong, H. C., *et al.*, *Chemistry of Materials*, 2009, **21**, 17, 3965-3972.
158. Hua, F. J., *et al.*, *Macromolecules*, 2006, **39**, 10, 3476-3479.
159. Lutz, J. F., *et al.*, *Qsar & Combinatorial Science*, 2007, **26**, 11-12, 1151-1158.
160. Pasparakis, G., *et al.*, *Angewandte Chemie-International Edition*, 2008, **47**, 26, 4847-4850.
161. Wischerhoff, E., *et al.*, *Angewandte Chemie-International Edition*, 2008, **47**, 30, 5666-5668.
162. Tan, I., *et al.*, *ACS Applied Materials & Interfaces*, 2009, **1**, 9, 1869-1872.
163. Kessel, S., *et al.*, *Langmuir*, **26**, 5, 3462-3467.
164. Roth, P. J., *et al.*, *Biomacromolecules*, **11**, 1, 238-244.
165. Wiss, K. T., *et al.*, *Macromolecules*, 2009, **42**, 12, 3860-3863.
166. Lele, B. S., *et al.*, *Biomacromolecules*, 2005, **6**, 6, 3380-3387.
167. Bontempo, D., *et al.*, *Journal of the American Chemical Society*, 2005, **127**, 18, 6508-6509.
168. Mantovani, G., *et al.*, *Journal of the American Chemical Society*, 2005, **127**, 9, 2966-2973.
169. Lutz, J. F., *et al.*, *Macromolecules*, 2006, **39**, 19, 6376-6383.
170. Nicolas, J., *et al.*, *Chem. Commun.*, 2006, 45, 4697-4699.
171. Bays, E., *et al.*, *Biomacromolecules*, 2009, **10**, 7, 1777-1781.
172. Wang, X. S., *et al.*, *Chem. Commun.*, 1999, 18, 1817-1818.
173. Wang, X. S., *et al.*, *Macromolecules*, 2000, **33**, 18, 6640-6647.
174. Abuchowski, A., *et al.*, *Biochimica Et Biophysica Acta*, 1979, **578**, 1, 41-46.
175. Abuchowski, A., *et al.*, *J. Biol. Chem.*, 1977, **252**, 11, 3582-3586.

176. Kodera, Y., *et al.*, *Prog. Polym. Sci.*, 1998, **23**, 7, 1233-1271.
177. Bornscheuer, U. T., *Angew. Chem.-Int. Edit.*, 2003, **42**, 29, 3336-3337.
178. Dyal A., *et al.*, *J. Am. Chem. Soc.*, 2003, **125**, 7, 1684-1685.
179. Ding, Z. L., *et al.*, *Bioconjugate Chem.*, 1996, **7**, 1, 121-125.
180. Huber, R., *et al.*, *Accounts of Chemical Research*, 1978, **11**, 3, 114-122.
181. Gaertner, H. F., *et al.*, *Enzyme and Microbial Technology*, 1992, **14**, 2, 150-155.
182. Goldstein, L., *Biochemistry*, 1972, **11**, 22, 4072-4084.
183. Gauthier, M. A. K., H. A., *Polymer Chemistry*, 2010, **1**, 9.
184. Munch, O., *et al.*, *Biocatalysis*, 1991, **5**, 1, 35-47.
185. Ding, Z. L., *et al.*, *J. Biomed. Mater. Res.*, 1998, **39**, 3, 498-505.
186. Raghava, S., *et al.*, *Artificial Cells Blood Substitutes and Biotechnology*, 2006, **34**, 3, 323-336.
187. Matsukata, M., *et al.*, *Bioconjugate Chem.*, 1996, **7**, 1, 96-101.
188. Tang, W., *et al.*, *Macromolecules*, 2007, **40**, 6, 1858-1863.
189. Laschewsky, A., *Current Opinion in Colloid & Interface Science*, 2003, **8**, 3, 274-281.
190. Kubowicz, S., *et al.*, *Angew. Chem.-Int. Edit.*, 2005, **44**, 33, 5262-5265.
191. Lutz, J. F., *et al.*, *Macromolecular Chemistry and Physics*, 2005, **206**, 8, 813-817.
192. Forster, S., *et al.*, *Angew. Chem.-Int. Edit.*, 2002, **41**, 5, 689-714.
193. Discher, D. E., *et al.*, *Science*, 2002, **297**, 5583, 967-973.
194. Gohy, J. F., in *Block Copolymers II*, Springer-Verlag, Berlin, 2005, pp. 65-136.
195. Rodriguez-Hernandez, J., *et al.*, *Prog. Polym. Sci.*, 2005, **30**, 7, 691-724.
196. Cameron, N. S., *et al.*, *Can. J. Chem.-Rev. Can. Chim.*, 1999, **77**, 8, 1311-1326.
197. Li, Z. B., *et al.*, *Science*, 2004, **306**, 5693, 98-101.
198. Pochan, D. J., *et al.*, *Science*, 2004, **306**, 5693, 94-97.
199. Kubowicz, S., *et al.*, *Angewandte Chemie International Edition*, 2005, **44**, 33, 5262-5265.
200. Lutz, J.-F., *et al.*, *Macromolecular Chemistry and Physics*, 2005, **206**, 8, 813-817.
201. Lutz, J.-F., *et al.*, *Soft Matter*, 2007, **3**, 6, 694-698.
202. Kotzev, A., *et al.*, *Macromolecules*, 2002, **35**, 3, 1091-1101.
203. Lutz, J. F., *et al.*, *Macromolecular Chemistry and Physics*, 2002, **203**, 10-11, 1385-1395.
204. Skrabania, K., *et al.*, *Langmuir*, 2007, **23**, 1, 84-93.
205. Lewis, W. G., *et al.*, *J. Am. Chem. Soc.*, 2004, **126**, 30, 9152-9153.
206. Golas, P. L., *et al.*, *Macromolecules*, 2006, **39**, 19, 6451-6457.

207. Arotcarena, M., *et al.*, *J. Am. Chem. Soc.*, 2002, **124**, 14, 3787-3793.
208. Liu, S. Y., *et al.*, *Angew. Chem.-Int. Edit.*, 2002, **41**, 8, 1413-1416.
209. Jiang, J. Q., *et al.*, *J. Am. Chem. Soc.*, 2005, **127**, 23, 8290-8291.
210. Vogt, A. P., *et al.*, *Macromolecules*, 2006, **39**, 16, 5286-5292.
211. Lutz, J. F., *et al.*, *Biomacromolecules*, 2006, **7**, 11, 3132-3138.
212. Tao, L., *et al.*, *J. Am. Chem. Soc.*, 2004, **126**, 41, 13220-13221.
213. Hassner, A., *et al.*, *Synthesis*, 1989, 1, 57-59.
214. Wankhede, K. S., *et al.*, *Tetrahedron Lett.*, 2008, **49**, 13, 2069-2073.
215. Himo, F., *et al.*, *J. Am. Chem. Soc.*, 2005, **127**, 1, 210-216.
216. Grecian, S., *et al.*, *Angew. Chem.-Int. Edit.*, 2008, **47**, 43, 8285-8287.
217. Lee, C. K. Y., *et al.*, *Journal of the Chemical Society, Perkin Transactions 2*, 2002, 12, 2031-2038.
218. Kele, P., *et al.*, *Angew. Chem.-Int. Edit.*, 2009, **48**, 2, 344-347.
219. Nurmi, L., *et al.*, *Chem. Commun.*, 2009, 19, 2727-2729.
220. DeForest, C. A., *et al.*, *Nat. Mater.*, 2009, **8**, 8, 659-664.
221. Polaske, N. W., *et al.*, *Macromolecules*, **43**, 3, 1270-1276.
222. Pfeifer, S., *et al.*, *J. Am. Chem. Soc.*, 2009, **131**, 26, 9195-9197.
223. Fournier, D., *et al.*, *Chem. Soc. Rev.*, 2007, **36**, 8, 1369-1380.
224. Lee, Y. G., *et al.*, *Macromolecules*, 2009, **42**, 20, 7709-7717.
225. Lee, Y. G., *et al.*, *Macromolecules*, **43**, 9, 4070-4080.
226. Lee, Y. G., *et al.*, *Chem. Lett.*, **39**, 4, 420-421.
227. Algay, V., *et al.*, *Org. Biomol. Chem.*, **8**, 2, 391-397.
228. Singh, I., *et al.*, *Org Biomol Chem*, 2009, **8**, 2, 451-456.
229. Pfeifer, S., *et al.*, *Chem.-Eur. J.*, 2008, **14**, 35, 10949-10957.
230. Pfeifer, S., *et al.*, *Macromol. Chem. Phys.*, **211**, 8, 940-947.
231. Malkoch, M., *et al.*, *J. Am. Chem. Soc.*, 2005, **127**, 42, 14942-14949.
232. Berthet, M. A., *et al.*, *Macromolecules*, **43**, 1, 44-50.
233. Coessens, V., *et al.*, *J. Macromol. Sci.-Pure Appl. Chem.*, 1999, **A36**, 5-6, 811-826.
234. Yang, Z., *et al.*, *Biomacromolecules*, 2007, **8**, 11, 3422-3428.
235. Harris, J. M., *et al.*, *Journal of Polymer Science: Polymer Chemistry Edition*, 1984, **22**, 2, 341-352.

- 236. Shanmugharaj, A. M., *et al.*, *Journal of Polymer Science Part A: Polymer Chemistry*, 2007, **45**, 3, 460-470.
- 237. Omura, K., *et al.*, *Tetrahedron*, 1978, **34**, 11, 1651-1660.
- 238. Nagase, K., *et al.*, *Langmuir*, 2008, **24**, 2, 511-517.
- 239. Zarafshani, Z., *et al.*, *Biomacromolecules*, **11**, 8, 2130-2135.
- 240. Ladmiral, V., *et al.*, *Polymer*, 2005, **46**, 19, 8536-8545.
- 241. Laemmli, U. K., *Nature*, 1970, **227**, 5259, 680-685.
- 242. Bradford, M. M., *Analytical Biochemistry*, 1976, **72**, 1-2, 248-254.
- 243. Candiano, G., *et al.*, *Electrophoresis*, 2004, **25**, 9, 1327-1333.
- 244. Erlanger, B. F., *et al.*, *Archives of Biochemistry and Biophysics*, 1961, **95**, 2, 271-278.
- 245. Berg, J. M., *et al.*, *Biochemistry*, W. H. Freeman, New York, 2006.
- 246. Chiu, H. C., *et al.*, *Bioconjugate Chem.*, 1993, **4**, 4, 290-295.
- 247. Lee, J. H., *et al.*, *J. Biomed. Mater. Res.*, 1989, **23**, 3, 351-368.
- 248. Roohi, F., *et al.*, *Journal of Chromatography A*, 2008, **1203**, 2, 160-167.

Acknowledgement

I would like to thank Professor André Laschewsky who gave me the possibility to do my thesis under his supervision. I would also like to show my great gratitude to Professor Jean-François Lutz for the excellent project leading and giving me the chance to work in his group and his supportive and friendly discussions which has brought me continuously motivation and knowledge during the work. I am also grateful to the members of the former group 'Nanotechnology for life science' at Fraunhofer Institute, especially Özgür Akdemir and Sebastian Pfeifer for the nice atmosphere in the lab and fantastic time in NATO-meeting in Antalya. I am greatly thankful to Dr. Toshihiro Obata (Max Planck Institute for Plant Physiology) for the great help in time-consuming SDS-PAGE measurements. My special thanks go also to Achille Bivigou Koumba for the friendly help and discussions in organic chemistry syntheses. I should also thank Dr. Carola Fanter and Mirjam Mai (Fraunhofer Institute) for the spectrophotometric measurements. And finally special thanks to all laboratory assistants, PhD students, and project collaborators at Fraunhofer Institute for Applied Polymer Science and Max Planck Institute for Colloids and Interfaces, Frances Heaney research group in the National university of Ireland, Maynooth and all kind people, without whose support this thesis would not have been possible.

